



Universidad  
Politécnica  
de Cartagena

Ph.D. Dissertation

**Conducting polymer actuator :  
From basic concepts to  
proprioceptive systems.**

Written by  
José Gabriel Martínez Gil



Universidad  
Politécnica  
de Cartagena

Ph.D. Dissertation

**Conducting polymer actuators:  
From basic concepts to  
proprioceptive systems.**

Written by  
José Gabriel Martínez Gil

Supervised by  
Prof. Dr. Toribio Fernández Otero

**Conducting polymer actuators: From basic concepts to proprioceptive systems.**

*To Gabriel, Pepa, Pepe and Pura, my grandparents*

This thesis is presented through a set of publications. It is supported by 12 papers, of the 27 co-authored by the candidate and published in different journals during the development of this thesis. All the papers are indexed in the Journal Citation Reports (ISI-JCR). Selected items reach 45 points according with the UPCT regulations (Artículo 33 del Reglamento de estudios oficiales de máster y doctorado de la Universidad Politécnica de Cartagena, aprobado por Consejo de Gobierno el 13 de abril de 2011 y modificado en Consejo de Gobierno el 11 de julio de 2012.), requiring a minimum of 12 points to allow the thesis presentation through a set of publications. Following those regulations this thesis includes: the objectives of the thesis, the state of the art, an extended abstract for every article (including the experimental procedure and the main achievements), a copy of each selected paper and the general conclusions.

List of selected papers:

1. Toribio F. Otero, Jose G. Martinez and Joaquin Arias-Pardilla. **Biomimetic electrochemistry from conducting polymers. A review. Artificial muscles, smart membranes, smart drug delivery and computer/neuron interfaces** *Electrochimica Acta*, year 2012, volume 84, pages 112-128. (ISI-JCR IF: 4.086, Q1 in Electrochemistry).
2. Toribio F. Otero and Jose G. Martinez. **Artificial Muscles: A Tool To Quantify Exchanged Solvent During Biomimetic Reactions** *Chemistry of Materials*, year 2012, volume 24, pages 4093-4099. (IF=8.535, Q1 in 'Materials science, Multidisciplinary' and 'Chemistry, Physical').
3. Toribio F. Otero and Jose G. Martinez. **Ionic exchanges, structural movements and driven reactions in conducting polymers from bending artificial muscles** *Sensors and Actuators B: Chemical*, year 2014, volume 199, pages 27-30. (IF=3.840, Q1 in 'Instruments & instrumentation', 'Chemistry, analytical' and 'Electrochemistry').
4. Toribio F. Otero and Jose G. Martinez. **Structural Electrochemistry: Conductivities and Ionic Content from Rising Reduced Polypyrrole Films** *Advanced Functional Materials*, year 2014, volume 24, pages 1259-1264. (IF=10.439, Q1 in 'Materials science, multidisciplinary', 'Nanoscience & nanotechnology', 'Physics, applied', 'Chemistry, multidisciplinary', 'Chemistry, physical' and 'Physics, condensed matter').
5. Jose G. Martinez, Toribio F. Otero and Edwin W. H. Jager. **Effect of the Electrolyte Concentration and Substrate on Conducting Polymer Actuators** *Langmuir*, year 2014, volume 30, pages 3894-3904. (IF=4.384,

Q1 in 'Materials science, multidisciplinary', 'Chemistry, multidisciplinary' and 'Chemistry, physical').

6. Toribio F. Otero, Juan J. Sanchez and Jose G. Martinez. **Biomimetic Dual Sensing-Actuators Based on Conducting Polymers. Galvanostatic Theoretical Model for Actuators Sensing Temperature** *The Journal of Physical Chemistry B*, year 2012, volume 116, pages 5279-5290. (IF=3.377, Q2 in 'Chemistry, physical').

7. Jose G. Martinez and Toribio F. Otero. **Biomimetic Dual Sensing-Actuators: Theoretical Description. Sensing Electrolyte Concentration and Driving Current** *The Journal of Physical Chemistry B*, year 2012, volume 116, pages 9223-9230. (IF=3.377, Q2 in 'Chemistry, physical').

8. Jose G. Martinez and Toribio F. Otero. **Mechanical awareness from sensing artificial muscles: Experiments and modeling** *Sensors and Actuators B: Chemical*, year 2014, volume 195, pages 365-372. (IF=3.840, Q1 in 'Instruments & instrumentation', 'Chemistry, analytical', and 'Electrochemistry').

9. Jose G. Martinez and Toribio F. Otero. **Structural Electrochemistry. Chronopotentiometric Responses From Rising Compacted Polypyrrole Electrodes: Experiments and Model** *RSC Advances*, year 2014, volume 4, pages 29139-29145. (IF=3.708, Q1 in 'Chemistry, multidisciplinary').

10. Toribio F. Otero and Jose G. Martinez. **Physical and chemical awareness from sensing polymeric artificial muscles. Experiments and modeling** *Progress in Polymer Science*, year 2014, DOI: 10.1016/j.progpolymsci.2014.09.002. (IF=26.854, Q1 in 'Polymer science').

11. Yahya A. Ismail, Jose G. Martinez and Toribio F. Otero. **Polyurethane microfibrillar mat template polypyrrole: Preparation and biomimetic reactive sensing capabilities** *Journal of Electroanalytical Chemistry*, year 2014, volume 719, pages 47-53. (IF=2.871, Q2 in 'Chemistry, analytical' and 'Electrochemistry').

12. Yahya A. Ismail, Jose G. Martinez and Toribio F. Otero. **Fibroin/Polyaniline microfibrillar mat. Preparation and electrochemical characterization as reactive sensor** *Electrochimica Acta*, year 2014, volume 123, pages 501-510. (IF: 4.086, Q1 in 'Electrochemistry').

Rest of co-authored articles published during thesis period:

- Toribio F. Otero and Jose G. Martinez. **Activation energy for polypyrrole oxidation: film thickness influence** *Journal of Solid State Electrochemistry*, year 2011, volume 15, pages 1169-1178. (IF: 2.234, Q2 in 'Electrochemistry').
- Toribio F. Otero, Jose G. Martinez, Kosuke Hosaka and Hidenori Okuzaki. **Electrochemical characterization of PEDOT-PSS-Sorbitol electrodes. Sorbitol changes cation to anion interchange during reactions** *Journal of Electroanalytical Chemistry*, year 2011, volume 657, pages 23-27. (IF: 2.871, Q2 in 'Chemistry, Analytical' and 'Electrochemistry').
- Yahya A. Ismail, Jose G. Martinez, Ahmad S. Al Harrasi, Seon J. Kim and Toribio F. Otero. **Sensing characteristics of a conducting polymer/hydrogel hybrid microfiber artificial muscle** *Sensors and Actuators B: Chemical*, year 2011, volume 160, pages 1180-1190. (IF=3.840, Q1 in 'Instruments & instrumentation', 'Chemistry, analytical', and 'Electrochemistry').
- Toribio F. Otero, Joaquin Arias-Pardilla, Maria I. Roca and Jose G. Martinez. **Electrochemical Kinetics in Dense, Reactive and Wet Gels. Biomimicking Reactions and Devices** *Molecular Crystals and Liquid Crystals*, year 2012, volume 555, pages 295-305. (IF: 0.491, Q4 in 'Crystallography').
- Salvador Aznar-Cervantes, Maria I. Roca, Jose G. Martinez, Luis Meseguer-Olmo, Jose L. Cenis, Jose M. Moraleda, Toribio F. Otero. **Fabrication of conductive electrospun silk fibroin scaffolds by coating with polypyrrole for biomedical applications** *Bioelectrochemistry*, year 2012, volume 85, pages 36-43. (IF: 3.870, Q1 in 'Biology', 'Biophysics' and 'Electrochemistry' and Q2 in 'Biochemistry & molecular biology').
- Ryoichi Kishi, Kazuaki Hiroki, Taiki Tominaga, Ken-Ichi Sano, Hidenori Okuzaki, Jose G. Martinez, Toribio F. Otero, Yoshihito Osada. **Electro-conductive double-network hydrogels** *Journal of Polymer Science Part B – Polymer Physics*, year 2012, volume 50, pages 790-796. (IF: 3.803, Q1 in 'Polymer science').
- Jose G. Martinez, Takushi Sugino, Kinji Asaka, Toribio F. Otero. **Electrochemistry of Carbon Nanotubes: Reactive Processes, Dual Sensing-Actuating Properties and Devices** *ChemPhysChem*, year 2012, volume 13, pages 2108-2114. (IF: 3.360, Q1 in 'Physics, atomic, molecular & chemical' and Q2 in 'Chemistry, physical').
- Jose G. Martinez, Toribio F. Otero, Concha Bosch-Navarro, Eugenio Coronado, Carlos Martí-Gastaldo, Helena Prima-Garcia. **Graphene**

**electrochemical responses sense surroundings** *Electrochimica Acta*, year 2012, volumen 81, pages 49-57. (IF: 4.086, Q1 in Electrochemistry).

- Toribio F. Otero and Jose G. Martinez. **Biomimetic intracellular matrix (ICM) materials, properties and functions. Full integration of actuators and sensors** *Journal of Materials Chemistry B*, year 2013, volume 1, pages 26-38. (Inmediacy index: 0.889).
- Toribio F. Otero and Jose G. Martinez. **Structural and Biomimetic Chemical Kinetics: Kinetic Magnitudes Include Structural Information** *Advanced Functional Materials*, year 2013, volume 23, pages 404-416. (IF=10.439, Q1 in 'Materials science, multidisciplinary', 'Nanoscience & nanotechnology', 'Physics, applied', 'Chemistry, multidisciplinary', 'Chemistry, physical' and 'Physics, condensed matter').
- Toribio F. Otero, Mercedes Alfaro, Venancio Martinez, Maria A. Perez and Jose G. Martinez. **Biomimetic Structural Electrochemistry from Conducting Polymers: Processes, Charges, and Energies. Coulovoltammetric Results from Films on Metals Revisited** *Advanced Functional Materials*, year 2013, volume 23, pages 3929-3940. (IF=10.439, Q1 in 'Materials science, multidisciplinary', 'Nanoscience & nanotechnology', 'Physics, applied', 'Chemistry, multidisciplinary', 'Chemistry, physical' and 'Physics, condensed matter').
- Toribio F. Otero, Jose G. Martinez and Buket Zaifoglu. **Using reactive artificial muscles to determine water exchange during reactions** *Smart Materials and Structures*, year 2013, volume 22, article number 104019. (IF: 2.449, Q1 in 'Instruments & instrumentation' and 'Materials science, multidisciplinary').
- Gonzalo Abellan, Jose G. Martinez, Toribio F. Otero, Antonio Ribera and Eugenio Coronado. **A chemical and electrochemical multivalent memory made from FeNi<sub>3</sub>-graphene nanocomposites** *Electrochemistry Communications*, year 2014, volume 39, pages 15-18. (IF: 4.287, Q1 in 'Electrochemistry').
- Laura Valero, Toribio F. Otero and Jose G. Martinez. **Exchanged Cations and Water during Reactions in Polypyrrole Macroions from Artificial Muscles** *ChemPhysChem*, year 2014, volume 15, pages 293-301. (IF: 3.360, Q1 in 'Physics, atomic, molecular & chemical' and Q2 in 'Chemistry, physical').
- Toribio F. Otero, Jose G. Martinez, Masaki Fuchiwaki and Laura Valero. **Structural Electrochemistry from Freestanding Polypyrrole Films: Full Hydrogen Inhibition from Aqueous Solutions** *Advanced Functional Materials*, year 2014, volume 24, pages 1265-1274. (IF=10.439, Q1 in 'Materials science, multidisciplinary',

**Conducting polymer actuators: From basic concepts to proprioceptive systems.**

'Nanoscience & nanotechnology', 'Physics, applied', 'Chemistry, multidisciplinary', 'Chemistry, physical' and 'Physics, condensed matter').

- Masaki Fuchiwaki, Jose G. Martinez, and Toribio F. Otero. **Structural Electrochemistry from Freestanding Polypyrrole Films: Full Hydrogen Inhibition from Aqueous Solutions** *Advanced Functional Materials*, year 2015, volume 25, pages 1535-1541. (IF=10.439, Q1 in 'Materials science, multidisciplinary', 'Nanoscience & nanotechnology', 'Physics, applied', 'Chemistry, multidisciplinary', 'Chemistry, physical' and 'Physics, condensed matter').







**CONFORMIDAD DE SOLICITUD DE AUTORIZACIÓN DE DEPÓSITO DE  
TESIS DOCTORAL POR EL/LA DIRECTOR/A DE LA TESIS**

D. Toribio Fernández Otero, Director/a de la Tesis doctoral “Conducting polymer actuators: From basic concepts to proprioceptive systems.”

**INFORMA:**

Que la referida Tesis Doctoral, ha sido realizada por D. José Gabriel Martínez Gil, dentro del programa de doctorado “Electroquímica. Ciencia y Tecnología”, dando mi conformidad para que sea presentada ante la Comisión de Doctorado para ser autorizado su depósito.

La rama de conocimiento en la que esta tesis ha sido desarrollada es:

- Ciencias
- Ciencias Sociales y Jurídicas
- Ingeniería y Arquitectura

En Cartagena, a 18 de marzo de 2015

EL DIRECTOR DE LA TESIS



Fdo.: Toribio Fernández Otero

**COMISIÓN DE DOCTORADO**



**CONFORMIDAD DE DEPÓSITO DE TESIS DOCTORAL  
POR LA COMISIÓN ACADÉMICA DEL PROGRAMA**

D. Enrique Herrero Rodríguez, Presidente de la Comisión Académica del Programa Electroquímica. Ciencia y Tecnología.

**INFORMA:**

Que la Tesis Doctoral titulada, “Conducting polymer actuators: From basic concepts to proprioceptive systems.”, ha sido realizada, dentro del mencionado programa de doctorado, por D. José Gabriel Martínez Gil, bajo la dirección y supervisión del Dr. Toribio Fernández Otero.

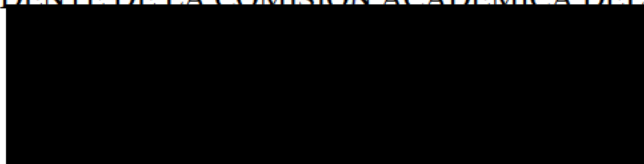
En reunión de la Comisión Académica de fecha 18/02/2015, visto que en la misma se acreditan los indicios de calidad correspondientes y la autorización del Director de la misma, se acordó dar la conformidad, con la finalidad de que sea autorizado su depósito por la Comisión de Doctorado.

La Rama de conocimiento por la que esta tesis ha sido desarrollada es:

- Ciencias
- Ciencias Sociales y Jurídicas
- Ingeniería y Arquitectura

En Alicante, a 11 de marzo de 2015

EL PRESIDENTE DE LA COMISIÓN ACADÉMICA DEL PROGRAMA



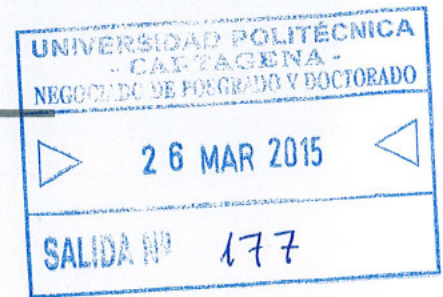
Fdo:-Enrique Herrero Rodríguez

**COMISIÓN DE DOCTORADO**





UNIVERSIDAD  
POLITÉCNICA DE  
CARTAGENA  
COMISIÓN DE DOCTORADO



**D. José Gabriel Martínez Gil**

Visto el informe favorable del Director de Tesis y el VºBº de la Comisión Académica para la presentación de la Tesis Doctoral titulada: **“Conducting polymer actuators: From basic concepts to proprioceptive systems”** en la modalidad de “compendio de publicaciones” solicitada por D. José Gabriel Martínez Gil, la Comisión de Doctorado de la Universidad Politécnica de Cartagena, en reunión celebrada el 26 de marzo de 2015, considerando lo dispuesto en el artículo 33 del Reglamento de Estudios Oficiales de Máster y Doctorado de la UPCT, aprobado en Consejo de Gobierno el 13 de abril de 2011 y modificado el 11 de julio de 2012,

**ACUERDA**

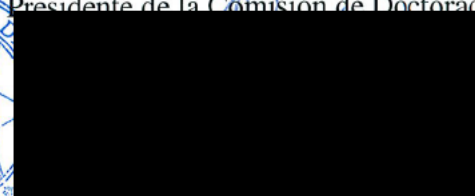
**Autorizar la presentación de la Tesis Doctoral a D. José Gabriel Martínez Gil en la modalidad de compendio de publicaciones.**

Contra el presente acuerdo, que no agota la vía administrativa, podrá formular recurso de alzada ante el Sr. Rector-Magnífico de la Universidad Politécnica de Cartagena, en el plazo de un mes a partir de la notificación de la presente.

Cartagena, 26 de marzo de 2015



El Presidente de la Comisión de Doctorado



Fdo.: Pablo Fernández Escámez



# Acknowledgements

The work exposed here would not have been possible without support of many other people. I would like to thank all of them. In order to do that, I will take the license to do it into the language I usually speak to them.

En primer lugar agradecer al profesor Toribio Fernández Otero, director de este trabajo. Me siento un total privilegiado al haber podido trabajar codo con codo con uno de los grandes. Gracias por confiar en mi desde un primer momento, incluso sin conocerme de nada. Y gracias también por el tiempo que me has dedicado. Espero haberlo aprovechado lo mejor posible y haber aprendido lo máximo.

Thanks to everyone who has worked in, or visited for different periods of time, our lab during this time. Joaquín, Gema, María, Laura, Mercedes, Inés, Angelita, Venancio, Pablo, Francisco, Bea, Juan, Yahya, Buket, Gonzalo, Bram, Sander, Rudolf, Masaki, Javi. From each of you I have learnt something. Thank you.

Thanks also to the staff members of the Biosensors and Bioelectronics centre from the Linköping University who welcomed me as if I was at home and made me feel warm despite the cold Swedish wintertime. I would like to devote a special mention to Edwin, my supervisor during my stay there and to Amy and Carlos, who gave me the opportunity to share a roof over our heads.

Thanks to the rest of our collaborators from other universities and centres around the world. Without all of you, some of the works would have just simply been impossible.

Gracias a Juan, Rosillo, Nani, Javo, Chema e Ismael, mis seis compañeros de Automática.

Gracias también a toda la gente que ha formado y forman parte de mi familia cartagenera: Pedro, Pablo, Paco, Carlos, Nacho, Juan, Rosillo, Lluís, Alicia, Silvia, Mamen, Almudena, Mercedes, Hugo, Manu, con los cuales he compartido mis estudios universitarios y todo lo que les rodea.



Gracias a Ana por aguantarme en buenos y malos momentos, y sobre todo por hacerme ver lo increíblemente afortunado que soy al poder dedicarme a lo que me apasiona.

Gracias también a los gorrinos calasparreños: Vero, Jota, Pulga, Rios, Torrente, Fernando, Edu, Bego,...

Gracias al ensemble La Danserye, mi familia musical: Fer, Juan Alberto, Luis y Edu. Motor y motivación constante, en música, ciencia, deporte...

Gracias a todos y cada uno de mis maestros y profesores por transmitirme cada uno parte de su conocimiento.

Gracias a todas las entidades que han financiado estas investigaciones: el Ministerio de Educación, Cultura y Deporte que me ha pagado mi salario durante los últimos años (AP2010-3460), to the ESNAM (European Scientific Network for Artificial Muscles) Cost Action MP1003, that funded my stay in Linköping, al Ministerio de Economía y Competitividad, y a la Fundación Séneca que financian y/o financiaron la compra de los reactivos y equipos que hacen posible nuestro trabajo y/o becas/contratos para los jóvenes investigadores, las cuales tuve la oportunidad de disfrutar durante mis primeros meses de tesis.

Gracias a todo el personal de la UPCT, por facilitarme la vida durante este tiempo, especialmente con las tediosas labores burocráticas y con la utilización de grandes equipos. Especial mención requieren las secretarias del departamento, Eva y Lilly; Yolanda, por su ayuda gestionando mi FPU; Ana y Marisa gestionando matrículas y papeleo que se requiere para ser alumno de doctorado y poder presentar esta tesis; y Alberto y María José, que han sido eficaces a la vez que didácticos con todos los grandes equipos del SAIT.

Y por último pero por ello no menos importante, a mi familia entera, que siempre están ahí dando todo el apoyo necesario y más. **Muy especialmente me gustaría agradecer a mis padres y a mi hermana por, simplemente, todo.**

¡Gracias! Thanks! Tack!

## Abstract

Designers and engineers have been dreaming for decades of motors sensing, by themselves, working and surrounding conditions, as biological muscles do originating proprioception. Here bilayer full polymeric artificial muscles were checked up to very high cathodic potential limits (-2.5 V) in aqueous solution by cyclic voltammetry. The electrochemical driven exchange of ions from the conducting polymer film, and the concomitant Faradaic bending movement of the muscle, takes place in the full studied potential range. The presence of trapped counterion after deep reduction was corroborated by EDX determinations giving quite high electronic conductivity to the device. The large bending movement was used as a tool to quantify the amount of water exchanged per reaction unit (exchanged electron or ion). The potential evolutions of self-supported films of conducting polymers or conducting polymers (polypyrrole, polyaniline) coating different microfibers, during its oxidation/reduction senses working mechanical, thermal, chemical or electrical variables. The evolution of the muscle potential from electrochemical artificial muscles based on electroactive materials such as intrinsically conducting polymers and driven by constant currents senses, while working, any variation of the mechanical (trailed mass, obstacles, pressure, strain or stress), thermal or chemical conditions of work. One physically uniform artificial muscle includes one electrochemical motor and several sensors working simultaneously under the same driving reaction. Actuating (current and charge) and sensing (potential and energy) magnitudes are present, simultaneously, in the only two connecting wires and can be read by the computer at any time. From basic polymeric, mechanical and electrochemical principles a physicochemical equation describing artificial proprioception has been developed. It includes and describes, simultaneously, the evolution of the muscle potential during actuation as a function of the motor characteristics (rate and sense of the movement, relative position, and required energy) and the working variables (temperature, electrolyte concentration, mechanical conditions and driving current). By changing working conditions experimental results overlap theoretical predictions. The ensemble computer-generator-muscle-theoretical equation constitutes and describes artificial mechanical, thermal

and chemical proprioception of the system. Proprioceptive tools and most intelligent zoomorphic or anthropomorphic soft robots can be envisaged.

# Contents

Acknowledgements .....	19
Abstract .....	21
Contents .....	23
List of figures .....	27
List of tables.....	29
List of acronyms and symbols .....	31
Objectives .....	35
State of the art .....	37
Present automatic control systems.....	37
Bio-inspired and bio-mimetic materials, elements and systems.....	40
Electrochemical reaction: The origin of biomimetic properties and devices .....	42
Artificial muscles: Classification .....	46
Models for the actuation of conducting polymer actuators.....	49
<i>Bending beam method</i> .....	50
<i>Finite elements method</i> .....	50
<i>Equivalent transmission line model</i> .....	51
<i>Faradaic behaviour of conducting polymer actuators</i> .....	51
<i>Conformational movements suffered by the polymeric chains influence         the material electrochemical response: Electrochemically Stimulated         Conformational Relaxation (ESCR) model</i> .....	53
Experimental variables affect the electrochemical reaction.....	55
Experimental.....	59
Materials.....	59
Generation of conducting polymer .....	60
<i>Chemical polymerization</i> .....	60
<i>Electrochemical polymerization</i> .....	61
Construction of actuators (Bilayers).....	62
Physical Characterization .....	64
<i>Fourier transform infrared spectroscopy (FTIR)</i> .....	64

<i>Scanning electron microscope (SEM)</i> .....	65
Electrochemical characterization.....	65
<i>Cyclic voltammetry</i> .....	66
<i>Coulouvoltammetry</i> .....	67
<i>Chronoamperometry</i> .....	68
<i>Chronopotentiometry</i> .....	69
Mechanical characterization of the actuators .....	70
<i>Video recording of actuators' movement</i> .....	70
Publications.....	73
‘Biomimetic electrochemistry from conducting polymers. A review. Artificial muscles, smart membranes, smart drug delivery and computer/neuron interfaces’.....	73
<i>Experimental</i> .....	73
<i>Results and achievements</i> .....	73
‘Artificial Muscles: A Tool To Quantify Exchanged Solvent During Biomimetic Reactions’ .....	74
<i>Experimental</i> .....	74
<i>Results and achievements</i> .....	75
‘Ionic exchanges, structural movements and driven reactions in conducting polymers from bending artificial muscles’ .....	78
<i>Experimental</i> .....	78
<i>Results and achievements</i> .....	79
‘Structural Electrochemistry: Conductivities and Ionic Content from Rising Reduced Polypyrrole Films’ .....	81
<i>Experimental</i> .....	81
<i>Results and achievements</i> .....	82
‘Effect of the Electrolyte Concentration and Substrate on Conducting Polymer Actuators’ .....	85
<i>Experimental</i> .....	85
‘Biomimetic Dual Sensing-Actuators Based on Conducting Polymers. Galvanostatic Theoretical Model for Actuators Sensing Temperature’ ....	89
<i>Experimental</i> .....	90
<i>Results and achievements</i> .....	90

**Conducting polymer actuators: From basic concepts to proprioceptive systems.**

‘Biomimetic Dual Sensing-Actuators: Theoretical Description. Sensing Electrolyte Concentration and Driving Current’ .....	93
<i>Experimental</i> .....	93
<i>Results and achievements</i> .....	94
‘Mechanical awareness from sensing artificial muscles: Experiments and modeling’ .....	96
<i>Experimental</i> .....	96
‘Structural Electrochemistry. Chronopotentiometric Responses From Rising Compacted Polypyrrole Electrodes: Experiments and Model’ .....	99
<i>Experimental</i> .....	99
<i>Results and achievements</i> .....	100
‘Physical and chemical awareness from sensing polymeric artificial muscles. Experiments and modeling’ .....	102
<i>Experimental</i> .....	103
<i>Results and achievements</i> .....	103
‘Polyurethane microfibrinous mat template polypyrrole: Preparation and biomimetic reactive sensing capabilities’ .....	105
<i>Experimental</i> .....	105
<i>Results and achievements</i> .....	105
‘Fibroin/Polyaniline microfibrinous mat. Preparation and electrochemical characterization as reactive sensor’ .....	107
<i>Experimental</i> .....	107
<i>Results and achievements</i> .....	108
Conclusions .....	109
References .....	113
Annex I: Papers.....	135
Annex II: Justification of impact.....	257



## List of figures

Figure 1: Scheme of an open-loop control system.....	38
Figure 2: Scheme of a closed-loop control system.....	40
Figure 3: Scheme of a proprioceptive system. ....	41
Figure 4: Conformational movements in conducting polymers. (a) Fully oxidized polymeric film. (b) Polymeric film at the beginning of the oxidation. ....	46
Figure 5: Electrochemical cell employed to study a bilayer conducting polymer/non-conducting polymer film artificial muscle.....	49
Figure 6: Artificial muscles based on electrochemical reactions (1) or (2) have proprioceptive properties. ....	57
Figure 7: Initiation of the polymerization in pyrrole monomers. ....	60
Figure 8: Polymerization of polypyrrole. ....	60
Figure 9: Three electrodes electrochemical cell employed during the electrochemical experiments. ....	61
Figure 10: Fabricating a bilayer artificial muscle: (a) Electrogenerated conducting polymer film; (b) Cutting the borders; (c) Removing the conducting polymer film from the metallic electrode used during the electrogeneration; (d) Free-standing conducting polymer film; (e) Cutting a smaller sample; (f) Small free-standing conducting polymer film ready to fabricate the bilayer; (g) Attaching the free-standing polymer film to the conventional tape; (h) Mechanical pressure over the bilayer to ensure the proper attachment; (i) Cutting the borders of the tape; (j) Removing the isolating parts not attached to the bilayer; (k) Bilayer artificial muscle; (l) Ensuring the electrical contact with a metallic clamp; (m) Painting the bilayer artificial muscle with paint to fill the pores and avoid the electrolyte contact with the metallic clamp by capillarity; (n) Electrochemical cell used during bilayer artificial muscle actuation. (n') scheme of the connections of the electrochemical cell.....	64
Figure 11: Cyclic voltammetry. (a) Symmetrical triangular potential wave applied to the working electrode. (b) Measured current when the potential wave in (a) is applied. (c) Cyclic voltammogram. ....	67
Figure 12: Coulovoltammetry. (a) Cyclic voltammogram. (b) Coulovoltammogram.....	68
Figure 13: Chronoamperometry. (a) Potential applied to the working electrode (referred to the reference electrode). (b) Measured current flowing through the working electrode during potential steps shown in (a).....	69



Figure 14: Chronopotentiometry. (a) Applied current versus time. (b) Measured potential evolution versus time when current from (a) was applied. ....	70
Figure 15: Electrochemical cell and angle described by a bilayer artificial muscle recorded by a video camera. Two frames in different moments of the movements were overlapped. ....	71
Figure 16: Bending movement in a bilayer artificial muscle based on electrochemical reactions on conducting polymers with reversible solvent molecules and counterions exchange. ....	76
Figure 17: Electrochemical setup for the study of length variations in free-standing films under electrochemical reactions. The mechanical measurements are performed in the inner part of an electrochemical cell designed for 'in situ' measurements. ....	79
Figure 18: Electrochemical reaction (1). ....	83
Figure 19: The laser scanner (LSM) set-up: 1. PC running GPES software, 2. Potentiostat, 3. LSM display unit, 4. Electrode support table, 5. LSM, 6. Lab jack, 7. Electrochemical cell. ....	87
Figure 20: Attached steel masses during the study of the effect of the different masses in the proprioceptive properties of conducting polymers. .	97
Figure 21: Experimental procedure followed to obtain the experimental responses: (a) In order to erase any previous structural memory, the free-standing electrode was submitted a potential of -0.5 V for 60 s, then the potential was stepped to 0.5 V kept during 60 s and then the potential was stepped again to the reduction-compaction potential (usually -0.9 V) for 60 s. (b) Chronoamperometric responses to those potential steps. Finally, a constant current of 0.5 mA was applied (c) during 100 s to obtain the chronopotentiometric responses (d). ....	100

## List of tables

Table 1: Bio-mimetic properties of conducting polymers that are driven by the electrochemical reaction, mimicked biological functions and related organs.....	44
---	----



## List of acronyms and symbols

$\alpha$	Angle
$\alpha'$	Electrochemical symmetry factor
$\alpha_0$	Initial angle
$\lambda$	Length of an elemental polymeric chain
$\eta$	Oxidation overpotential
$\eta_c$	Applied reduction overpotential related to the closing potential
$\tau$	Time constant
$\tau_0$	Pre-exponential factor of the relaxation time
$\kappa$	Constant characteristic of every electrolyte
$\nu$	Scan rate
$\omega$	Angular rate
$\Lambda_m$	Molar conductance
$\Lambda_m^0$	Molar conductance at a very low concentration
$\Delta$	Variation
$[A^-]$	Concentration of anions
$[Pol^*]$	Concentration of active centres
$A$	Area of the polymer film
$A^-$	Anion
active	Relative to the active part
AFM	Atomic force microscopy
APS	Ammonium persulfate
ATP	Adenosine triphosphate
ATR	Attenuated total reflectance
$C^+$	Cation
$C_1$ and $C_2$	Impedance constant
CE	Counterelectrode
CP	Conducting polymer
$D$	Diameter
$d$	Reaction order related with the concentration of anions in solution
DBS	Dodecylbenzenesulfonate
E	Electrical potential
$e$	Reaction order related with the concentration of active centres in the polymer
$e^-$	Electron

$E_0$	Standard potential
$E_{\text{ini}}$	Initial potential
ECM	Extracellular matrix
EDX	Energy dispersive X-ray spectroscopy
ESCR model	Electrochemically stimulated conformational relaxation model
EQCM	Electrochemical quartz crystal microbalance
$F$	Faraday constant ( $F=96485 \text{ C mol}^{-1}$ )
film	Relative to the full CP film.
FTIR	Fourier transform infrared spectroscopy
gel	Gel
$H$	Energy of the system in absence of any electric fields
$h$	Thickness
H <sub>2</sub> O	Relative to water molecule
$I$	Constant electrical current
$i$	Electrical current
$i_0$	Initial current
ICM	Intracellular matrix
$i_d$	Diffusion current
$i_{\text{EDL}}$	Electrical double layer current
if	At the interface
ion	Relative to the ion
IR	Infrared
$i_r$	Relaxation current
$K$	Constant, relationship between angle and consumed charge for bending artificial muscles
$k$	Reaction's rate constant or rate coefficient
$K_0$	Pre-exponential factor
$l$	Length
LiTFMS	Lithium trifluoromethanesulfonate
LSM	Laser scan micrometre
M	Monomeric unit
m	Mass
$M^{\bullet+}$	Radical cation
$MA^-$	Macroanion
MSA	Methane sulfonic acid
$N$	Number of counterions
$n$	Number of charges
$n'$	Relative number of solvent molecules
$N_0$	Number of oxidation nuclei

**Conducting polymer actuators: From basic concepts to proprioceptive systems.**

$N_A$	Avogadro's number ( $N_A=6.022 \times 10^{23} \text{ mol}^{-1}$ )
PANI	Polyaniline
$P$	Pressure
$p_n(t)$	Unitary pulse function
$Pol^0$	Neutral polymer chains
$Pol^*$	Active centres on polymeric chains
PPy	Polypyrrole
PPy-DBS	Polypyrrole-dodecylbenzenesulfonate
PU	Polyurethane
PU/PPy	Polyurethane/polypyrrole
$Q$	Total consumed charge
$Q_d$	Diffusion charge
$Q_r$	Relaxation charge
$R$	Universal gas constant ( $R=8.314 \text{ J K}^{-1} \text{ mol}^{-1}$ )
$r$	Reaction rate
$R_0$	Initial curvature radius
$R_\infty$	Curvature radius at the equilibrium
$S$	Solvent molecules
$s$	Solid
SEM	Scanning electron microscope
$T$	Temperature
$t$	Time
$U$	Electrical energy
UV-vis	Ultraviolet-visible spectroscopy
$V$	Volume
WE	Working electrode
$x$	vertical displacement
$Y$	Young's modulus
$Z$	Impedance
$z$	Valence
$z_c$	Charge consumed to compact one mole of polymeric segments
$z_r$	Charge required to relax of one mole of polymeric segments



# Objectives

During reaction, conducting polymers immersed in solution change their composition in a reversible way. Such changes promote variations in several biomimetic properties (volume, conductivity, colour...). Some of them may change simultaneously announcing new multi-functional biomimetic devices: several tools working simultaneously under reaction control in one device. A new field is open here, where only one physically uniform device is needed to perform several simultaneous actions. This possibility is explored here using electro-chemo-mechanical actuators mimicking the consecutive events occurring in natural muscles. While they produce a mechanical effect, they will sense, simultaneously, working physical and chemical conditions. The study and clarification of such simultaneous actuating-sensing (proprioceptive) properties will allow the development of simpler, cheaper and more reliable systems. In order to be able to attain a general acceptance and use of these novel multi-functional devices, a better understanding of the processes occurring in the material under influence of different variables and the development of reliable models is required. These are the aims of this thesis.

Specific objectives of this thesis are:

- To update the state of the art (kind of actuators, sensors and models).
- To study how the composition evolves during actuation in actuators constituted by different families of conducting polymer.
- To study how the ion exchanged by the conducting polymer during reaction driven actuation influences the polymer volume changes.
- To study how the conductivity evolves during mechanical actuation in conducting polymers in the full operating range.
- To check how peripheral elements such as the metallic background present nowadays in most of actuators influence both, actuation and lifetime.
- To check how the temperature affects the actuating and electrochemical responses from conducting polymers.
- To develop a model able to explain the electrochemical behaviour of conducting polymers at different temperatures.
- To check how the electrolyte concentration affects the actuating and electrochemical responses from conducting polymers.
- To develop a model able to explain the electrochemical behaviour of conducting polymers in different electrolyte concentrations.



- To check how the applied current affect the actuating and electrochemical responses from conducting polymers.
- To develop a model able to explain the electrochemical behaviour of conducting polymers after applying different constant currents.
- To check how the mechanical conditions affect the actuating and electrochemical responses from conducting polymer actuators. To check bilayer artificial muscles carrying different attached masses.
- To develop a model able to explain the electrochemical behaviour of conducting polymer actuators carrying different attached masses.
- To check how the initial state of the conducting polymer affects its electrochemical responses.
- To develop a model able to explain the electrochemical behaviour of conducting polymers from different initial states.
- To establish the basics of a full model able to explain the full electrochemical behaviour of conducting polymers originating multi-functionality.
- To check the validity of such model with new materials.

# State of the art

Designers and engineers have been dreaming for decades of motors sensing, by themselves, working and surrounding conditions, as biological muscles do. Thus, one physically uniform device must include one actuator and several sensors working simultaneously. In this case, the information from the sensors must be contained in the same two connecting wires used for the actuator feeding: both, actuating and sensing information should be simultaneously read/applied by the computer at any time. Using this technology, simpler systems with fewer connections and faster responses can be designed. A lower number of components and connections means cheaper and more reliable systems [1,2].

## Present automatic control systems

In the control process-engineering field, a process is a set of interrelated tasks that, together, transform inputs into outputs. Such processes (transformations) can be carried out by actuators using resources [3]. An actuator is a device able to transform one kind of energy into a different one to modify a process. Thus, mechanical actuators, as those treated in this work, transform the input energy (electrical, chemical, electrochemical, optical, magnetic, and so on) into mechanical energy output. Actuators can be people (worker), nature (i.e. sun for heating), or machines. Those processes where only machines are employed are automatic processes. Actuators are used in a huge number of applications in our everyday life [4].

The introduction of the assembly lines was a remarkable milestone in the history of industry. It allows large productions of standardized commodities saving money and increasing the quality of the products. Very specialized and repetitive processes are the basic elements where human errors can produce waste of incomes [5]. Automatic processes decrease or eliminate such errors with parallel increase of the productivity and quality of the commodities. They use machines to perform the repetitive work without any direct human intervention. In this case, human work is only needed for high-level supervision tasks [3].

Thus, the simple process of keeping a comfortable temperature in a room can be considered as a reference. This can be done by a person who turns the heater on and off according to his own feelings or without the direct

human interaction using an automatic system. The automatic control of a process can be made by means of an open-loop system or using a closed-loop (feedback control) system [6,7]. The open-loop systems (Figure 1) control a process through the perfect knowledge of the process. The elements of the open-loop systems are:

- Input: signal equivalent to the desired result of the process.
- Controller: element that according with the input generate the proper signal to get the desired final result of the process.
- Control signal: signal offered by the controller that applied to the actuator is expected to transform the process to reach the desired final result.
- Actuator: element transforming the energy from the control signal into another kind of energy, modifying the process.
- Output: result of the process.



Figure 1: Scheme of an open-loop control system.

Back to the example, it is possible to calculate the heat losses through the walls, windows, doors of the room, etc.; and from those losses, the energy that the heater must produce to compensate such losses. The controller's designer includes the calculation program in the controller. When an input equivalent to the desired temperature is given to the system, the controller is able to calculate the energy that the actuator must produce to keep the desired temperature. That information (control signal) is applied to the heater (actuator) that produces the required thermal energy (output) to maintain a constant comfortable room temperature.

But, if someone opens the door heat losses increase and the room temperature decreases. The original program didn't include those losses. Thus, temperature drops. This kind of system is commanded only by the applied input, not considering the real output so they are not able to compensate unexpected disturbances coming from the process itself or from missed elements during the controller design. In open loop systems every input is related with a unique control signal, so a unique effect of the actuator. Thus, the output of the system depends on the proper calibration of the system and the absence of any unknown, or undesired, disturbance. When this occurs, which is very common in real applications, the output can

be any (not the desired one), depending on, besides in input, the disturbances.

Such possible disturbances typical of real systems (someone opening the door of the room, for example) can be corrected considering the real output. This is possible through the inclusion of sensors/transducers able to quantify variables in the systems and convert them to make them understandable by the rest of the components in the system [7]. If there is a temperature sensor in the room, the value of such temperature is relevant information that can be used for the system to perform a better control. Thus, the control system becomes a closed-loop control system, Figure 2, where the output (room's temperature) has an effect in the process (energy consumed by the heater). In this way, if the temperature is lower than the desired value, a greater energy can be applied to the heater to compensate such difference.

In this kind of systems, the input is the desired output (or a signal equivalent to it, understandable for the controller). The real output, quantified and adapted by a sensor is compared with the desired output resulting in an error signal (difference between the desired output and the real one). The controller tends to minimize such errors using the available actuators in the system. If the error is null, the actuators do nothing. Closed-loop systems are less sensitive to errors in the design, noise, disturbances and changes in the environment than open-loop systems as they are able (if they are properly designed) to correct them by themselves. Besides, it is not needed to know the process as well as in the case of open-loop systems where everything needs to be known. In fact, there are some techniques that allow, using some very primitive models, to obtain a model able to fulfil the imposed control requirements from some very easy experiments [8]. However, they also have some disadvantages, being closed-loop systems usually more expensive and complex, containing more elements than open-loop systems with the subsequent increment in costs and probability of failures.

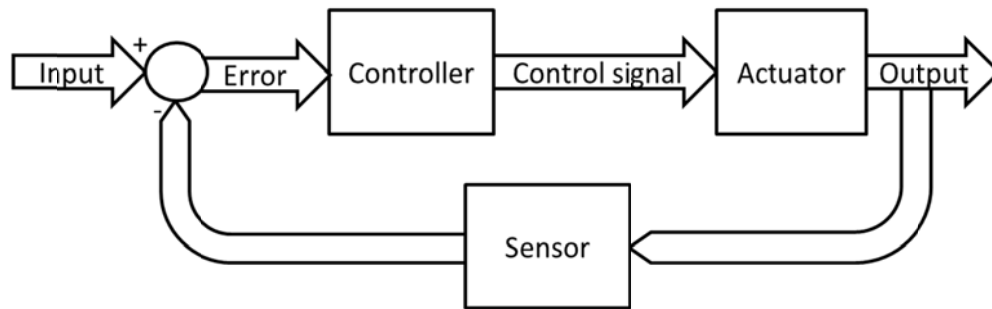


Figure 2: Scheme of a closed-loop control system.

Commercial electronics are cheaper and faster every day [9]. This has influenced automatic control systems, allowing more complex designs every day. Most of them have become closed-loop systems including hierarchical and complex structures with many controllers and a huge number of sensors, actuators, controllers, connections and interfaces. This allows advanced control of the processes able to predict failures, to save energy, to make it faster, cheaper,...[10] For this reason, it is very important to develop new components (actuators, sensors, controllers, connections, interfaces,...) able to reduce costs and failures.

Actuators and sensors are the elements of a control system requiring more resources in both, initial investment and energy feeding and maintenance due to the great number of them used. So far, every sensor is an independent device needing, at least, two cables for their electrical connection to close the electrical circuit and transmit the information. However, in most of the cases, four cables are needed for their connection: two of them to transmit the information of the measured signal in a closed electrical circuit and another two to feed (with energy) the sensor in a different closed electrical circuit. Great efforts are being made in order to simplify the sensing systems: reducing the complexity of the sensor networks [11–13], making sensors smaller [14–18] and more efficient [19], or without the need of wires for their connection [11,12,20–23].

## **Bio-inspired and bio-mimetic materials, elements and systems**

Motors sensing by themselves working and surrounding conditions could simplify present systems, reducing the number of components and making systems simpler and cheaper. When a human being moves an object grasped in his hand, he knows the object (hand) position at any time related to any other part of his body, the rate and direction of the movement, the presence

of obstacles in its way, if he can displace the obstacle or not, the force and energy that he must produce to move it and so on, even if he does not see the object while he is moving it. This kind of awareness is known as proprioception [24,25]. Proprioception is based on haptic muscles: muscles sensing by themselves the working mechanical conditions. Developing proprioceptive artificial systems require devices able to actuate and sense (employing a unique uniform device) simultaneously, as biological systems do. Thus, in artificial proprioceptive control systems actuators should sense by themselves surrounding and working conditions. Besides, the information must flow two ways simultaneously: actuating signal from the generator to the actuator and sensing signals from the actuator-sensor to the controller, figure 3. Related to figure 2, this configuration would save components and connections, allowing a simpler, cheaper and more reliable system. Returning to the example of the control of room temperature, in the new system the heater should be, simultaneously, the temperature sensor providing information that can be used by the controller.

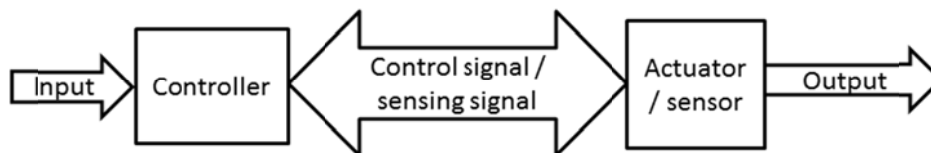


Figure 3: Scheme of a proprioceptive system.

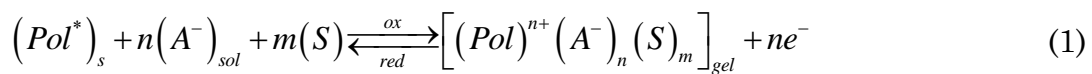
Automatic systems inspired by biological systems (bio-inspired) are being developed nowadays trying to imitate organs, functions, or parts of them from living beings (and their advantages). They cover the full range of design: from full system (robots [26–30], drug delivery systems [31], energy conversion systems [32,33], actuators [34],...) to individual components (as sensors [35–37], sensor networks [20,38], controllers [40],...) and even the materials used to build the different components [40–47]. However, while biological organs are constituted by soft, wet and reactive materials, those bio-inspired systems are based on hard and dry materials having a constant composition during actuation and working by change of the material physical properties.

A second family of bio-mimetic systems are based on new materials mimicking properties from living cells. The extracellular matrix (ECM) of the cells (external coverage of the living cells) is being successfully imitated by several kinds of materials allowing very high biocompatibility so living cells can grow on them, adhere, proliferate, etc. on their surface [48–55]. This is broadly used at the present in biomedicine for prosthesis [56–58].

On the other hand, materials mimicking the processes occurring in the inner part of the living cells (intracellular matrix, ICM) are aimed to be successfully imitated. The reactions occurring in the ICM are responsible for their actuation, sensing (proprioception) and self-repairing properties. They involve reactive macromolecules, conformational movements, ionic exchange and solvent [59]. Recently it has been proposed that new reactive materials (most as gels) can be considered, during reactions, as biomimetic material models mimicking, in its simplest expression, the ICM [60,61]. They are available from different carbon based materials such as conducting polymers, porphyrines, carbon nanotubes or graphenes. When they are immersed in solution, they are capable of react reversibly. Such reaction makes them soft and wet biomimetic materials, including polymer chains (macromolecules), ions and solvent that reacts and changes their composition and properties in a continuous way for several orders of magnitude when the reaction evolves. This thesis is focused in the study of bio-mimetic proprioception (dual sensing-actuating properties) with reactive bio-mimetic conducting polymers. A change from dry materials which composition is constant to wet reactive materials would allow the development of more efficient systems.

## Electrochemical reaction: The origin of biomimetic properties and devices

The reversible oxidation/reduction reactions involving conducting polymer materials include reactive macromolecules, conformational reaction driven chain movements, ionic and solvent exchange (as in the ICM). For CPs exchanging anions it can be written in a very simplified version as [62]:

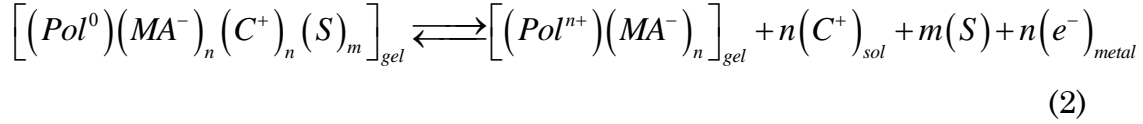


where the different sub-indexes mean: s, solid; sol, solution; Pol\* represents the active sites on the neutral polymer film, understood as those points on the conducting polymer chains where a positive charge will be present after removing electrons from the neutral chains during oxidation; A<sup>-</sup> represents the anions exchanged between the film and the electrolyte to keep the electroneutrality inside the material; S represents solvent molecules exchanged for osmotic pressure balance forming a dense polymeric gel (indicated by the sub index gel) and n represents either: the number of electrons (e<sup>-</sup>) removed from each of the polymeric chains during oxidation (injected during reduction) or the number of monovalent anions (A<sup>-</sup>)

### Conducting polymer actuators: From basic concepts to proprioceptive systems.

penetrating from (or expelled to, during reduction) the solution to keep the electroneutrality in the gel.

Other families of conducting polymers exchange cations during oxidation/reduction reactions [63]:



where  $MA^-$  represents any macroscopic anion (organic, polymeric or inorganic) trapped inside the CP material during its polymerization and  $C^+$  represents a cation required to balance the charge of the trapped macro-anion.

In both cases, the gel composition (polymer-ions-solvent relative content) is given at any time by the value of  $n$  (number of electrons extracted during oxidation). The value of  $n$  is given by the consumed charge during oxidation/reduction (forward/backward) reactions (1) or (2):

$$n = Q \frac{N_A}{F} \quad (3)$$

being  $Q$  the consumed charge (C),  $N_A=6.022 \times 10^{23} \text{ mol}^{-1}$  is the Avogadro's constant and  $F$  is the Faraday's constant ( $F=96485 \text{ C mol}^{-1}$ ).

Different values of  $n$  result in different gel composition that means different materials, each of them with different properties. The composition change is one, among several biomimetic properties from the CP, the value of which changes in a continuous and reversible way driven by reactions (1) or (2): composition dependent properties. Those reversible changes in the biomimetic properties allow the development of biomimetic actions, organs (biomimetic artificial devices) and other artificial devices collected by table 1 [64].



Property	Action	Inspired organ	Other artificial devices
Electrochemomechanical	Change of volume	Muscles	
Electrochromic	Change of colour	Mimetic skins	Smart windows and mirrors
Charge storage	Current generation	Electric organs	Smart batteries
Chemical or pharmacological storage	Chemical modulation or chemical dosage	Glands	Chemical dosage / drug delivery
Electron/neurotransmitter	Channel V action	Nervous interface	
Electroporosity (permselectivity)	Transversal ionic flow	Membrane	
Electron/ion transduction	Potential variation (Chemical/Physical properties)	Bio-sensors	

Table 1: Bio-mimetic properties of conducting polymers that are driven by the electrochemical reaction, mimicked biological functions and related organs. Reproduced from [64] with the permission of Elsevier.

Each of the composition dependent properties can be exploited to develop a different family of actuators. Thus, reversible colour changes in thin films allows to build smart windows, mirrors and glasses [65–68]; reversible changes in the stored charge allows the development of polymeric batteries [69–71]; the ability to store and deliver chemical ions allows to develop smart drug delivery systems [72–75]; when those chemicals are neurotransmitters, nervous interfaces for artificial chemical synapses can be developed, suitable to communicate artificial electronics systems and neurons [76–81]; the reversible variation of the inter and intra-chain distances during reactions (1) or (2) allows designing and building smart membranes with reversible control of the transversal ionic conductivity [82–86]; the changes experienced into the chemical equilibrium allow the development of sensors [87–93] and reversible film volume changes allows artificial muscles to be built [94,95].

The previous paragraph includes a traditional technological development procedure. Now new unexpected and unparalleled technological possibilities are open. Properties from table 1 may change simultaneously

during electrochemical reactions (1) or (2). This fact can be used for the development of new multi-functional devices where two, or more tools, work simultaneously by exploiting the simultaneous change of two or more composition dependent properties. Some preliminary empirical results have been advanced in this field as dual sensor-actuators: artificial muscles sensing chemical working conditions[96–100], muscles sensing thermal conditions[96,98,100,101], muscles sensing mechanical conditions as trailed masses [96,97] or the presence of obstacles giving tactile muscles[102]; Vidal et al. have reported the development of dual electrochromic (UV-vis or IR) artificial muscles [103].

From now on this thesis will be focused on the study, control and modelling of the simultaneous volume (giving mechanical actuators, artificial muscles or polymeric motors) and the muscle potential variation (giving mechanical, chemical, thermal or electrical sensors) driven simultaneously by the electrochemical reaction, or reactions, of the CP film (or films) constituting the sensing-muscle. The final aim is the construction of artificial devices mimicking haptic muscles and one of its most fascinating properties: proprioception.

Focussing now on reaction (1) reversible volume variations are originated and controlled by the reversible CP oxidation/reduction [similar concepts can be applied to reaction (2)]. The flow of an anodic current through the material immersed in an electrolyte originates the extraction of electrons from the polymeric chains generating radical-cations (polarons) along the chains. Electrostatic repulsion forces between neighbour polarons generate conformational movements of the polymeric chains getting free volume. Instantaneously the new volume will be occupied by counterions ( $A^-$ ), in order to keep the material electroneutrality (polaron-anion), and solvent in order to keep the osmotic pressure balance in the resulting dense gel. The final result is conformational and macroscopic volume variations driven by reaction (1), figure 4. Summarizing: an electronic pulse promotes an electrochemical reaction driving chain conformational movement, ionic and aqueous exchange and film volume variations.

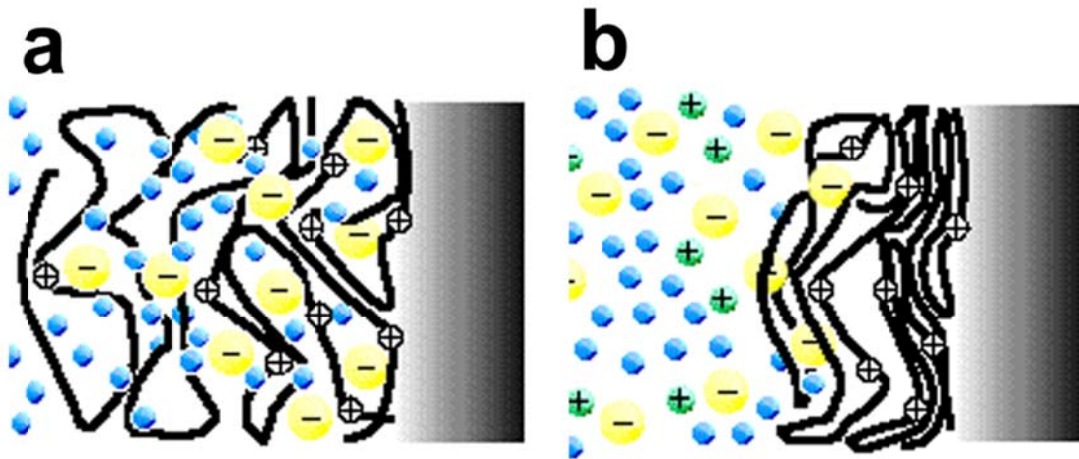


Figure 4: Conformational movements in conducting polymers. (a) Fully oxidized polymeric film. (b) Polymeric film at the beginning of the oxidation.

Similar stages occur during activation of natural muscles in mammals: an electric pulse arriving from the brain to the muscle through the nervous system promotes liberation of calcium ions inside the sarcomere, chemical reactions (ATP hydrolysis) and conformational changes along the natural polymeric chains (actin and myosin) and water exchange originating the sarcomere contraction [104,105].

Artificial muscles [63,94,95,106] include, mimicking natural muscles, electric pulses, polymeric chains, aqueous solutions, ionic exchanges, volume variations and strain and stress changes. In the 1950s, some pioneering devices were constructed employing films of ionic conducting polymer gels in aqueous solutions [107–109]. After that, only a few works [110–112] were performed in the field until 1992, when the term ‘artificial muscle’ was first employed. In that year, papers from two different research groups appeared presenting artificial muscles or polymeric actuators from conducting polymers: Prof. Otero’s group [94] and Prof. Inganäs’ group [95,106].

## Artificial muscles: Classification

The term artificial muscle has been employed since then to designate a wide variety of polymeric actuators. In broad terms, two different families of mechanical actuators can be differentiated [64,113]:

- Electromechanical actuators [99,114–117]: they are based on electroactive and electronic insulator polymers able to move under the effect of a very high electric field. The dimensional variation is proportional to the square of the electric field (for electrostrictive actuators) or following a linear dependence from the applied electric

## Conducting polymer actuators: From basic concepts to proprioceptive systems.

field. In electromechanical actuators, the polymeric chains do not participate in any chemical reaction during actuation; only physical effects are present reorganizing the physical structure of the material.

- Electrochemomechanical actuators [61,99]: they are based on reactive materials, as conducting polymers, which dimensions change driven by chemical reactions involving the polymer chains as reactants. Under electrochemical driven reactions the dimensional variations of the material are produced (and perfectly controlled) by the electrochemical reaction [as reactions (1) or (2)].

This thesis is focused on electrochemomechanical actuators based on conducting polymers. From now on, the terms artificial muscles, actuators or polymeric motors refer to electrochemomechanical actuators based on reactions (1) or (2). The electrochemical reaction shifts simultaneously the magnitude of different material properties (Table 1). The development of simultaneous actuating and sensing properties will be here studied broadly in order to explore the possibility of getting and modelling dual sensing-actuators mimicking haptic muscles.

A conducting polymer film itself (free-standing film) is the simplest actuator. Electrochemical reactions (1) or (2) promote volume variations (along each of the three dimensions, figure 4). By focusing on the variation of only one of the three dimensions, linear actuators are obtained [118–121].

In order to study and characterize the CP oxidation/reduction [reactions (1) or (2)] driven actuation, different electrochemical techniques such as: potential sweeps (cyclic voltammetry) [122–125], square potential steps (chronoamperometry) [122,126–128] or square current steps (chronopotentiometry) [129,130] have been used. Volumetric and dimensional variations also are being characterized by the simultaneous (to the electrochemical) use of different techniques as: in situ AFM [131–134], laser scan micrometers [135] to study thickness variations, universal mechanical test machines to study length variations (or strains and stresses produced by the polymer) [122–125,129,130], or lasers [136–138] to measure small displacements.

Experimental results reveal that the reaction driven [by reactions (1) or (2)] volume changes depend on different factors such as: the used conducting polymer, the dopant [138–140], the conditions used during the CP synthesis [63] or the electrolyte and solvent [141] used during the actuator control, among others. Different strategies were used to improve the properties of such kind of primitive actuators as optimization of the CP synthesis

conditions [63], by including metal (sputtered) layers in the actuator trying to increase its electronic conductivity [142], by obtaining (by extrusion) fibres of conducting polymers [124] or covering any background fibre with a conducting polymer by chemical polymerization [143].

Dimensional variations of actual linear actuators are still quite low, suitable for microscopic devices but not applicable to real macroscopic devices.

One of the simplest ways to convert the small local volume changes suffered by the conducting polymer during reactions (1) or (2) into macroscopic movement is through multilayer bending structures. The simplest one is a bilayer structure (figure 5). The device is composed by two layers: one active layer (conducting polymer) changing its volume under control of the electrochemical reaction and a passive (non-reactive) layer keeping constant its volume, both properly adhered to avoid glissades, peel-off and efficiency loss. Thus, electrochemically induced local length variations in the active layer promote a stress gradient between the two layers and subsequently a bending motion. The direction (clockwise or anticlockwise) of the movement depends on the sense of the conducting polymer film length variation during reaction due to the prevalent ionic exchange (anions or cations). Conducting polymers with a prevalent exchange of anions [following reaction (1)] swell by oxidation, pushing the non-reactive layer towards the concave side of the bending motion. Conducting polymers with prevalent cation exchange [following reaction (2)] shrink during oxidation, pulling the non-reactive layer towards the convex side of the bending movement. Having the same relative position of the active and passive layer actuators exchanging anions or cations move in opposite sense (i.e. clockwise vs anticlockwise) during the CP oxidation. Opposite movement is attained during the active layer reduction in both cases: polymers exchanging anions shrink, trailing the non-reactive layer, while polymers exchanging cations swell pushing the non-reactive layer. Different passive layers have been used: commercial available tapes [94,95,144,145], sputtered metals [146–148], a piece of paper [149,150], plastic films [151] or solid electrolyte membranes [152,153].

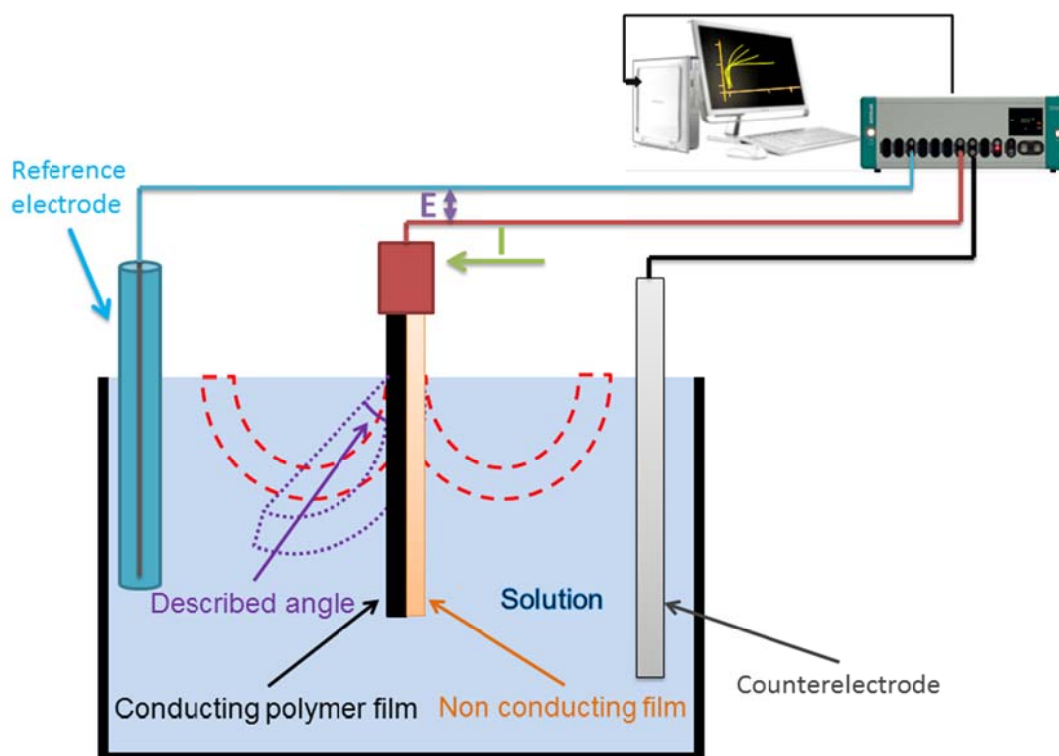


Figure 5: Electrochemical cell employed to study a bilayer conducting polymer/non-conducting polymer film artificial muscle.

For the electrochemical control and characterization of those bilayer actuators, or of free-standing films of conducting polymers, a metal counterelectrode (CE) is required to close the electrical circuit allowing the current flow that promote reactions (1) or (2) in the CP film (Figure 5).

Moreover bilayer structures, trilayer actuators conducting polymer film-support (passive) film-conducting polymer film allow the connection of one of the CP films to the working electrode (WE) and that of the second CP film to the CE, the current flowing by the cell is used two times to produce reverse volume variations. [98,154–158].

## Models for the actuation of conducting polymer actuators

In order to use extensively conducting polymer actuators, models able to fulfill control requirements are needed. Some models have been developed for the study of mechanical and dynamic properties of actuators:

### ***Bending beam method***

The analogy existing between a bending artificial muscle and a solid-state bending beam can be used to attempt modelling the mechanical behaviour of bending bilayer and multilayer artificial muscles from conducting polymers [159,160].

This mechanical model assumes several characteristics related with the study of traditional mechanical bending beam: (I) the thickness of the beam is small compared to the minimum radius of curvature, (II) a linear relationship exists between stress and strain of the material and (III) the Young's modulus,  $Y$ , and the actuation expansion coefficient of the conducting polymer, keep constant: they do not depend on spatial location inside each layer.

The actuator curvature radius ( $R_\infty$  is the radius at the equilibrium and  $R_0$  is the initial radius) is related to either, the Young's modulus ( $Y$ ) and the thicknesses ( $h$ ) of the conducting and non-conductive films (indicated by subscripts 1 and 2 respectively), and to the volume changes locally produced at the interface between both films  $\Delta V_{if}$  [106,161,162]:

$$\frac{1}{R_\infty} - \frac{1}{R_0} = \frac{6\Delta V_{if}}{\frac{(Y_1 h_1^2 - Y_2 h_2^2)^2}{Y_1 Y_2 h_1 h_2 (h_1 + h_2)} + 4(h_1 + h_2)} \quad (4)$$

The basis of this model has been used to improve its features. Christophersen et al. [163] expanded the model by including strain and modulus variations along the direction of film thickness. Actuator's position, rate of the movement and force generated by the actuator [154,164] were simulated and applied to the design of biomimetic device (propulsion fins) [165]. Du et al. [166] have developed a general model for a multilayer system to link the actuation strain of the actuator to the bending curvature.

### ***Finite elements method***

The finite elements methodology is a well know mathematical treatment for engineering designs [167] that can be applied to solve the movement of the artificial muscles. Alici et al. [168,169] developed a model based on a lumped-parameter mathematical model for actuators employing the analogy between thermal strain and the real strain (due to the insertion/extraction of ions inside the polymeric film) in polypyrrole actuators actuating in air. An optimization of the geometry was required, in order to obtain the greater output properties from a determined input voltage. Shapiro et al. [170] developed a two dimensional model (along a full area) to obtain curvature

and angular moment of the actuators. Thus, they combined the results from the previous method (bending beam method) with finite element method to attain a solution. Another example of the employment of this method was carried out by Gutta et al. who applied it to study the movement of a cylindrical ionic-polymer metal composite actuator [171].

### ***Equivalent transmission line model***

Electrochemical systems, as many other systems, can be studied as equivalent systems of a different nature. Thus, they can be studied as equivalent electrical circuits and electrochemomechanical actuators have been treated by the equivalent transmission line method. This resource is a practical tool due to the great number of facilities available for the study of electrical circuits through different steps or modules. Such treatments are employed by engineers and physicists, or electrochemists, in order to explain the claimed capacitive behaviour of CP [172–174]. Ren et al. [175] proposed equivalent electrical circuits to model the electron transport and electron transfer in composite polypyrrole-polystyrenesulfonate films based on Albery's works. Fang et al. [176,177] have developed a scalable method including dynamic actuation performance under a given voltage input, joining three different modules for different aspects of the actuator: electrochemical dynamics, stress-generation by charge and mechanical dynamics. Shoa et al. [178] developed a dynamic electromechanical method for electrochemically driven conducting polymer actuators based on a 2-D impedance model using an RC transmission line equivalent circuit to predict the charge transfer during actuation. In addition, a mechanical model (based on the bending beam model) is considered after the equivalent circuit that simulates ion "diffusion" through the thickness and electronic resistance along the length [179]. If the angular movement is not linear along the full geometry of the actuator, the bending beam method has to be modified, for example for cantilever type conducting polymer actuators [180].

In order to successfully achieve the imposed requirements for the control of an actuator, it is possible to use one or several of the mentioned models [181].

### ***Faradaic behaviour of conducting polymer actuators***

Unlike the models previously exposed here, based on analogies with different kinds of systems, this one is based on the device electrochemical nature under driving reactions (1) or (2). When the flow of a constant electrical current,  $I$ , is imposed through a bilayer artificial muscle, the reaction induced volume variations in the conducting polymer promote a



macroscopic bending movement because strain and stress prompted across the bilayer interface. Gel volume and ionic gel composition (number of exchanges ions, equation (3)) are controlled by the number of electrons extracted from the neutral polymeric chains. This number of electrons determines the charge consumed charge during reactions (1) or (2) and, through the charge, equation (3), the number of counterions exchanged to keep the gel electroneutrality and the number of solvent molecules exchanged to balance the osmotic pressure. The number of exchanged solvent molecules must be proportional to the ionic concentration gradient between the film and the solution: a linear relationship should be expected between the consumed charge and the volume (ions plus solvent) variation. That means that the same charge gradient should give the same angular displacement, totally independent of the fact that the charge gradient is applied to a neutral polymer film or to a partially oxidized polymer film.

Empirical results corroborate the linear relationships between the described angle and the charge consumed by a bending bilayer artificial muscle device [99,182–184]:

$$\alpha = \alpha_0 + KQ \quad (5)$$

where  $\alpha$  is the described angle,  $\alpha_0$  is the initial angle,  $Q$  is the consumed charge and  $K$  is a constant depending on the system (conducting polymer, electrolyte, passive polymer, attachment between layers). Equation (5) corroborates the Faradaic nature of bending movement in artificial muscles. According with the Faraday's law the charge controls the number of exchanged ions and solvent molecules, thus the volume variation, the transversal stress gradient variation and the angular displacement. Equation (5) is followed by bending artificial muscles working under different driving currents, for different electrolyte concentrations, in different electrolytes, working at different temperatures for conducting polymers exchanging anions or cations during reactions [99,182,183].

Equation (5) states that bending artificial muscles are electro-chemo-positioning devices: any new position requiring an angular displacement  $\alpha$  is attained by imposing the flow of a charge  $Q=\alpha/K$  [185] through the muscle.

By differentiating equation (5) a linear relationship is obtained between the angular rate ( $\omega$ ) and the applied current ( $i$ ):

$$\frac{d\alpha}{dt} = \frac{d}{dt}(KQ) \Leftrightarrow \frac{d\alpha}{dt} = K \frac{dQ}{dt} \Leftrightarrow \omega = Ki \quad (6)$$

Equation (6) describes that the angular rate of the bending movement is under linear control of the applied current. The sense of the bending movement can be reversed by reversing reactions (1) and (2) (from forwards to backwards and vice versa) changing the anodic constant current flow by a cathodic constant current flow.

Equations (5) and (6) are much simpler than any of the complex equations attained with the rest of the models. In addition those linear equations describe a perfect actuation control: the rate and sense of the angular movement is controlled by the value of anodic or cathodic applied currents and the muscle relative position is fully characterized by the consumed charge.

In addition, those actuators are very robust and fully reproducible. The faradaic control persists whatever the muscle geometry or the mass of the active polymer working in the muscle is [182,183] and for polymers exchanging anions [183] or cations [99] during reaction. Thus, the electrochemomechanical behaviour of any artificial muscle moving in the same electrolyte, the muscle constituted by the same material whatever the geometry of the device is (shape, thickness, surface area, length, width, etc.) can be predicted. Experiments from only one muscle are required in order to obtain its electrochemomechanical characteristics (constant  $K$  from equations (5) or (6)), whatever its configuration, mass and shape. Once attained, the behaviour of different muscles can be modelled.

***Conformational movements suffered by the polymeric chains influence the material electrochemical response: Electrochemically Stimulated Conformational Relaxation (ESCR) model***

Conformational movements of the constituent polymer chains driven by electrochemical reactions (1) or (2) are the origin of volume changes (actuation), figure 4. Such conformational movements in the gel promote during its oxidation/reduction different macroscopic basic structural processes: oxidation-relaxation, oxidation-swelling, reduction-shrinking, and reduction-packing of gels exchanging anions [reaction (1)] and oxidation-shrinking, oxidation-compaction, reduction-relaxation and reduction swelling for gels exchanging cations [reaction (2)].

During reduction, reaction (1) backwards, counterions are expelled from the oxidized and swollen film, under diffusion kinetic control, towards the solution: the gel film shrinks and the polymer chains become closer and closer. The average distance between neighbour polymeric chains is high enough to allow the diffusion of counterions and solvent molecules across

the polymeric gel. The reduction rate is fast, expending low energy (at low overpotential) under diffusion control. Going on the gel reduction, reaction (1) backwards, the average distance between the polymeric chains becomes, at the closing potential, smaller than the diameter of the moving counterion units (probably solvated counterions). The fast reaction rate under diffusion control finish and a slow reduction rate goes on, now under kinetic control of the slow conformational movements that allows the counterions (and solvent) to find its way through the rising conformational packed structure towards the solution. The reaction rate is much slower and consuming rising amounts of energy. Similar reaction induced conformational phenomena, named allosteric, occur in biological systems [186–188].

Such conformational effects influence, and were detected from, the shape of the gel electrochemical responses during reaction (1) [189]. The reaction driven conformational effects have been theoretically described by the Electrochemically Stimulated Conformational Relaxation (ESCR) model [190–202]. The transition from the faster reduction-shrinking rate, under diffusion kinetic control, to the slower reduction-compaction under conformational kinetic control is clearly visualized from the slope of the charge consumed during voltammetric experiments (coulovoltammetric responses) [200,203]. Any film begins its oxidation after reduction and conformational compaction by oxidation-relaxation of the packed conformational structure starting by relaxation-nucleation (visualized from electrochromic films) at those points of the film/electrolyte interface having a higher mobility of the chains [204,205].

Thus, the involved energy during the polymeric reactions includes, according with the ESCR model three different structural components, for conducting polymers exchanging anions [reaction (1)]:

- the energy variation of the system in absence of any electric fields,  $\Delta H$ , or electrochemical reaction as for any gel material;
- the energy variation due to the conformational compaction by reduction of one mole of polymeric segments ( $z_c \eta_c$ , where  $z_c$  is the charge consumed to compact one mole of polymeric segments and  $\eta_c$  is the applied reduction overpotential related to the closing potential) with expulsion of a number of balancing ions defined (Faraday's law) by the consumed charge: the conformational compaction molar energy;
- the energy required to relax by oxidation-nucleation one mole of compacted polymeric segments ( $z_r \eta$ ,  $z_r$  is the charge required to relax one mole of polymeric segments and  $\eta$  is the oxidation overpotential)

with entrance of a number of balancing ions defined by the consumed charge: the conformational relaxation molar energy.

Different experimental ways allow getting different, and each of them in a very reproducible way, conformational packed states of the conducting polymer film starting every time from an oxidized and swollen state. Rising conformational compacted states are obtained by gel reduction at increasing cathodic overpotentials (beyond the closing potential) each potential applied for a constant time [190,193,206,207]. Alternatively rising conformational compacted states, starting from the same oxidized and swollen state every time, are got by gel reduction at the same cathodic overpotential (enough to achieve the closing of the polymeric structure) applied for rising reduction times [201,208]. Similar results are got by submitting the gel electrode to potential cycles until a different cathodic potential limit every time [190,194,197,199].

Similar methodologies and concepts can be applied to those conducting polymer families where reaction (2) prevails, but taking into account that here the conformational gel structure relaxes and swells during reduction, shrinking and packing during the gel oxidation. In addition a new slope change during coulometric reduction responses has revealed the existence of a new reaction driven structural processes, not totally clarified yet [203].

## **Experimental variables affect the electrochemical reaction**

Among the different gel properties changing simultaneously with the gel composition driven by the reactions (1) or (2), table 1, here we will focus on the gel potential, which has allowed the development of sensors and biosensors [14,87–93,209–214] and the volume variation, which has led to the development of artificial muscles [94,95].

In accordance with the Le Chatelier's principle [215], any variable acting on a chemical reaction affects its equilibrium, modifying also the products of such reaction.

In this thesis it is proposed that even outside the equilibrium (in the case of electrochemical devices based on conducting polymers, while a charge is consumed or a current is applied and the gel composition is varying) electrochemical reactions (1) and (2) are influenced by those experimental (physical and chemical) variables affecting the reaction rate. The existence

of this influence should be detected by different electrochemical responses for different values of the studied variable. So if any experimental variable affecting electrochemical reactions (1) or (2) is changed, a new and different electrochemical response should be expected.

In this way, previous empirical results corroborate that, submitted to a constant current flow from the same initial oxidation level to the same final (different from the first one) oxidation level, the evolution of the gel potential or that of the consumed electrical energy change for different values of the working variables: temperature, electrolyte concentration, different salts, different solvents or mechanical conditions [216–220]. Similar results were got from films of carbon nanotubes or graphene [221–224]. The most important empirical results related to this thesis is that the muscle potential evolution and the consumed electrical energy evolution during bilayer or trilayer muscles actuation sense, while moving, the influence of the same physical and chemical variables, giving sensing and tactile artificial muscles. The dual actuating-sensing property is observed from artificial muscles constituted by both families of conducting polymers: exchanging anions or cations [96,98,99,101,102]. Using the experimental setup shown in figure 5 the muscle potential response is recorded while a current is applied to the artificial muscle, producing a mechanical work. Under flow of a constant current (constant reaction rate) the achieved potential evolution is lower when a variable favouring the electrochemical reaction increases. This is the case for temperature [96,98–101] or electrolyte concentration [96–99,225]. On the other hand, the potential evolution shifts to higher values for rising values of those variables retarding the reaction rate (it needs more energy to happen): the muscle moves higher masses [99] or moving faster the same mass by applying now rising currents [98,100,184]. When a free muscle moves driven by a constant current and finds an obstacle in his way, the potential steps to higher values at the touching time: more electrical energy is required to move the obstacle. The potential increment reveals both, the obstacle contact time and the opposed mechanical resistance. If the muscle can develop a higher energy the obstacle is shifted. Related to this property, artificial muscles with tactile sensitivity have been developed [102].

Being the potential evolution a sensor of the working variables, the electrical energy ( $U$ ) consumed by the device during actuation and obtained by integration:

$$U(t) = \int E(t)I(t)dt \quad (7)$$

**Conducting polymer actuators: From basic concepts to proprioceptive systems.**

where  $t$  is the elapsed time,  $E(t)$  is the potential evolution during the actuation time and  $I$  is the applied current. The energy,  $U$ , also senses the same physical and chemical perturbations.

Thus, using experimental setups from figure 5, a current (so a charge) is applied to the actuator, varying the composition and volume of its constituent conducting polymer films and controlling both, the position and the angular rate of the muscle movement through equations (5) and (6). At the same time, it is possible to follow the evolution of the potential difference between the same two wires used to close the electrical circuit allowing current flow. Such potential contains information about the experimental variables and can be used as a sensing signal. A uniform device includes the simultaneous work of different tools: a mechanical actuator and several sensors. Actuating and sensing information is present at any time in the two connecting wires and can be read by the computer at any time. This information can be used by the computer-galvanostat controller for taking instantaneous decisions for the control of the actuator. The result mimics human proprioception, figure 6, making automatic systems simpler, cheaper and more reliable.

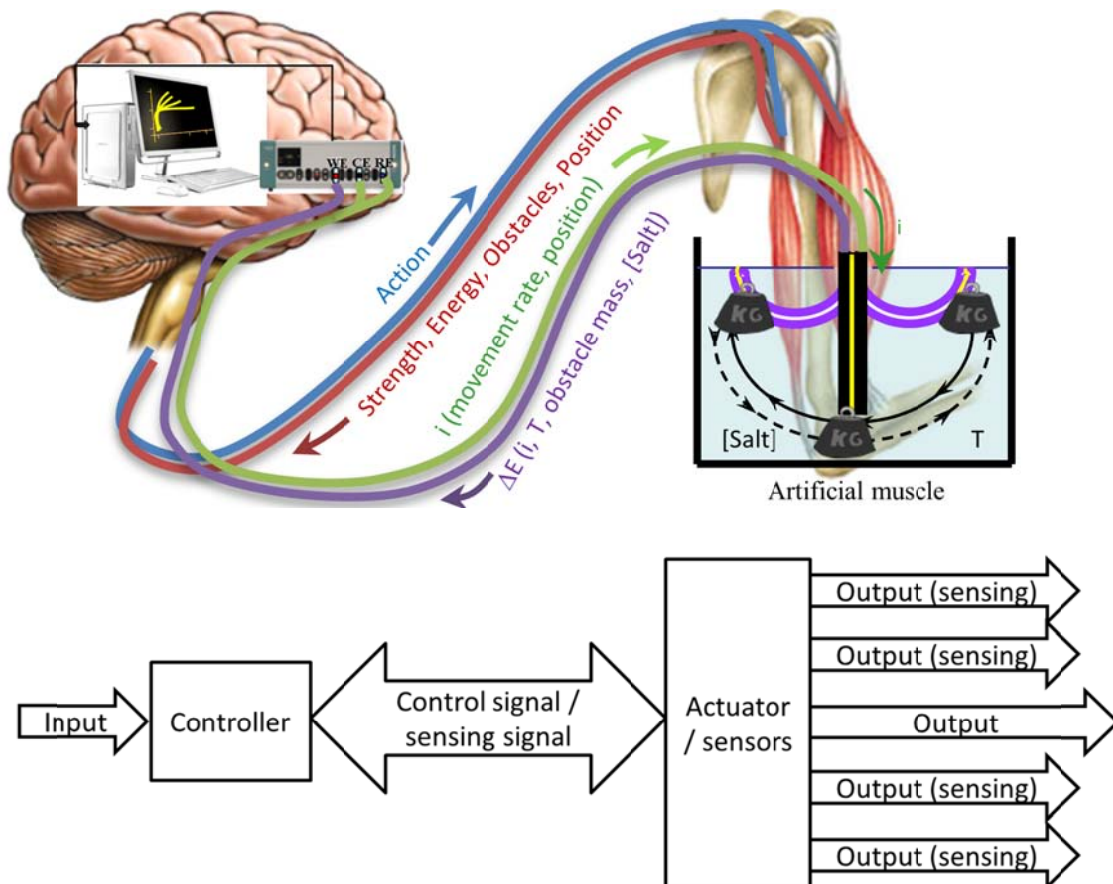


Figure 6: Artificial muscles based on electrochemical reactions (1) or (2) have proprioceptive properties.

These proprioceptive properties are here studied deeply, studying new systems that present such properties and developing a model able to explain and quantitatively describe them.

# Experimental

Here, general experimental procedures used in most of the publications included in this thesis are presented. Specific experimental procedures will be developed in each of the involved publications, as specified by the regulations (Artículo 33 del Reglamento de estudios oficiales de máster y doctorado de la Universidad Politécnica de Cartagena, aprobado por Consejo de Gobierno el 13 de abril de 2011 y modificado en Consejo de Gobierno el 11 de julio de 2012).

## Materials

Pyrrole (Fluka or Sigma-Aldrich) and Aniline (Fluka) were purified before use by distillation at constant temperature (38 °C) under vacuum using a diaphragm vacuum pump MZ 2C SCHOTT and stored at -10 °C.

Anhydrous lithium perchlorate salt  $\text{LiClO}_4$  (Aldrich), trisodium phosphate 12-hydrate  $\text{Na}_3\text{PO}_4 \cdot 12\text{H}_2\text{O}$  (Panreac), disodium hydrogen phosphate 12-hydrate  $\text{Na}_2\text{HPO}_4 \cdot 12\text{H}_2\text{O}$  (Panreac), sodium peroxodisulphate  $\text{Na}_2\text{S}_2\text{O}_8$  (Panreac), sodium chloride  $\text{NaCl}$  (Panreac, Aldrich or Merck), sodium perchlorate  $\text{NaClO}_4$  (Sigma-Aldrich), sodium carbonate  $\text{Na}_2\text{CO}_3$  (Merck), sodium nitrate  $\text{NaNO}_3$  (Merck), sodium iodide  $\text{NaI}$  (Sigma), polyurethane (Aldrich, average molecular weight of  $1.2 \times 10^5 \text{ g mol}^{-1}$ ), ferric chloride (Aldrich), Lithium trifluoromethanesulfonate  $\text{LiTFMS}$  (Aldrich), silk fibroin meshes (provided by the Instituto Murciano de Investigación y Desarrollo Agrario, IMIDA), Ammonium persulfate APS (Fluka), Methane Sulfonic Acid MSA (Sigma-Aldrich), Lithium Bromide  $\text{LiBr}$  (Acros Organics) and sodium dodecylbenzenesulfonate  $\text{NaDBS}$  (Aldrich, Sigma or TCI Europe) were used as received.

Acetonitrile (Panreac, HPLC grade), Hexafluoroisopropanol (Sigma) and Ethanol (Panreac) were used as received. Ultrapure water was obtained from Millipore Milli-Q equipment.



## Generation of conducting polymer

### Chemical polymerization

The way to initiate the polymerization is through the generation of radical anions, or radical cations, with the subsequent polycondensation of the radical-ions [226]. The initial radical cations are generated by electrochemical, chemical, or photochemical oxidation of the monomer, figure 7. All those methodologies require an initial solution of: monomer, solvent, and salt. The salt is essential to provide conductivity to the solution allowing the current flow (closing the electrical circuit) and the anions required for the polymer doping (oxidation) during the electropolymerization. From every monomeric unit (M) the polymerization is initiated by physical (light, heat, mechanical,...), chemical or electrochemical generation of radical-cations ( $M^{\bullet+}$ ) and release of electrons ( $e^-$ ):



Figure 7: Initiation of the polymerization in pyrrole monomers.

The energy required to extract one electron from the monomer HOMO level and start the polymerization can be provided chemically by different redox couples in solution, as  $Fe^{3+}/Fe^{2+}$  for example. Thus, radical cations can meet forming dimers, trimers and so on, figure 8.

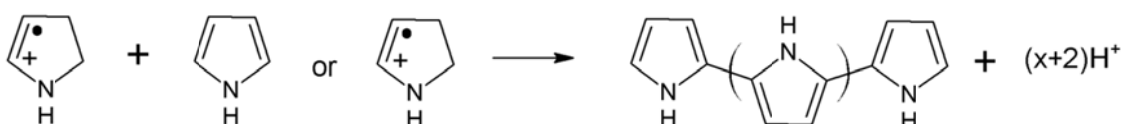


Figure 8: Polymerization of polypyrrole.

This is the most usual procedure for coating a non-conducting material (textile, natural fibres, wood) with a thin layer of conducting polymer. When the redox couple penetrates into the basic material an interpenetrated network is generated avoiding exfoliation of the conducting polymer film during the subsequent applications. The final product from the same monomeric solutions is an oxidized film on different materials and lumens, or powder of conducting polymer. The thickness of the conducting polymer film is controlled by different kinetic variables, the most direct being the polymerization time.

In this thesis chemical polymerization was used to coat a polyurethane microfibrinous mat with polypyrrole (PU/PPy) and to coat a silk fibroin mesh with polyaniline (Silk fibroin/PANI).

### ***Electrochemical polymerization***

During the electrochemical polymerization, the initiation (see chemical polymerization, figure 7), is promoted by an electronic current flow in an electrochemical cell (figure 9).

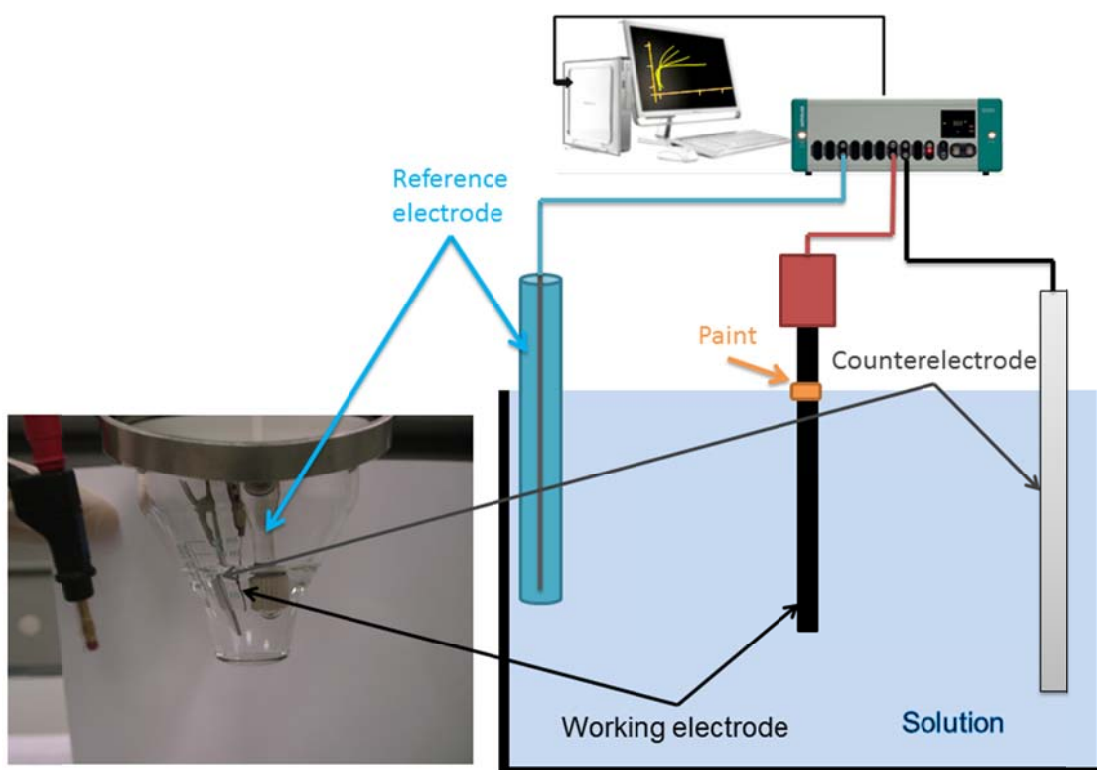


Figure 9: Three electrodes electrochemical cell employed during the electrochemical experiments.

The three electrodes electrochemical cell contains the monomeric solution and three electrodes, each of them with a specific function. The working electrode (WE) is the electrode under study: steel metals supporting the electrogeneration of conducting polymer, a metal coated with a conducting polymer film, a self-supported CP film or a CP from an artificial muscle. All the electrochemical responses presented in this thesis follow currents or potential evolutions with time in the WE. In order to close the electrical circuit, the counterelectrode (CE) is needed, so the current can flow back to the potentiostat/galvanostat. The reference electrode (in this thesis, an Ag/AgCl 3M KCl from Metrohm was used) is an ideal non-polarizable electrode allowing the measurement of any variation of the potential

gradient at the WE/electrolyte interface. Through this electrode there is not current flow.

Thick polypyrrole films were used in this thesis. For their electrogeneration, three stainless steel electrodes having a surface area of 6 cm<sup>2</sup> were used, one of them as working electrode and the other two as counterelectrodes (in shortcut). The working electrode was placed in the middle of the counterelectrodes and parallel with them, separated by 1 cm, in order to create a uniform electric field over the working electrode during current flow. Typically, the electrogeneration was carried out from a 0.2 M pyrrole and 0.1 M LiClO<sub>4</sub> acetonitrile solution having 1% water content. The films were electrodeposited by consecutive square potential waves from -0.322 V, kept for 2 s, to 0.872 V, kept for 8 s for the time required to achieve the desired polymerization charge (oxidation minus reduction charge). Consumption of different polymerization charges promotes the generation of conducting polymer films with different thicknesses. In the different works presented in this thesis, different charges were used (see each of the papers for the specific details) attaining films of different thicknesses. Results are very reproducible: by consumption of the same charge under the same electrochemical conditions the attained films have the same physical (thickness, mass, conductivity) and electrochemical (involved charge during oxidation/reduction reactions) properties. Once the electrogeneration was ended, the films were reduced at -0.322 V for 300 s, and next dried in air.

## **Construction of actuators (Bilayers)**

Bilayer actuators were always constructed from electrochemically generated polypyrrole (Figure 10a) through the same steps:

1. The electrode borders of the electrogenerated polypyrrole film on the steel electrode are scraped (Figure 10b). The polypyrrole film is removed from the steel background electrode with help of a plane sharp surface (Figure 10c) to get the free-standing conducting polymer film (Figure 10d).
2. Longitudinal strips are cut (Figure 10e) from the self-supported conducting polymer film, with the desired dimensions (Figure 10f). Each film is weighed and its dimensions are determined. One of those strips is used as the working electrode for some of the papers included in this thesis: the electrical connection is produced through a metal clamp at the electrode top (step 5) and a transversal strip is painted below the clamp (step 6) in order to avoid direct contact between the clamp and the electrolyte by capillarity. This self-supported

### **Conducting polymer actuators: From basic concepts to proprioceptive systems.**

conducting polymer film is used as the working electrode by immersion in the electrolyte, the transversal painted strip remaining above the electrolyte border.

3. One of the polypyrrole free-standing film strips is adhered to a flexible thin commercial tape (Figure 10g) by applying mechanical pressure with a cylindrical dipstick (Figure 10h) to guarantee the proper attachment. Any tape can be used as passive layer, but choosing a proper tape (as much flexibility as possible, with lower mass and stickier as possible) allows getting bigger displacements.
4. To cut the uncovered borders of the tape (Figure 10i) and to remove the rest of the non-attached parts (Figure 10j) getting a bilayer artificial muscle (Figure 10k).
5. To ensure with a metallic clamp the electrical contact between the bilayer artificial muscle and the electrical pulses generator (potentiostat-galvanostat) (Figure 10l).
6. To paint a transversal strip around the bilayer artificial muscle and below the clamp in order to avoid the electrolyte ascension by capillarity, its direct contact with the metallic clamp and its electrochemical reactions (Figure 10m). The selected paint must be insoluble in the cell electrolyte. Here, nail paint soluble in acetone was used. Let the paint dry.
7. To set the electrochemical cell for the experiments (Figure 10n), including a reference electrode to set a reference for the potential and a counter electrode to close the electrical circuit, see electrochemical characterization section.

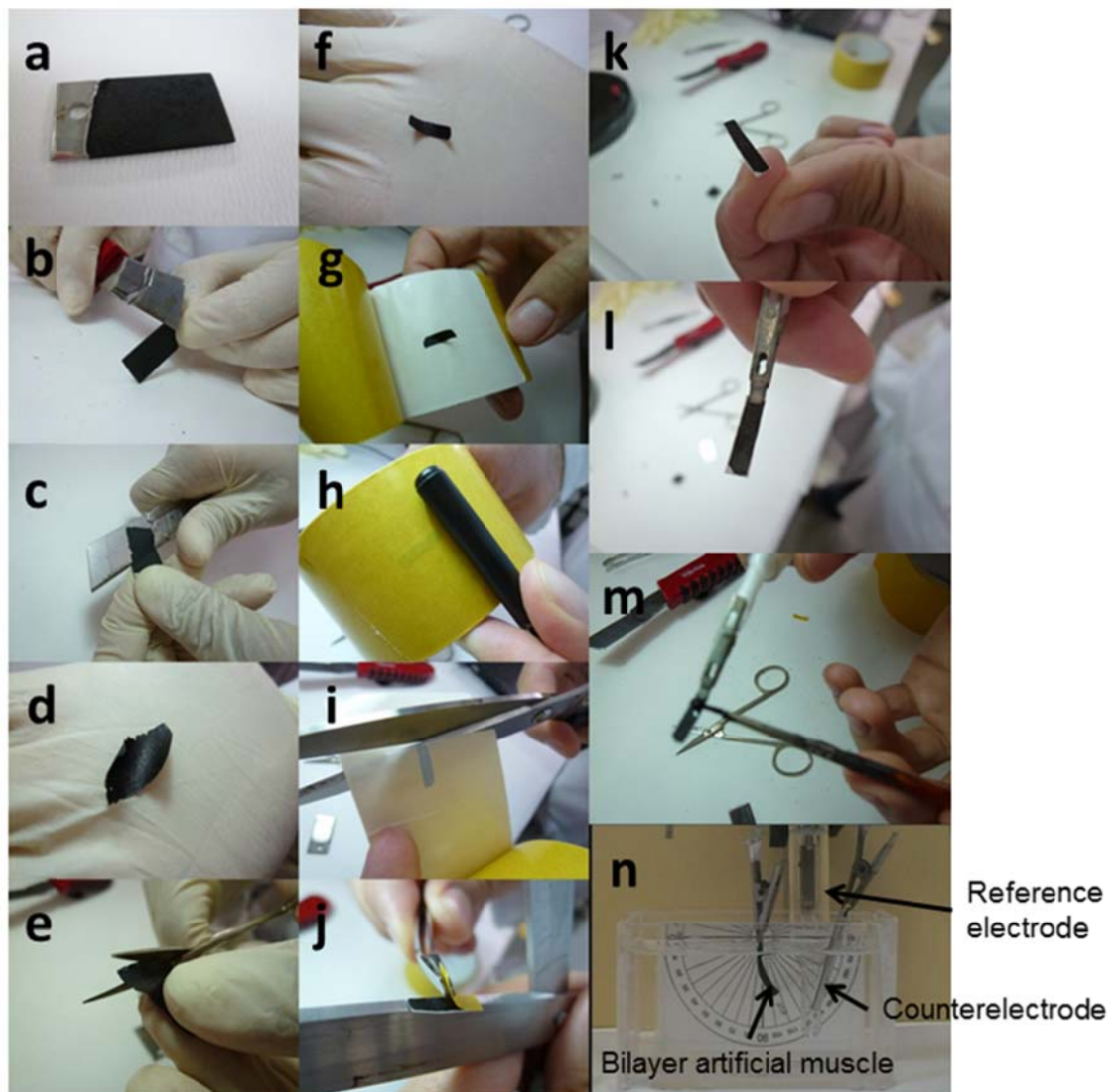


Figure 10: Fabricating a bilayer artificial muscle: (a) Electrogenerated conducting polymer film; (b) Cutting the borders; (c) Removing the conducting polymer film from the metallic electrode used during the electrogeneration; (d) Free-standing conducting polymer film; (e) Cutting a smaller sample; (f) Small free-standing conducting polymer film ready to fabricate the bilayer; (g) Attaching the free-standing polymer film to the conventional tape; (h) Mechanical pressure over the bilayer to ensure the proper attachment; (i) Cutting the borders of the tape; (j) Removing the isolating part not attached to the bilayer; (k) Bilayer artificial muscle; (l) Ensuring the electrical contact with a metallic clamp; (m) Painting the bilayer artificial muscle with paint to fill the pores and avoid the electrolyte contact with the metallic clamp by capillarity; (n) Electrochemical cell used during bilayer artificial muscle actuation. (n') scheme of the connections of the electrochemical cell

## Physical Characterization

### *Fourier transform infrared spectroscopy (FTIR)*

Fourier transform infrared spectroscopy (FTIR) is a well-known technique to characterize molecules [227]. FTIR is based on infrared spectroscopy. Different molecules absorb different specific frequencies. This is a

characteristic of their structure, related with the strength of their bonds. When a molecule is under influence of an electromagnetic light having a specific frequency (the same of a vibrational frequency of a chemical bond in the molecule), absorption is observed at the concomitant frequency.

By using this technique, it is possible to analyse and identify macroscopic or microscopic samples with very high accuracy and selectivity without destroying the sample in only a few minutes.

For the experiments performed during this thesis, attenuated total reflectance (ATR) accessory was used. It allows characterizing solid or liquid samples without further preparation (also polymeric gels). In this case, the infrared beam is directed onto an optically dense crystal with a high refractive index at a certain angle. The beam, once reflected, arrives to the sample (in contact with such dense crystal) and absorption bands are observed at the vibrational frequency of the polymeric bonds.

During this thesis, a Nicolet 5700 FTIR spectrometer (Thermo Electron Corporation) with smart orbit accessories (ATR technology) was used for the characterization of the different materials.

### ***Scanning electron microscope (SEM)***

The scanning electron microscope is also a widely used technique nowadays [228].

A scanning electron microscope is a kind of microscope that produces images of a sample by scanning it with a focused beam of electrons. In such microscopes, the electrons are accelerated in the presence of an electric field. Once properly accelerated, the electrons are directed to the sample and interact with its atoms. Such interactions promote changes in the electrons that can be detected by the microscope.

During this thesis a Scanning Electron Microscope Hitachi S-3500 was used for the characterization of the different materials.

## **Electrochemical characterization**

Electrochemical reactions (1) or (2) can be promoted through different ways: applying a potential difference between the working electrode and the reference electrode which induces a current flow to achieve a new equilibrium state (such current flow changes the polymeric gel composition and properties to a new specific oxidation/reduction state); or applying a current between the working electrode and the counterelectrode promoting

a variation in the potential of the working electrode (compared with the reference electrode) promoting the variation of the gel composition at a controlled rate.

Different electrochemical techniques such as cyclic voltammetry, chronoamperometry and chronopotentiometry were used for the experiments presented in this thesis.

### ***Cyclic voltammetry***

Using this technique, a potential sweep between a cathodic potential limit (most negative potential set for the experiment) and an anodic potential limit (most positive potential set for the experiment) is applied. The potential is varied at a constant rate. Once a potential limit is achieved, the potential sweep goes on in the opposite way to the other potential limit at the same rate (symmetrical triangular potential wave), figure 11a. This is repeated as many times as necessary.

During the potential sweep, the current flowing at any time is recorded, figure 11b, and usually presented as a function of the applied potential. The current recorded during both, anodic (from the cathodic potential limit to the anodic one) and cathodic (from the anodic potential limit to the cathodic one) sweeps are usually presented over the same potential axes giving, in many cases (when the study is in the steady state) a closed loop, figure 11c.

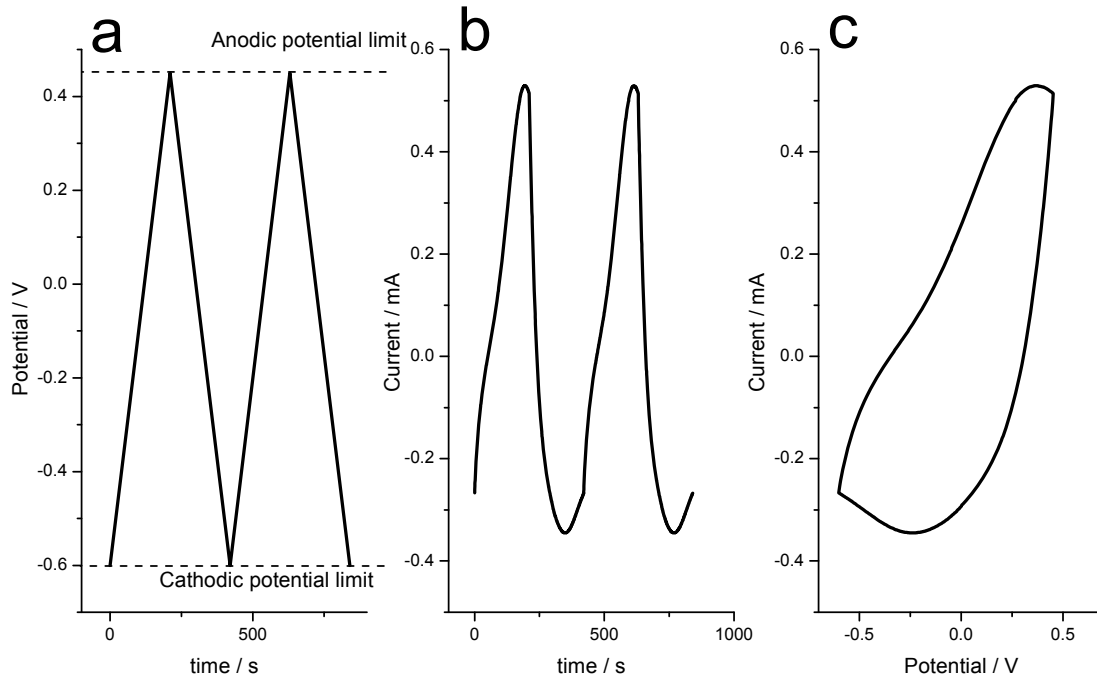


Figure 11: Cyclic voltammetry. (a) Symmetrical triangular potential wave applied to the working electrode. (b) Measured current when the potential wave in (a) is applied. (c) Cyclic voltammogram.

### Coulovoltammetry

This technique is based on results from the previous one (cyclic voltammetry). It consists of the study of the consumed charge during the potential sweeps. It is possible to get the consumed charge directly integrating the current from the voltammetric results (figure 11b):

$$Q(t) = \int_0^t i(t) dt \quad (9)$$

where  $Q$  is the consumed charge,  $t$  is the elapsed time and  $i$  is the current.

However, it is not usual to have these results but rather the voltammogram (figure 12a). In order to get the consumed charge directly from the voltammogram, it is of interest to consider the relationship between time and potential,  $E(t)$ :

$$E(t) = E_{ini} + vt \quad (10)$$

with  $E_{ini}$  the initial potential,  $t$  the elapsed time and  $v$  the scan rate. Differentiating:



$$dE = v dt \Leftrightarrow \frac{dE}{v} = dt \quad (11)$$

Thus, from equations (9) and (11) it is possible to obtain the consumed charge (coulvoltammogram, figure 12b) during the voltammetric experiment just numerically integrating the voltammogram and dividing the result by the scan rate.

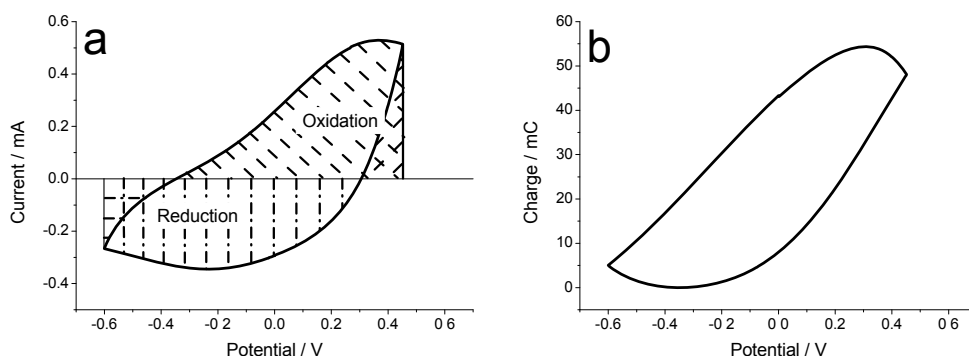


Figure 12: Coulovoltammetry. (a) Cyclic voltammogram. (b) Coulvoltammogram.

### ***Chronoamperometry***

This electrochemical technique consists of applying a constant potential to the working electrode (referred to the reference electrode) during a constant time. In this thesis this time it is usually enough to achieve a very low current (the material has achieved a stationary oxidation/reduction state). Once the specified time is elapsed, the potential difference between the reference electrode and the working electrode is stepped to a new value, figure 13a. The number of steps can be different every time. While the potential steps, the current flow is recorded and presented versus the elapsed time as the result of the chronoamperometric experiment, figure 13b.

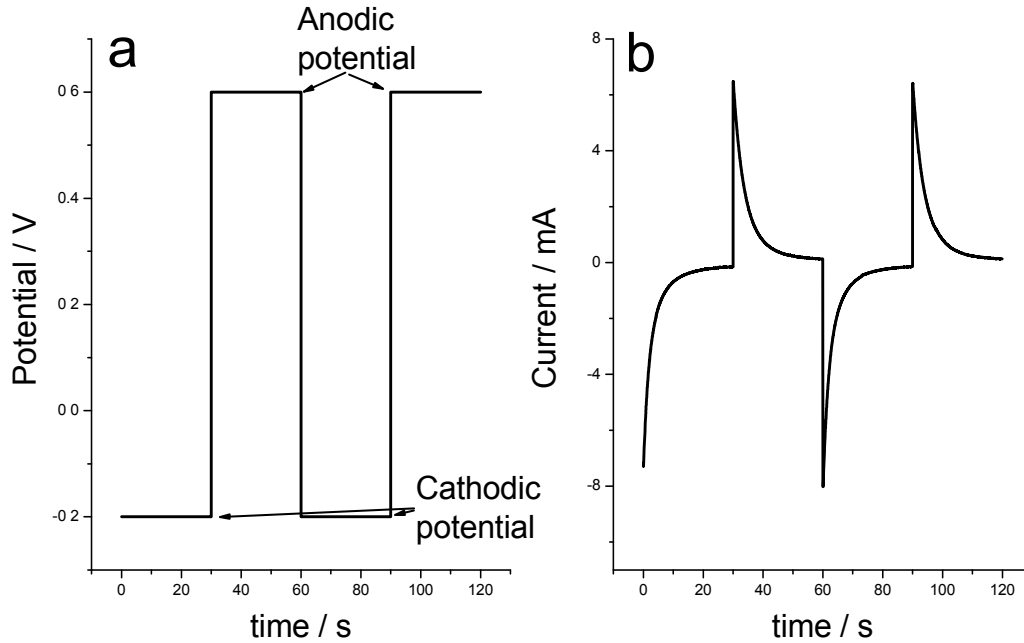


Figure 13: Chronoamperometry. (a) Potential applied to the working electrode (referred to the reference electrode). (b) Measured current flowing through the working electrode during potential steps shown in (a).

### ***Chronopotentiometry***

When instead of applying square potential waves, square current waves are applied, it is called chronopotentiometry. A constant current is passed through the working electrode during a constant time and then step the current to a different value. During current flow the potential evolution between the working electrode and the reference electrode is recorded. In this thesis a constant current,  $I$ , through the electrode during a time,  $t$ , needed to consume a fixed value of charge,  $Q$  has been fixed. Such time can be calculated from the current definition, equation (9):

$$I = \frac{Q}{t} \Leftrightarrow t = \frac{Q}{I} \quad (12)$$

Once such value of charge had been consumed, the same current during the same time was passed through the electrode, but into the reverse direction so a square current wave was applied to the working electrode, so as the same charge was consumed during oxidation and reduction processes, the same initial and final oxidation/reduction (same composition of the polymeric gel) is attained. Such square current wave can be repeated as many times as needed, figure 14a. The potential evolution (referred to the reference electrode) is measured and presented versus the elapsed time, figure 14b.

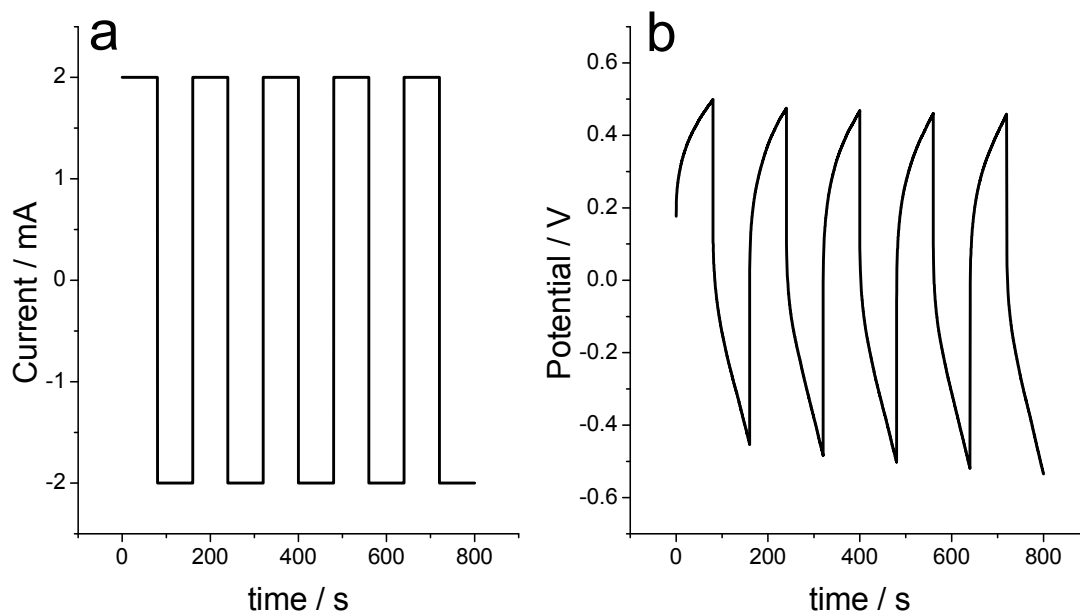


Figure 14: Chronopotentiometry. (a) Applied current versus time. (b) Measured potential evolution versus time when current from (a) was applied.

## Mechanical characterization of the actuators

Some techniques have been used to characterize the mechanical properties of the actuators such as their movement, the force produced or the volume variations in the conducting polymer itself. The technique most used during this thesis was the video recording of the movement of actuators during electrochemical experiments. The other techniques will be developed in each of the articles where used.

### *Video recording of actuators' movement*

Usually, the movement of bilayer actuators during electrochemical experiments already mentioned was video recorded employing a video camera EVI-D31/B (Sony) connected to a computer through a Matrox Meteor II video acquisition card controlled by home-made software [229]. Such software is able to get an image every second, so it is possible to relate every acquired frame with the moment of the experiment, with the subsequent video and electrochemical results relationships.

Different angles were measured between the horizontal line between the electrolyte border and the line joining the actuator end and the actuator contact with solution as indicated in figure 15.

Conducting polymer actuators: From basic concepts to proprioceptive systems.

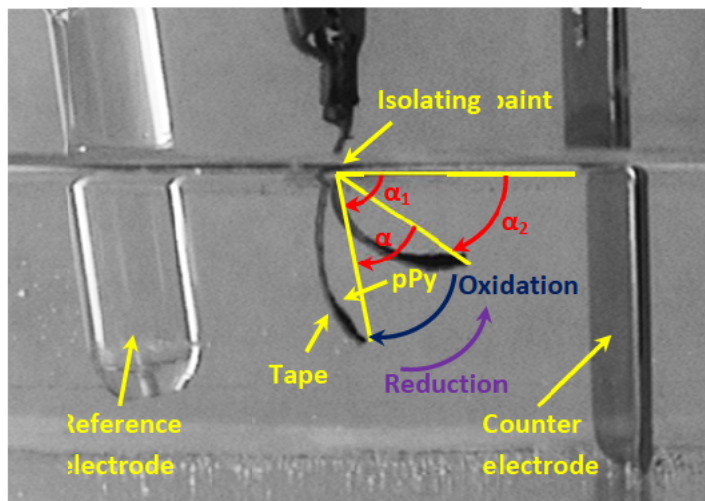


Figure 15: Electrochemical cell and angle described by a bilayer artificial muscle recorded by a video camera. Two frames in different moments of the movements were overlapped.



# Publications

The results of this thesis have been published in different international journals. Among those papers the most significant for the objectives have been selected for this thesis. Now an abstract of those papers with some specific experimental details and the most significant scientific achievements attained, in the context of the general aims of this thesis, will be presented.

## **'Biomimetic electrochemistry from conducting polymers. A review. Artificial muscles, smart membranes, smart drug delivery and computer/neuron interfaces'**

Toribio F. Otero, Jose G. Martinez and Joaquin Arias-Pardilla.

Published in **Electrochimica Acta**, year 2012, volume 84, pages 112-128. (IF: 4.086, Q1 in Electrochemistry).

### ***Experimental***

No new experimental work was performed for this work.

### ***Results and achievements***

This paper is a review. A careful revision of the state-of-the-art in basic electrochemistry of conducting polymers and their main applications as soft, wet and reactive materials was performed, fulfilling the first of the objectives of this thesis.

Electrochemical reactions (1) and (2) presented in the introduction part and similar for different conducting polymers based materials with different doping mechanisms and processes involved were reviewed here. Each electron extracted from the polymeric chains promotes a new polymeric gel with a new composition (counterions and solvent content). Such reaction driven composition changes originate parallel changes in some composition dependent properties of the conducting polymer materials. Changes in volume, colour, stored charge, porosity or permselectivity, stored chemicals, wettability and so on open the way to new applications mimicking similar property changes in organs from living beings. They are reversible, allowing

the construction of electrochemical devices mimicking biological processes in cells.

The change under electrochemical control of each of those properties is being exploited to develop several biomimetic reactive and soft devices. Here, the revision was focused on artificial muscles (sensing-actuators) including models and developed applications, smart membranes, smart drug delivery systems and computer/neuron interfaces, and their ability to sense surroundings during actuation as corresponds to the main aim of this thesis. Working under constant current (driving signal), the evolution of the device potential or the evolution of the consumed electrical energy (sensing signals) gives quantitative information about (senses) any experimental variable acting on the reaction rate.

Examples of the tools and products, start-up companies, increasing evolution of the scientific literature and patents and scientific and technological challenges are also considered.

## **'Artificial Muscles: A Tool To Quantify Exchanged Solvent During Biomimetic Reactions'**

Toribio F. Otero and Jose G. Martinez.

Published in **Chemistry of Materials**, year 2012, volume 24, pages 4093-4099. (IF=8.535, Q1 in 'Materials science, Multidisciplinary' and 'Chemistry, Physical').

### ***Experimental***

The go and back described angle (the bending movement was video recorded) from bilayer (polypyrrole/tape) artificial muscles submitted to square current waves immersed in electrolytes containing the same cation ( $\text{Na}^+$ ) and different anions ( $\text{Cl}^-$ ,  $\text{I}^-$ ,  $\text{NO}_3^-$ ,  $\text{ClO}_4^-$ ,  $\text{S}_2\text{O}_8^{2-}$ ,  $\text{HPO}_4^{2-}$  and  $\text{PO}_4^{3-}$ ) was studied.

In order to get a good reproducibility and comparable results from different muscles the mass of each polypyrrole film was obtained using a balance with a precision of  $10^{-6}$  g. The electroactive polypyrrole mass,  $(m_{PPy})_{active}$ , below the paint strip inside the solution was estimated from the total mass of the reduced film,  $(m_{PPy})_{film}$ , the length of the film,  $l_{film}$ , and the length of active (immersed) film,  $l_{active}$  below the paint strip inside the solution:

$$\left(m_{PPy}\right)_{active} = \frac{l_{active}}{l_{film}} \left(m_{PPy}\right)_{film} \quad (13)$$

The reproducibility of the experiments from different muscles was characterized in 0.5 M NaClO<sub>4</sub> through five consecutive potential cycles between -0.7 V and 0.5 V vs Ag/AgCl at 10 mV s<sup>-1</sup> to ensure stationary voltammetric responses. The charges consumed during the full cyclic voltammetry were directly attained from GPES software and the specific charge (by unit of mass, equation (13)) was calculated. When the specific charge differs over 5% from that of the reference muscle, the bilayer was discarded and a new one was employed to go on the experiments. Thus a reproducible electroactivity between each of the studied muscles was ensured.

In addition a good reproducibility (< 8%) was corroborated for the amplitude of the bending movement under consumption of constant anodic and cathodic specific charges of 25 mC mg<sup>-1</sup>, by flow of a constant current of ±1 mA mg<sup>-1</sup> during 25 s, through the bilayer artificial muscles. For larger deviations the bilayer was discarded and substituted by a fresh one to go on with the experiments.

Once the reproducibility (electroactivity and actuation) was guaranteed, the amplitude of the bending movement by consumption of the same anodic and cathodic specific charges was determined in aqueous solutions of different salts (NaCl, NaI, NaNO<sub>3</sub>, NaClO<sub>4</sub>, Na<sub>2</sub>S<sub>2</sub>O<sub>8</sub>, Na<sub>2</sub>HPO<sub>4</sub>, Na<sub>3</sub>PO<sub>4</sub>) while recording the concomitant chronopotentiometric responses.

After characterization of the muscle bending movement in each of the studied electrolytes, the electrochemomechanical reproducibility of the bilayer was checked in the reference electrolyte (NaClO<sub>4</sub>) by cyclic voltammetry. If both, the bilayer voltammetric response (peak current and oxidation or reduction charges) and described angle deviation, related to the previous controls, differ less than 5% from those of the previous controls, the same muscle was used for the study of a new electrolyte. When the difference was greater than 5 % a new actuator was prepared and its reproducibility was checked to go on with the experimental series.

## ***Results and achievements***

In this work, bilayer artificial muscles are used as a tool to determine the number of solvent molecules exchanged during biomimetic reaction (1) per unit of charge involved. The solvent exchange plays an important role during actuation of artificial muscles based on conducting polymers, as a



greater amount of solvent exchanged will promote greater volume variations and a larger angular displacement by consumption of the same charge.

Conformational movements of the polymeric chains during electrochemical reaction (1), forwards and backwards, promote volume variations to lodge or expel, respectively, counterions required to keep the membrane electroneutrality and solvent molecules to keep the membrane osmotic pressure balance. When a conducting polymer film is part of a bilayer artificial muscle, such volume variations drives the bending described angle, which will be a function of the number (and volume) of exchanged counterions and solvent molecules, figure 16.

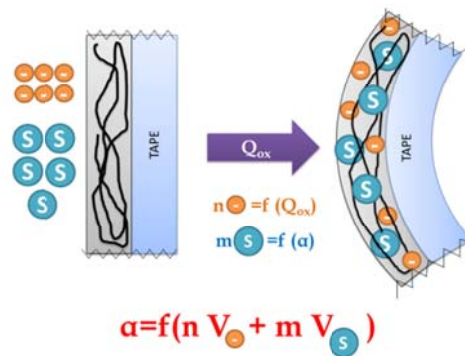


Figure 16: Bending movement in a bilayer artificial muscle based on electrochemical reactions on conducting polymers with reversible solvent molecules and counterions exchange.

According with equation (5), the described angle follows in each of the studied electrolytes a linear relationship with the consumed charge with a different slope, different  $K$ . A constant specific charge ( $\text{mC g}^{-1}$ ) gives a different angular displacement in each of the studied electrolytes. Higher values of  $K$  means that a constant consumed charge promotes a higher volume variation (actuation) giving a larger angular displacement.

The number of counterions exchanged for the oxidation or reduction of the CP film between two different redox states according with reaction (1),  $N$ , is calculated from the consumed charge,  $Q$ , and the counterion valence,  $z$ :

$$N = Q \frac{N_A}{zF} \quad (14)$$

where  $N_A = 6.022 \times 10^{23} \text{ mol}^{-1}$  is the Avogadro's number (number of ions in one mole) and  $F$  is the Faraday constant ( $F = 96485 \text{ C mol}^{-1}$ ).

With the number of exchanged ions,  $N$ , the change of volume in the CP film required to lodge those counterions is attained using the crystallographic ionic volume,  $V_{ion}$ :

$$\Delta V = NV_{ion} \quad (15)$$

Nevertheless volume variations due to the ionic exchanges cannot explain the experimental angles described by actuation of the same bilayers in different electrolytes (different values of  $K$ ) consuming the same specific charge. A parallel exchange of water (solvent) molecules (different in each electrolyte) is required to explain the empirical results. Under this assumption the relative number of solvent molecules,  $n'$ , can be calculated from the experimental described angle and the volume variation due to the exchange of  $N$  counterions, taking as reference the electrolyte showing the lowest angular displacement, Cl<sup>-</sup> here:

$$n' = \frac{\frac{\alpha(anion)}{\alpha(Cl)} V_{Cl} - \frac{V_x}{z}}{V_{H_2O}} \quad (16)$$

where  $\alpha(anion)$  is the angular displacement in a specific electrolyte,  $\alpha(Cl)$  is the described angle in the reference electrolyte (NaCl),  $V_{Cl}$  is the Cl<sup>-</sup> crystallographic volume,  $V_x$  is the crystallographic volume of the counterion present in the studied solution, and  $V_{H_2O}$  is the volume of the solvent molecule (water in this case).

Thus, the number of solvent molecules exchanged between the polymeric membrane and the electrolyte at the same time that each counterion (apparent solvation number) or when an electron was extracted from the polymer chains (apparent hydration number) during reaction was calculated for the different electrolytes. The highest number of exchanged water molecules per ion was attained for the electrolyte showing the largest angular displacement for the same consumed charge, NaNO<sub>3</sub> that exchanged 4.91 water molecules per anion, followed by Na<sub>2</sub>HPO<sub>4</sub> (3.22 water molecules per anion), Na<sub>3</sub>PO<sub>4</sub> (1.47 water molecules per anion), NaClO<sub>4</sub> (1.07 water molecules per anion), NaI (0.71 water molecules per anion), Na<sub>2</sub>S<sub>2</sub>O<sub>8</sub> (0.16 water molecules per anion) and NaCl (0.00 water molecules per anion).

During actuation the chemical nature of the film changes and the intermolecular forces between the different chemical species in the CP film change. The attained results constitute the basis for the accumulation of experimental results for future modelling of the variation of the

intermolecular forces (polymer-polymer, polymer-solvent, polymer-anion, anion-solvent, cation-polymer, and cation-solvent) inside a polymeric film along reaction (1). Developed models could be extended to similar biological processes originating health and diseases.

## **'Ionic exchanges, structural movements and driven reactions in conducting polymers from bending artificial muscles'**

Toribio F. Otero and Jose G. Martinez.

Published in **Sensors and Actuators B: Chemical**, year 2014, volume 199, pages 27-30. (IF=3.840, Q1 in 'Chemistry, analytical', 'Electrochemistry' and 'Instruments & instrumentation').

### ***Experimental***

Free-standing polypyrrole films and bilayer (polypyrrole/tape) artificial muscles were attained as stated in the experimental part. Length variations suffered by free-standing polypyrrole films were obtained, under constant load, by using a universal test frame machine, MTS QTest, with a special electrochemical cell designed and developed in our own laboratory. It allows in-situ characterization of the mechanical response (length variation) from films immersed in solution during oxidation/reduction processes [129,130], figure 17. The polypyrrole film, under a constant force of 0.1 N, was oxidized and reduced in 0.1 M LiClO<sub>4</sub> aqueous solution by imposing the flow of five consecutive square current waves ( $\pm 0.4$  mA) following, simultaneously, film length variations. The original dimensions of the polypyrrole film in absence of any applied load were 7.32 mm x 1.94 mm x 34  $\mu$ m.

## Conducting polymer actuators: From basic concepts to proprioceptive systems.

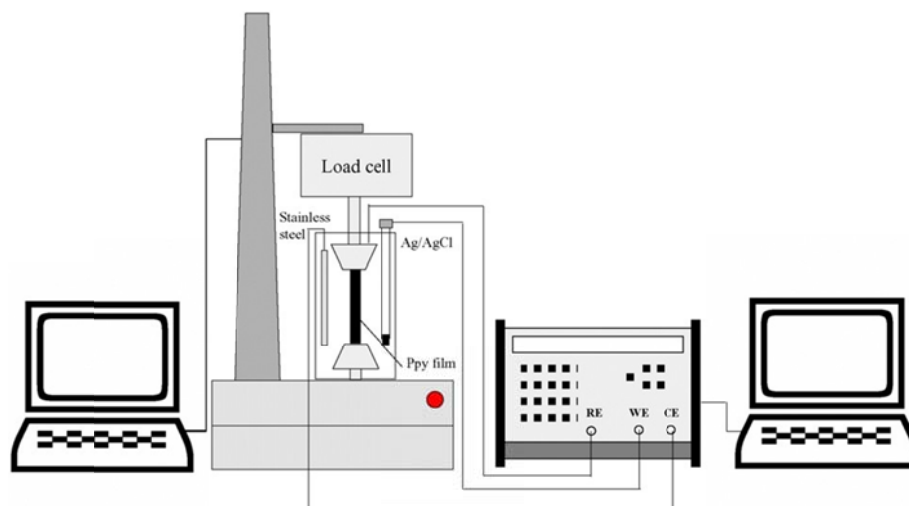


Figure 17: Electrochemical setup for the study of length variations in free-standing films under electrochemical reactions. The mechanical measurements are performed in the inner part of an electrochemical cell designed for 'in situ' measurements.

Using the same electrolyte bending bilayer (polypyrrole/tape) artificial muscles were submitted to consecutive potential cycles between 1 and -2.5 V vs Ag/AgCl at a sweep rate of 5 mV s<sup>-1</sup>. Voltammetric, or coulometric results and angular displacements were integrated in the same plot to get dynamo-voltammetric (angle vs potential) and coulo-dynamic (angle vs consumed charge) responses.

### **Results and achievements**

The literature presents controversial results related to the nature of the ions exchanged during the oxidation/reduction of conducting polymer and the potential range where those exchanges occur [86,219,230–234]. Volume changes from free-standing polypyrrole films or from the polypyrrole film of the (polypyrrole/tape) bilayer muscles are used here to try to reveal the nature of the ionic exchanges from the macroscopic dimensional changes observed during oxidation/reduction.

Length variations from free-standing polypyrrole film electrodes were followed using a universal test frame machine with a special electrochemical cell able to take the mechanical experiments while electrochemical experiments are carried out [130]. Under a constant force of 0.1 N shows the PPy film length increment during oxidation and its length decreases during its electrochemical reduction. Those results indicate that the material swells by oxidation promoting the increase of the film length and shrinks by reduction with the subsequent decrease of the film length. Nevertheless the amplitude of the displacements is not large enough to attain a good precision in narrow potential ranges.

From that point of view the bending movement from a bilayer (PPy/tape) muscle gives a very large amplitude of the bending movement during a similar electrochemical experiment. This reversible bending movement was video recorded during potential cycles from a very high cathodic potential limit (-2.5 V vs Ag/AgCl) until an anodic potential limit of 1.0 V at a scan rate of 5 mV s<sup>-1</sup>. Simultaneously voltammetric and coulometric responses from the muscles were recorded. From the coulometric results and the angle described by the muscle at each potential the coulodynamic responses were attained.

The closed loop coulometric response indicates that only reversible PPy oxidation/reduction processes are present. The film volume decrease driven by consumption of reduction charges is present in the full studied potential range: from the coulometric maximum, going to -2.5 V and at the beginning of the anodic sweep until the coulometric minimum. The film volume increase driven by consumption of oxidation charges is present between the coulometric minimum and its maximum. If irreversible reactions, such as hydrogen release, are present: the coulometric response would show open parts. These results point to reaction (1) with exchange of anions as origin of the observed movements.

Abrupt slope changes are observed from the coulometricograms during both oxidation and reduction processes. The slope represents the reaction rate and changes of the reduction reaction rate mean the presence of a new structural change in the film driven by the reaction. Through such changes it is possible to study the different structural processes affecting the electrochemical responses [235] that can be explained through the ESCR model. At the coulometric maximum the PPy film presents an open and swollen structure. Going through the cathodic potential sweep a fast reduction-shrinking is observed. Around -0.75 V vs Ag/AgCl, the slope changes to a slower reduction rate: the distance between polymeric chains has decreased during reduction-shrinking and now free space between chains is too low to allow the free expulsion of the counterions and solvent (the closing potential), and the expulsion of counterions by film reduction-conformational compaction goes on more slowly under conformational kinetic control. During oxidation, at the beginning the polymer opens its structure (oxidation-relaxation) and then it is oxidized faster (oxidation-swelling) until the coulometric maximum.

The coulodynamic responses corroborate both, the faradaic nature of the bending movement and that reaction (1) drives the exchange of anions in the full studied potential range. Those results contradict some results published for Electrochemical Quartz Crystal Microbalance (EQCM)

[86,219,230–234] indicating the presence of cation exchanges at the most cathodic potential limits. The presence of a metal between the PPy film and the quartz crystal originate hydrogen evolution in that region.

Summarizing coulometric and coulodynamic responses are excellent tools to clarify and quantify ionic exchanges, structural reaction driven processes and the Faradaic nature of the polymeric motor driven by reaction (1).

## **'Structural Electrochemistry: Conductivities and Ionic Content from Rising Reduced Polypyrrole Films'**

Toribio F. Otero and Jose G. Martinez.

Published in **Advanced Functional Materials**, year 2014, volume 24, pages 1259-1264. (IF=10.439, Q1 in 'Materials science, multidisciplinary', 'Nanoscience & nanotechnology', 'Physics, applied', 'Chemistry, multidisciplinary', 'Chemistry, physical' and 'Physics, condensed matter').

### ***Experimental***

Polypyrrole-Dodecylbenzenesulfonate (PPy-DBS) films were prepared at room temperature ( $20\pm 2^\circ\text{C}$ ) in dark conditions in a one-compartment electrochemical cell using 50 mL of an aqueous solution containing 0.2 M dodecylbenzenesulfonic acid and 0.2 M pyrrole monomer. The working electrode was a stainless steel plate having a surface area of 10 cm<sup>2</sup> on each side. Deposition was performed on both sides of the immersed part of the electrode having an area of 6.6 cm<sup>2</sup> on each side. Two large stainless steel electrodes having an area of 13.75 cm<sup>2</sup> were used as counterelectrodes. They were symmetrically placed at a distance of 1 cm from the working electrode to obtain a uniform electric field. A standard Ag/AgCl (3M KCl) electrode from Metrohm® was used as reference electrode. The PPy-DBS film was electrogenerated by applying a constant anodic current density of 0.75 mA cm<sup>-2</sup> for 100 minutes.

Free-standing polypyrrole films synthesised as described above in the general experimental part and free-standing PPy-DBS films were cut in narrow longitudinal strips getting several working electrodes from the same pristine film. Each self-supported electrode was submitted to consecutive potential sweeps. After attaining steady state voltammetric response the last potential sweep was stopped at a different potential for each of the studied films in order to get a different redox state (ionic composition) of

electrode. The higher expected concentrations correspond to oxidized polypyrrole (PPy), according with reaction (1), or to the reduced polypyrrole-dodecylbenzenesulfonate (PPy-DBS), according with reaction (2): The lower expected ionic concentrations should correspond to the most reduced and conformational packed state: PPy film after reduction up to the cathodic potential limit and PPy-DBS films after oxidation up to the anodic potential limit. Two intermediate redox states were also attained for each of the materials.

Each of the films, after water rinsing and drying, was analysed by Energy Dispersive X-ray Spectroscopy (EDX) at the SEM microscope. When electrons interact with atoms from the sample, they produce specific X-rays. EDX is based on the separation and analysis of such X-rays allowing the detection and relative quantification of the different sample elements. EDX is a semi-quantitative technique which is able to detect the presence of the different elements in each of the prepared samples and its relative content.

A Bruker AXS Microanalysis probe located in the previously mentioned scanning electron microscope (SEM-Hitachi S-3500N) was used with this aim.

The solid-state electronic conductivity of the different samples was also determined. Measurements were performed using an Agilent digital multimeter attached to a computer allowing to record I-E curves controlled by home-made software, having a precision of 1 picoampere. Each sample was washed with ultrapure water, dried and kept in dry nitrogen atmosphere in order to avoid its oxidation by the air oxygen. Conductivity measurements were performed in a glove box (MBraum) containing less than 1.2 parts per million of oxygen. The two points methodology was used, following the evolution of the current as a function of the applied potential gradient ranging between  $-5$  V and  $+5$  V. These measurements were performed at the 'Instituto de Ciencia Molecular' (IcMol) in Valencia, where the equipment is set and used every day.

## ***Results and achievements***

As stated in the previous paper, ionic exchanges during redox reaction (1) determine the actuating properties of the conducting polymer materials. This paper tries to verify the ionic composition changes there described by the coulodynamic responses. On the other hand different models from the literature are trying to explain the evolution of the electronic conductivity and ionic content in conducting polymers as a function of the oxidation state. The conducting-insulator transition model and the percolation model [236–257] claim the full reduction of every polymeric chain taking part at

## Conducting polymer actuators: From basic concepts to proprioceptive systems.

the end of the voltammetric reduction maximum, which corresponds with the closing potential from the coulombometric response. The chains from the film should become neutral (without any charge) insulators with a  $\sigma$  bond between consecutive monomeric units by total expulsion of the balancing counterions, figure 18.

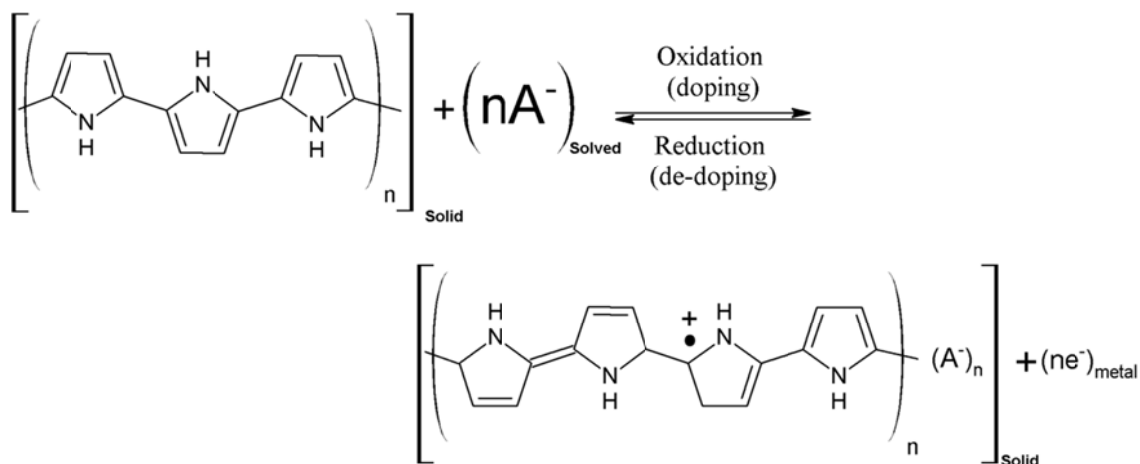


Figure 18: Electrochemical reaction (1).

On the other hand, the ESCR model[191,193–199, 202,258,259] claims that the theoretically total insulator state can not be achieved in real conducting polymers due to mechanical limitations of the conformational movements of the conducting polymer chains. For rising reduced state the distance between chains decreases, the structure closes trapping counterions, which expulsion rate (reduction rate) through the rising packed conformational structure drops requiring rising energetic consumption for subsequent expulsions of counterions. Getting full reduced, neutral and insulating chains become a long time consuming process. Most of the reduced states must include a relatively high counterion's content.

Different free-standing polypyrrole film electrodes were subjected to two consecutive voltammetric cycles in 0.1 M NaCl aqueous solutions at  $1 \text{ mV s}^{-1}$  between -1.50 and 0.65 V vs Ag/AgCl. During the second cycle, the cathodic potential was stopped at a different potential for every film: 0.65 V (oxidized and swollen material), -0.70 V (closing potential), or -1.50 V (deep reduced and packed material). A still more reduced state was attained using a different film by stopping the cathodic potential cycle at -1.50 V for 30 minutes. The anion (Cl-) content attained from energy-dispersive X-ray spectroscopy (EDX) analysis drops for rising reduced states. Even after reduction at -1.50 V for 30 min around a 15% of counterions remain trapped inside the film. The cation present in solution ( $\text{Na}^+$ ) was not detected in the polymeric film, pointing that it does not participate in the reduction processes (as claimed from EQCM results [86,219,230–234]). Summarizing,



reaction (1) describes the only oxidation/reduction reactions occurring in the film. In addition, it was not possible getting a deep reduced PPy film free of counterions.

Parallel electronic conductivities (measured in absence of oxygen to avoid oxidation in air) show decreasing values from rising reduced and conformational packed states. Samples reduced at -1.5V for 30 minutes still present a relatively high conductivity ( $0.0025 \text{ S cm}^{-1}$ ) according with the content of counterions and balanced polarons. Those conductivities are far from the insulator state expected from the conducting-insulator transition or the percolation models.

A similar study was repeated for PPy-DBS films that are expected to follow reaction (2), thus exchanging cations during redox reactions. In this case each PPy-DBS film was submitted to two consecutive voltammetric cycles in 0.1 M NaCl aqueous solutions at  $1 \text{ mV s}^{-1}$  between -1.50 and 0.65 V vs Ag/AgCl. During the second cathodic potential sweep, the potential was stopped at a different potential for every film: -1.50 (reduced and swollen material), -0.50 V (closing potential), or 0.50 V (oxidized and packed material). A more oxidized state was attained using a different film by keeping the final potential of 0.50 V for 30 minutes. EDX results show increasing concentrations of  $\text{Na}^+$  for deeper reduced films, corroborating the entrance of cations during film reduction as expected from reaction (2). Nevertheless, after the closing potential, now taking place at anodic potentials, increasing amounts of  $\text{Cl}^-$  are detected in deep oxidized (and supposedly packed) films. A mixed exchange of the ions present in solution (anions and cations) for the material at high oxidized states (the more packed states) is observed. Such detected anions does not influence the movement of bilayers [184]. Probably they are exchanged to compensate positive charges on deep oxidized PPy chains not compensated by  $\text{DBS}^-$ .

Again, the conductivity of these films was in the range of semiconductors and conductors for the different studied states (from  $0.36$  to  $12.35 \text{ S cm}^{-1}$ ). In this case, after oxidation at 0.5 V for 30 min. the conductivity decreases up to  $5.10 \text{ S cm}^{-1}$  indicating that a partial polymeric degradation (overoxidation) occurred during this polarization [260,261]. The attained values for the electronic conductivity are always in the conductor-semiconductor range allowing the subsequent re-oxidation of the film without any requirement of a back metal support in solution.

In both materials experimental conductivities and the ionic content were far from the expected for an insulator material. Thus, even for very reduced films, the conductivity is high enough to support currents of tenths of mA

cm<sup>-2</sup>. Consequently, free-standing polypyrrole films can support consecutive oxidation/reduction cycles. After reduction at high cathodic potentials the conductivity of the material is high enough to allow its re-oxidation not requiring any back metal inside the solution to support this electronic conductivity.

Thus, here it was clarified how both, the ionic content and conductivity in the polymeric gel changes along the different redox states during actuation according with reactions (1) or (2).

## **'Effect of the Electrolyte Concentration and Substrate on Conducting Polymer Actuators'**

Jose G. Martinez, Toribio F. Otero and Edwin W. H. Jager.

Published in **Langmuir**, year 2014, volume 30, pages 3894-3904. (IF=4.384, Q1 in 'Materials science, multidisciplinary', 'Chemistry, multidisciplinary' and 'Chemistry, physical').

### ***Experimental***

The influence of the presence of a metallic background and the electrolyte concentration on the actuating properties in conducting polymers has been studied employing a novel equipment recently developed at Linköping University (LiU) [135].

Sodium chloride (NaCl, from Merck) and Sodium dodecylbenzenesulfonate (NaDBS, from TCI Europe for electrogeneration and Aldrich for characterization) were used as received. Pyrrole (Sigma-Aldrich) was distilled before use under vacuum and stored at -18 °C in the refrigerator under nitrogen atmosphere. Ultrapure water was obtained from Millipore Milli-Q equipment.

Gold (Ø 0.5 mm) and platinum (Ø 1 mm) wires from Good-fellow were used as the working electrodes. The wires were electrically insulated with an electrically insulating heat-shrink polymer, but letting a length of 10 mm in the middle of the wire uncoated. Each of those wires was used for the polypyrrole electrodeposition. The counter electrode was a cylindrical gold coated plastic film, ensuring a uniform electrical field around the working electrode and thus a uniform polypyrrole coating. The gold counter electrode was constructed by first depositing a chromium layer, 3 nm thick, onto an acetate sheet. On this adhesion layer a gold film, 200 nm thick, was then

deposited. This flexible material was cut into the right shape to fit the electrochemical cell.

For the electrogeneration, a cylindrical electrochemical cell with a diameter of 2 cm was used. The working electrode was set in the centre of the cell, surrounded by the counter electrode. A silver/silver chloride (Ag/AgCl) electrode from BASi was used as the reference electrode located very close to the upper part of the working electrode. Every potential in this work is referenced to this electrode. The PPy-DBS coating was obtained in 8 mL of 0.1 M NaDBS and 0.1 M pyrrole aqueous solution by applying a constant potential of 0.55 V versus Ag/AgCl, during the time required to consume a constant charge of 140 mC. The procedure was repeated obtaining reproducible films:  $6.12 \pm 1.08 \mu\text{m}$  thick and  $0.23 \pm 0.06 \text{ mg}$  on gold and  $3.12 \pm 0.51 \mu\text{m}$  thick and  $0.21 \pm 0.03 \text{ mg}$  on platinum.

After generation the coated electrode was immersed in water during 20 seconds and then was dried for 3 minutes in air. The thickness of the polymer films were determined by difference between the diameter of the coated and uncoated wire, both measured with a Laser Scan Micrometre (LSM), keeping the position of the electrode constant. Then the polypyrrole coated electrode was weighed and the PPy-DBS mass was obtained by mass difference between coated and uncoated electrode using a Sartorius BP210D balance (precision  $10^{-5} \text{ g}$ ).

The electrochemical characterization and parallel determination of the induced dimensional variations, i.e. the expansion of the PPy-DBS layer, was performed in a transparent plastic cell of 50 mL with a rectangular cross-section. A flat and rectangular platinized titanium electrode was used as counter electrode. The reference electrolyte was 0.1 M NaDBS aqueous solution (NaCl aqueous solutions were used for the study of different electrolyte concentrations), which was filtrated through a  $0.2 \mu\text{m}$  filter to remove any potential particulate matter than could interfere with the LSM.

The LSM used here is from Mitutoyo (Mitutoyo LSM-501H) controlled through a display unit (Mitutoyo LSM-6100). From these diameter variations the diametrical (out-of-plane or perpendicular) expansion and strain of the conducting polymer could be calculated with a precision of  $0.1 \mu\text{m}$ . To obtain dynamic measurements, the output signal of the LSM (diameter of the working electrode) was fed to the potentiostat-galvanostat (for this work, Autolab PGSTAT-20) allowing a simultaneous record of electrochemical and optical responses [135], figure 19.

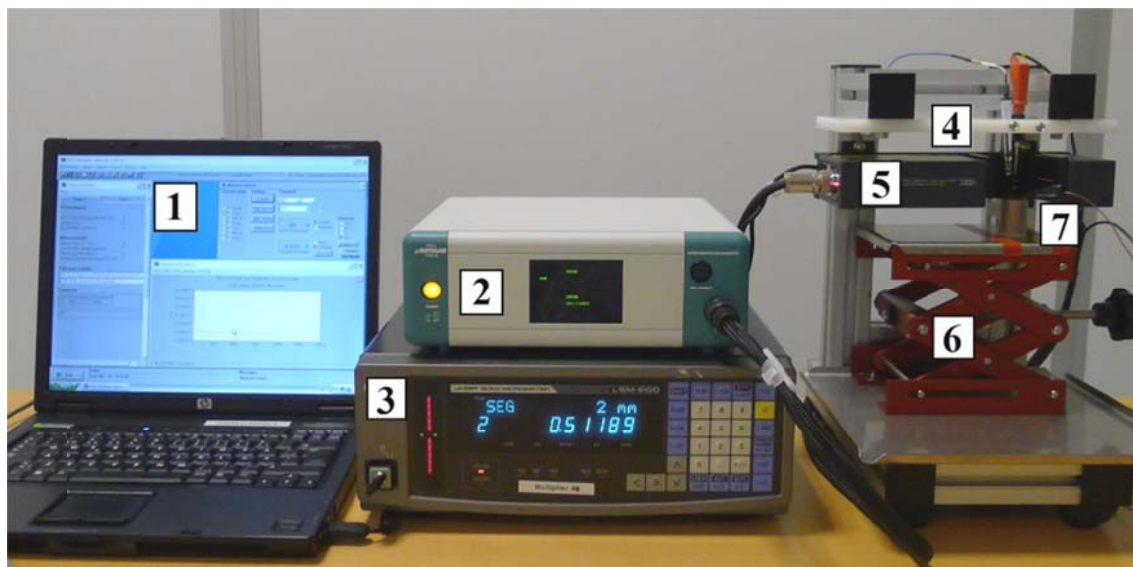


Figure 19: The laser scanner (LSM) set-up: 1. PC running GPES software, 2. Potentiostat, 3. LSM display unit, 4. Electrode support table, 5. LSM, 6. Lab jack, 7. Electrochemical cell.

Voltammetric and coulometric results were attained from both, the uncoated and PPy-DBS coated wires. From the PPy-DBS coated metallic wires, the diameter variations along consecutive potential cycles were recorded from solutions with different electrolyte concentrations. By submitting the electrode to consecutive potential steps parallel chronoamperometric and diameter variation responses were also attained.

### **Results and achievements**

Two different goals are studied here: the effect of the metallic substrate used in most of the conducting polymer actuators from the literature on the actuator electroactivity, actuating properties and lifetime; and the effect of the electrolyte concentration again on both, the electroactivity and actuating properties of the conducting polymer.

For that, a laser scan micrometre was used to detect thickness variations during electrochemical reactions with the experimental setup developed at LiU (see experimental part) during a short stay at Linköping University (Sweden) financed by the European Scientific Network for Artificial Muscle (ESNAM-Cost Action IP1003, ref. COST-ISTSM-MP1003-11575).

Regarding the study of the effect of the metallic substrate, voltammograms and coulometric curves from PPy-DBS coated and uncoated gold and platinum wires were attained in 0.0375 M NaCl aqueous solution.

For uncoated background gold and platinum wires cycled between -1.2 V and 0.5 V at 20 mV s<sup>-1</sup>, very high cathodic currents were attained at more cathodic potentials than -0.8 V vs Ag/AgCl for both metal substrates. Open

coulvoltammograms were attained, indicating the existence of irreversible charge consumed by hydrogen evolution at the metal/electrolyte interface [235]. The irreversible charge and the concomitant hydrogen evolution was always much more important from the gold wire.

Similar voltammetric and coulvoltammetric experiments were performed using PPy-DBS coated gold or platinum wires. Two cathodic potential limits, -1 V or -0.8 V, were investigated. The cathodic current at those limits was quite low compared with the overall current passing through the electrode during electrochemical reactions (2). Coulvoltammetric responses from the PPy-DBS coated gold wire up to -1.0 V still reveal some irreversible reduction charge (hydrogen evolution). After 150 cycles, voltammetric currents and reversible film oxidation/reduction charges from the coulvoltammetric closed loop decrease indicating an important decrease of the PPy-DBS electroactivity. The diameter variation per cycle also decreases after the 150 cycles in a similar proportion to the diminution of the film electroactivity.

When the PPy-DBS coated platinum electrode was cycled until a cathodic potential limit of -0.8 V the coulvoltammetric response is a closed loop: only reversible reactions (2) occur in the studied potential range. After 150 cycles the film electroactivity remains constant showing overlapping coulvoltammetric loops and giving a constant film actuation measured as diameter variation per cycle.

Thus, any parallel reaction (as hydrogen evolution or overoxidation) to those driving the mechanical actuation (reactions (1) or (2)) influences the electroactivity, actuating properties and lifetime of the conducting polymer actuator. Parallel irreversible reactions promote the polymer degradation, decreasing its electroactivity, actuating properties and life-time. By using different metals and adjusting the potential range, such parallel reactions and associated degradation can be avoided with the concomitant increase of the actuator lifetime.

The electrochemical and electro-chemo-mechanical properties of the PPy-DBS coated metals were then studied in NaCl aqueous solutions with different electrolyte concentrations (0.0375 M, 0.075 M, 0.15 M, 0.3 M, 0.6 M, 1 M, 2 M and 3 M) avoiding the parallel generation of hydrogen, or the material overoxidation, by using a Pt substrate cycled between -0.8 and 0.0 V.

Voltammetric and coulvoltammetric responses show that the film redox charge increases for rising electrolyte concentrations up to 0.15 M or 0.3 M (measured values are very close) then decreasing for higher concentrations.

A parallel evolution was observed for the PPy-DBS film actuation (diameter variation). The maximum actuation was also found in 0.3 M NaCl aqueous solution. This maximum was attributed to the number of molecules of water exchanged per exchanged ion in every electrolyte concentration during the film redox reactions. When the electrolyte concentration increases, the film reduction rate and the amount of consumed charge (applying the same overpotential) is greater, as the number of solvent molecules increases. The easier conformational movements due to the presence of a higher content of water inside the film allow a deeper film oxidation and reduction: the average number of oxidation charges per chain increases with the electrolyte concentration. Nevertheless, going ahead by increasing the electrolyte concentration, the percentage of free solvent molecules in solution decreases (it takes part of the solvated ions, salting effect). Apparently, when the salt concentration is higher than 0.3 M, the concentration of free solvent is so low that starts to influence the reaction rate. Lower concentrations of free solvent give lower reaction rates, lower solvent penetrates in the film (lower actuation), the plasticity decreases and the reaction is harder, so applying the same overpotential, the reaction is not fully completed.

Whatever the ionic concentration the variation of the film diameter follows a linear dependence of the consumed charge: As bending muscles, linear actuators (diameter variation) are Faradaic motors. Higher consumed charges ( $\Delta Q$ ) promote larger wire diameter variation ( $\Delta D$ ):

$$\Delta D = K\Delta Q \quad (5)$$

where  $K$  is a constant depending on the system (conducting polymer, electrolyte, back metal).

## **'Biomimetic Dual Sensing-Actuators Based on Conducting Polymers. Galvanostatic Theoretical Model for Actuators Sensing Temperature'**

Toribio F. Otero, Juan J. Sanchez and Jose G. Martinez.

Published in **The Journal of Physical Chemistry B**, year 2012, volume 116, pages 5279-5290. (IF=3.377, Q2 in 'Chemistry, physical').

## ***Experimental***

Polypyrrole films were electrogenerated by consumption of 28 C (polymerization charge). Average final thickness of rinsed and dried films was 13  $\mu\text{m}$ , measured using an electronic micrometre having a precision of 1  $\mu\text{m}$ . The mass of the immersed polypyrrole film (1.6026 mg) was calculated by extrapolation from the immersed film area.

Consecutive square current waves were applied to the material,  $\pm 0.75$  mA, 200 s period (0.75 mA flow for 100 s followed by -0.75 mA flow for 100 s) in the background electrolyte (0.1 M  $\text{LiClO}_4$  aqueous solution) until stationary responses (4 cycles). Symmetrical square current waves guarantee transitions between the same two oxidation states (initial reduced and final oxidized for the oxidation reaction by consumption of the same charge) every time.

For experiments at different temperatures, the electrochemical cell temperature was maintained constant during each experiment by means of a Julabo F25 cryostat ( $\pm 0.1$  °C).

Theoretical simulations were performed using MATLAB 7.7.0.0471 (R2008b) software.

## ***Results and achievements***

Once the faradaic nature of the actuators under influence of different variables was corroborated the next challenge in this thesis is the study of the simultaneous presence and description of actuating and sensing properties: that means if the reacting material can sense by itself the working conditions. The development of a theoretical description is here initiated by a quantitative description of the chronopotentiometric responses from self-supported conducting polymer films cycled under different experimental temperatures. Related to the previous paper here the experimental conditions are selected to give only reversible slow redox reactions in conducting polymer films during the electrochemical kinetic control.

The material oxidation/reduction control is performed by electrochemical methodologies. It should be expected that the attained electrochemical responses could be described from basic electrochemical models. The electrochemical kinetics from complex reactions involving two or more reactants during electron transfer and having reactions order different than 1, as reaction (1), were described during the past century [262]. For the oxidation, reaction (1) forwards (equations for the reduction reaction can be found in the paper also):

$$r = \frac{i}{FV} = k [A^-]^d [Pol^*]^e \quad (17)$$

where  $r$  represents the polymer oxidation rate,  $k$  is the oxidation rate constant, or the rate coefficient, superscripts  $d$  and  $e$  are the reaction orders,  $[A^-]$  is the concentration of anions in solution,  $[Pol^*]$  is the concentration of active centres in the polymeric film, and  $V$  is the volume of the polymeric film. In this initial stage concentrations are used instead of the most correct magnitude: activities.

Including Buttler-Volmer equation into equation (17):

$$i = FV k_0 [A^-]^d [Pol^*]^e \exp\left(\frac{(1-\alpha')nF(E-E_0)}{RT}\right) \quad (18)$$

where  $E$  is the electrode potential,  $E_0$  is the standard potential,  $\alpha'$  is the electrochemical symmetry factor,  $k_0$  is the pre-exponential factor,  $R$  is the universal gas constant ( $R=8.314 \text{ J K}^{-1} \text{ mol}^{-1}$ ), and  $T$  is the working temperature.

From equation (18), it is possible to get the potential,  $E$ :

$$E(t) = E_0 + \frac{RT}{(1-\alpha')nF} \left\{ \ln\left(\frac{i}{FV}\right) - d \ln[A^-] - e \ln\left(\frac{[Pol^*]_{initial}}{FV} - \frac{it}{FV}\right) - \ln k_0 \right\} \quad (19)$$

with  $[Pol^*]_{initial}$  being the initial concentration of active centres in the film, which will decrease during the oxidation reaction as  $(it/FV)$ , being  $it=Q$ , the oxidation charge.

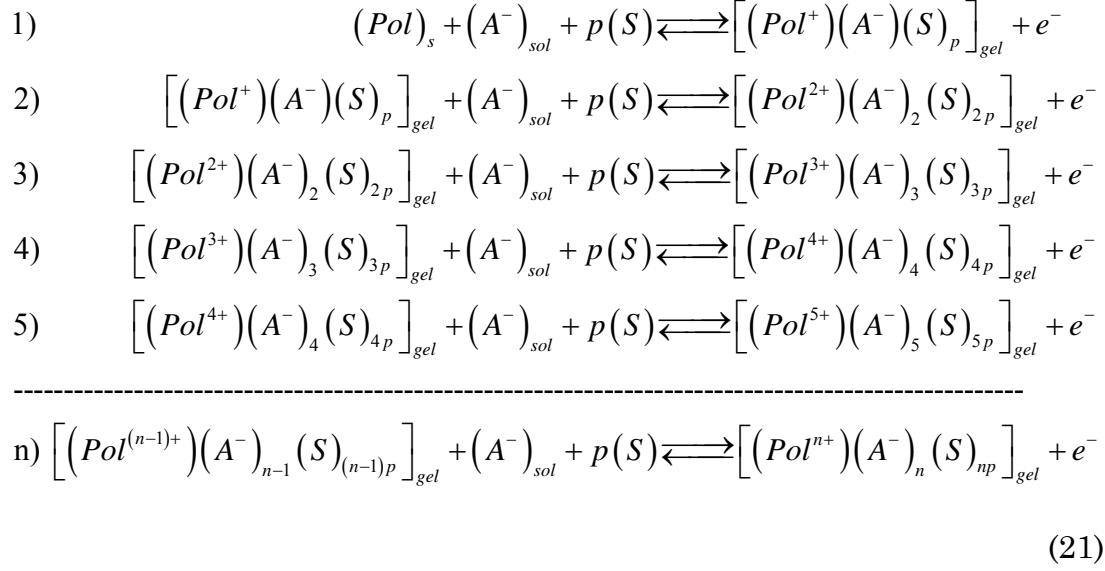
Equation (19) provides a mathematical relationship between the material potential at any oxidation time and each of the different experimental variables (temperature, electrolyte concentration, applied current). Regarding the experimental temperature influence, for a constant value of the other experimental variables, equation (19) describes a linear dependence of the material potential after a constant oxidation time from the same initial state. This relationship is in good agreement with experimental results attained from different families of conducting polymers.

Similar relationships can be attained for the consumed electrical energy by integration of the chronopotentiometric results:

$$U(t) = I \int E(t) dt \quad (20)$$



In reaction (1) the  $n$  electrons lost by chain are not equivalent. Considering the polymer science every chain has a first, second, third... ionization potential: the electrons are extracted one by one at different energies. Assuming a monodisperse film (film constituted by ideal chains of the same length) every chain loses  $n$  electrons under flow of anodic current through  $n$  consecutive oxidation steps of one electron per step:



Each of the electrochemical equilibria presented as equation (21) has increasing equilibrium potentials, as an extra energy is needed to extract an additional electron from the polymeric chain. The potential increment between that required to extract the last  $i^{\text{th}}$  electron from chains and that required to extract the first  $(i+1)^{\text{th}}$  electron is assumed to be constant ( $\Delta E$ ). Under those conditions, the theoretical stair function describes a high slope for the chronopotentiograms far from an almost constant potential expected if the  $n$  electrons were equivalent.

This can be introduced into the model through a stair function [263]:

$$E(t) = \sum_1^n E_n(t) p_n(t) = E_1(t) p_1(t) + E_2(t) p_2(t) + \dots + E_n(t) p_n(t) \tag{22}$$

where  $E_n(t)$  is given by equation (19) and  $p_n(t)$  is the unitary pulse function, being  $p_n(t)=1$  if the  $n^{\text{th}}$  electron is being extracted from every polymeric chain and  $p_n(t)=0$  if other electron different than  $n^{\text{th}}$  is being extracted under current flow.

The model was employed to simulate the responses at different temperatures. A good agreement was obtained between experimental (obtained using the experimental setup shown in figure 9) and theoretical results for both, the achieved potential at any time and the consumed

electrical energy during chronopotentiometric experiments. Sensing calibration curves were attained for both (based on potential and based on the consumed electrical energy) temperature sensors while working. Potential based sensors had a temperature sensitivity of  $-4.05 \text{ mV K}^{-1}$  for the oxidation and  $3.71 \text{ mV K}^{-1}$  for the reduction (average values). Energy based sensors sensitivity depends on the experimental time, as described by equation (19).

Equation (22) also simulates the fast empirical potential increase observed after oxidation of the active centres in the polymeric film, as expected after any oxidation (faradic) completion.

Equations (19) and (22) were obtained from basic electrochemical and polymeric principles. If the oxidation/reduction of conducting polymers sense the working temperature that means that any device based on those reactions (artificial muscles, actuators or polymeric motors; smart windows, mirrors or filters; batteries and supercapacitors; smart membranes; smart drug delivery devices, and so on) will sense the working temperature while working. All of them will be, simultaneously, temperature sensors. The device actuation signal (current) and the sensing magnitude (potential or consumed electrical energy) are present, simultaneously, in the only two connecting wires.

## **'Biomimetic Dual Sensing-Actuators: Theoretical Description. Sensing Electrolyte Concentration and Driving Current'**

Jose G. Martinez and Toribio F. Otero.

Published in **The Journal of Physical Chemistry B**, year 2012, volume 116, pages 9223-9230. (IF=3.377, Q2 in 'Chemistry, physical').

### ***Experimental***

As in the previous work, chronopotentiometric results from free-standing polypyrrole films were attained. In this case, repeating experiments from the same initial oxidation state to the same final state varying only one variable at a time: electrolyte concentration or applied current.

For the study of the influence of the electrolyte concentration, stationary (after 5 cycles) voltammograms were attained from every free-standing polypyrrole electrode in 0.1 M LiClO<sub>4</sub> aqueous solution between -1.0 and 0.6 V vs Ag/AgCl at 5 mV s<sup>-1</sup>. The potential cycling was stopped every time at

the cathodic potential limit. Then, the chronopotentiometric responses were obtained by applying five consecutive square current waves (0.75 mA for 30 s, then -0.75 mA for another 30 s). The procedure was repeated for every studied electrolyte concentration. The last (the fifth one) chronopotentiogram was used to validate the model. As in the previous paper, this procedure guarantees transitions between the same two oxidation states (initial reduced and final oxidized for the oxidation reaction by consumption of the same charge) every time, as required by the theoretical development. Experiments, under different current flow, between the same initial and final redox states, were guaranteed by keeping constant the consumed charge (2.25 mC): varying the time of current flow (equation (12)).

Theoretical simulations were also performed using MATLAB 7.7.0.0471 (R2008b) software.

### ***Results and achievements***

In order to simulate chronopotentiometric responses from conducting polymers immersed in different electrolyte concentrations or under flow of different constant currents through the working electrode (self-supported conducting polymer film or any device based on them), it was needed to include in the model a detailed description of the relationship between the electrochemical cell impedance (resistance and capacitance) with the electrolyte concentration and the applied current. An increment of the potential is expected because of the impedance of the electrochemical cell:

$$E_z = iZ \quad (23)$$

with  $E_z$  is the potential increment due to the cell impedance and  $Z$  is the cell impedance. Usually, the electrochemical characterization of conducting polymers is performed in electrochemical cells containing a volume of electrolyte high enough to accept that the concentration in the bulk remains constant during film oxidation/reduction reactions. Thus, it is possible to model the conductivity of any electrolyte as a function of the concentration of ions in solution as [215]:

$$\Lambda_m = \Lambda_m^0 - \kappa \sqrt{[A^-]} \quad (24)$$

where  $\Lambda_m$  (S cm<sup>-1</sup> mol<sup>-1</sup>) is the molar conductance,  $\Lambda_m^0$  (S cm<sup>-1</sup> mol<sup>-1</sup>) is the molar conductance at a very low concentration and the constant  $\kappa$  is a characteristic of every electrolyte.

The contribution of the electrolyte concentration  $[A^-]$  to the system impedance becomes:

$$Z = C_1 + \frac{C_2}{\sqrt{[A^-]}} \quad (25)$$

where  $C_1$  and  $C_2$  are constants.

Thus, the potential evolution is:

$$E_n(t) = E_0 + i \left( C_1 + \frac{C_2}{\sqrt{[A^-]}} \right) + (n-1)\Delta E + \frac{RT}{(1-\alpha')F} \left\{ \ln \left( \frac{i}{FV} \right) - d \ln [A^-] - e \ln \left( [Pol^*]_{initial} - \frac{it}{FV} \right) - \ln k_0 \right\} \quad (26)$$

Again, equation (26) is a dual sensing-actuating equation. In this case, the relationship is not as easy as in the case of the temperature as it is possible to find the same variables in different places.

However, looking carefully at the value of the variables, it was possible to observe that in the case of the flow of different currents, the term  $iZ$  is much more important (two orders of magnitude) than the rest of the terms where the current is present, so an almost linear relationship is expected between the applied current and the achieved potential. Similar concepts are applied to the terms where  $[A^-]$  is present.  $d \ln [A^-]$  has a very significant influence on the response and an almost semilogarithmic relationship is expected between the electrolyte concentration and the achieved potential.

Similar relationships are obtained from the consumed electrical energy in the paper.

As in the previous paper good agreements were finally attained between simulated and experimental results for both, the material potential evolution during reactions and the evolution of the consumed electrical energy.

Again, the concentration and current sensing calibration curves were attained during charge consumption (actuation). Sensitivities of the current sensor are 0.58 and 0.59 V A<sup>-1</sup>, for the theoretical and experimental, respectively, anodic currents and -0.52 or -0.54 V A<sup>-1</sup> for the theoretical and experimental, respectively, cathodic currents. Sensitivities of the concentration sensor are -62.20 and -59.20 mV M<sup>-1</sup> from the theoretical

and experimental, respectively, anodic chronopotentiograms and 48.40 and 49.40 mV M<sup>-1</sup> from the theoretical and experimental, respectively, cathodic chronopotentiograms. Again, sensitivities of the sensors, taking the consumed energy as sensing magnitude, depend on the experimental time.

## **'Mechanical awareness from sensing artificial muscles: Experiments and modeling'**

Jose G. Martinez and Toribio F. Otero.

Published in **Sensors and Actuators B: Chemical**, year 2014, volume 195, pages 365-372. (IF=3.840, Q1 in 'Chemistry, analytical', 'Electrochemistry' and 'Instruments & instrumentation').

### ***Experimental***

Bilayer (polypyrrole/tape) bending artificial muscles were constructed as specified in the experimental part (figure 10). The bilayer electrochemical behaviour was controlled in 0.5 M LiClO<sub>4</sub> aqueous solution by cyclic voltammetry between -0.7 and 0.4 V versus Ag/AgCl at 5 mV s<sup>-1</sup> (5 consecutive cycles to get stationary responses). The charge consumed during voltammetric experiments was attained by integration of the voltammetric branches. This is the maximum that the actuator can support under reversible behaviour. Outside this limit degradation processes start. Around 70 % of such charge was used for the chronopotentiometric experiments resulting in the application of five consecutive square current waves: oxidation by flow of 2 mA for 100 s (200 mC consumed charge), then reduction by flow of -2 mA for 100 s. Stationary chronopotentiometric responses were attained after two consecutive square current waves. The same displacement of the bilayer (angle, figure 15) was observed and video recorded during each cycle. This procedure was repeated trailing different steel masses attached to the muscle bottom, figure 20. The fourth of the oxidation and reduction chronopotentiometric responses were used to check the validity of the theoretical description.

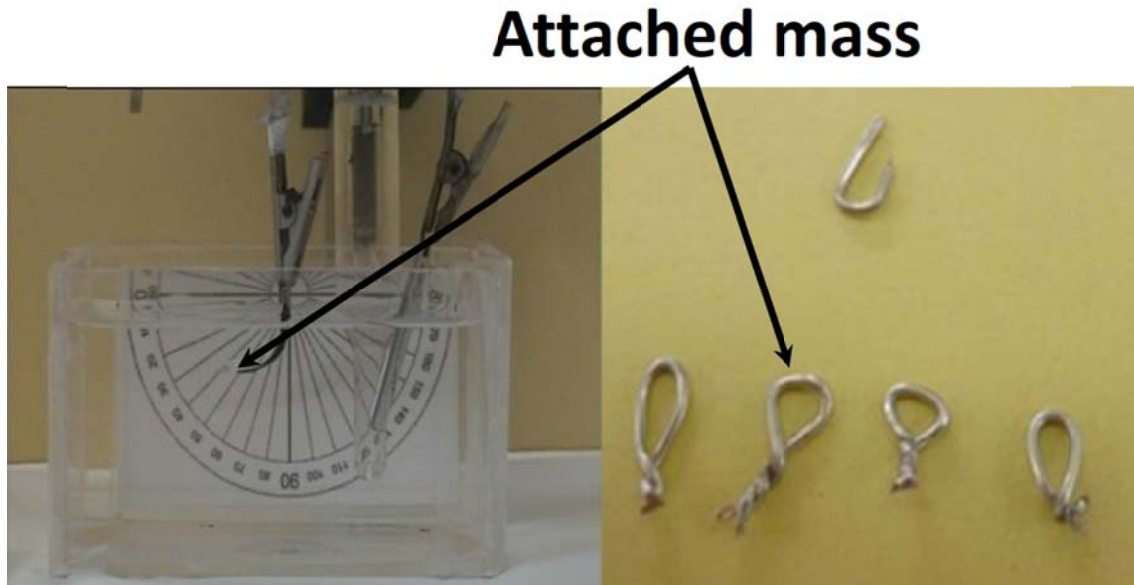


Figure 20: Attached steel masses during the study of the effect of the different masses in the proprioceptive properties of conducting polymers.

Young's modulus from the non-reactive tape and the polypyrrole films were measured with a universal test frame machine Qtest from MTS Systems. Five different samples of every material were employed to get the average values.

As in the previous works, mathematical treatment, simulations and integrals were performed employing Matlab R2008b software.

### ***Results and achievements***

Equation (19) describing the chronopotentiometric responses when artificial muscles, or self-supported film electrodes, are submitted to consecutive square current waves must include the influence of the mechanical conditions. The energetic component of the reaction coefficient is rewritten including now the mechanical work,  $\Delta(PV)$  [264]:

$$k = k_0 \exp\left(\frac{(1-\alpha)nF(E-E_0)}{RT}\right) \exp\left(\frac{\Delta(PV)}{RT}\right) \quad (27)$$

$\Delta$  means increment,  $P$  pressure and  $V$  volume.

Considering a bending bilayer artificial muscle, the term  $\Delta(PV)$  includes the different mechanical works involved in the muscle actuation and required to:

- a) bend the conducting polymer and the tape films.
- b) trail the mass of those films.
- c) trail any other mass attached to the muscle.

- d) touch and shift an obstacle.
- e) produce, or respond to, any change of internal or external pressure, strain or stress applied to the device while working.

Having here in consideration the three initial (a-c) components, equation (26) becomes:

$$E_n(t) = E_0 + iZ + \Delta E(n-1) - \frac{2l(Y_{Pol}x + Y_{tape}x + mg) \sin\left(\frac{kQ}{2}\right)}{(1-\alpha)F} + \frac{RT}{(1-\alpha)F} \left\{ \ln\left(\frac{i}{FV}\right) - d \ln[A^-] - e \ln\left([\text{Pol}^*]_{initial} - \frac{it}{FV}\right) - \ln k_0 \right\} \quad (28)$$

where  $Y_{Pol}x$  is the force required to bend the polymer layer following Hooke's law being  $Y_{Pol}$  the Young's Modulus of the conducting polymer film and  $x$  the vertical displacement produced by the bending movement;  $Y_{tape}x$  is the force required to bend the tape being  $Y_{tape}$  its Young's modulus;  $mg$  is the force required to elevate the mass  $m$  of those two layers plus any other object attached to the bilayer for a vertical distance  $x$ , being  $g$  the gravimetric acceleration ( $g=9.81 \text{ m s}^{-2}$ );  $\alpha$ , equation (5), is the angle described during the movement and  $l$  is the length of the bilayer bending inside the electrolyte.

Thus, considering the different components of the mechanical work involved in the muscle actuation the chronopotentiometric responses from artificial muscles pushing different masses attached to their bottom between the same initial and final positions were simulated. Theoretical results fit experimental results for bilayer artificial muscles carrying different attached masses.

Equation (28) describes the full multi-sensing actuating (proprioceptive) equation. It includes the different experimental variables sensed while the electrochemical device is working (a charge is being consumed). It predicts a linear relationship between the mass (muscle mass + attached mass) and the muscle potential for a constant actuation time. This equation was developed for a muscle driven by reaction (1) forwards. Similar results are attained for reaction (1) backwards-driving reaction [96] or from reactions (2). Equation (27) is a full proprioceptive equation including actuating (charge, current, through equations (5) and (6)) and sensing (potential) physical (temperature, trailed mass) and chemical (electrolyte concentration) variables was attained.

Equation (28) was attained from basic electrochemical, polymeric and mechanical concepts applied to reaction (1) forwards and backwards. Thus, any device based on conducting polymers driven by the same reaction will

behave as dual and simultaneous sensing (physical, chemical or mechanical)/actuators described by the same equations.

Again, the evolution of the consumed electrical energy with the actuation time follows similar relationships with the mechanical conditions of work.

As in the previous cases, the calibration curves of the mechanical sensor, taking the muscle potential as sensing magnitude sensitivities are  $1.00 \pm 0.10$  mV mg<sup>-1</sup> for the oxidation process and  $0.67 \pm 0.09$  mV mg<sup>-1</sup> for the reduction process. Sensitivities from sensors based on the consumed energies depend on the experimental time.

Also, a study of the energetic efficiency was carried out. Efficiencies up to 7.59%, depending on the trailed mass, were attained, higher than those reported on the literature [126,128,265,266].

The model developed in this and previous works is able to simulate and explain the biomimetic behaviour conducting polymer gel and the dual actuating-sensing (proprioceptive) behaviour of conducting polymers.

## **'Structural Electrochemistry. Chronopotentiometric Responses From Rising Compacted Polypyrrole Electrodes: Experiments and Model'**

Jose G. Martinez and Toribio F. Otero.

Published in **RSC Advances**, year 2014, volume 4, pages 29139-29145. (IF=3.708, Q1 in 'Chemistry, multidisciplinary').

### ***Experimental***

Free-standing polypyrrole films were attained as specified in the experimental part. The electrochemical behaviour was controlled in 0.5 M LiClO<sub>4</sub> aqueous solution by potential sweeps (20 consecutive cycles to ensure stationary responses) between -0.5 and 0.5 V vs Ag/AgCl at 5 mV s<sup>-1</sup>. Next, in the same solution the reproducible initial conformational state for each experiment was attained through potential steps: -0.5 V for 60 s, stepping then to 0.5 V for 60 s. Then the potential was stepped to the cathodic potential of reduction and conformational compaction (different for each experiment to get different reduction/compaction states) kept for 60 s, getting the chronoamperometric responses (figure 21) as in many other works [207,267,268]. After this reduction-packing the free-standing polypyrrole film was oxidized by applying a constant current, usually 0.5



mA (figure 21c) and the chronopotentiogram was attained (figure 21d). This experimental procedure was repeated by changing only one of the experimental variables, reduction potential, electrolyte concentration or oxidation current, every time. The influence of the applied current was studied for a constant oxidation charge (by changing the time of current flow) as in the previous works.

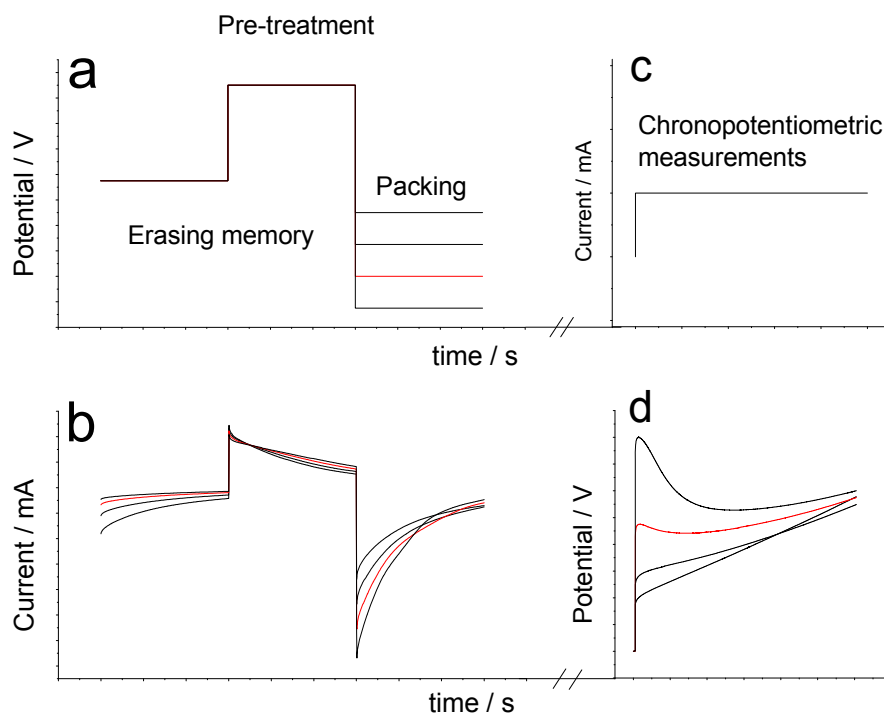


Figure 21: Experimental procedure followed to obtain the experimental responses: (a) In order to erase any previous structural memory, the free-standing electrode was submitted a potential of  $-0.5$  V for 60 s, then the potential was stepped to  $0.5$  V kept during 60 s and then the potential was stepped again to the reduction-compaction potential (usually  $-0.9$  V) for 60 s. (b) Chronoamperometric responses to those potential steps. Finally, a constant current of  $0.5$  mA was applied (c) during 100 s to obtain the chronopotentiometric responses (d).

Again, mathematical simulations were performed employing Matlab R2008b.

## **Results and achievements**

The Electrochemically Stimulated Conformational Relaxation (ESCR) model was developed to describe the effect of the initial conformational compacted states on the subsequent voltammetric, chronoamperometric or coulombometric responses from conducting polymers [189,196,199,200]. Here the goal is to expand that theoretical description to the effect of the initial conformational packed states on the chronopotentiometric responses attained when rising packed states of the material are oxidized by flow of a constant current. The theoretical equation must describe the influence of

each of the different experimental variables on the chronopotentiometric response.

Using as initial state a reduced and partially packed conformational polymeric structure, the subsequent polymeric oxidation includes two components: first the oxidation starts the conformational relaxation of the packed structure in order to allow the insertion of counterions and solvent consuming the relaxation charge,  $Q_r$ . Then, the open polymeric structure allows the free diffusion of counterions and solvent through the polymeric swollen structure until oxidation completion: the oxidation-swelling is completed under diffusion kinetic control consuming the diffusion charge,  $Q_d$ . Thus,  $Q_r$  should be considered null if the applied cathodic potential is lower than the closing potential: neither the conformational compaction nor the subsequent relaxation occur because the structure is already relaxed allowing the free diffusion of counterions and solvent. Beyond the closing potential, polymeric structure starts packing and subsequent relaxation charge could be attained from the evolution of coulombammogram at those potentials.

This has been already described for chronoamperometric experiments as [198]:

$$i(t) = i_r(t) + i_d(t) + i_{EDL}(t) = 2aQ_r t \exp(-at^2) + bQ_d \exp(-bt) + i_0 \left[ 1 - \exp\left(-\frac{t}{\tau}\right) \right] \quad (29)$$

where  $i_r(t)$  is the current fraction employed to relax and open the polymeric structure in order to open the structure so there is enough free space to allow the subsequent penetration of balancing counterions and solvent;  $i_d(t)$  is the current consumed during oxidation-swelling completion under diffusion kinetic control of the counterions;  $i_{EDL}(t)$  is the current employed to charge the electrical double layer (EDL);  $a = \frac{\pi N_0 \lambda^2}{\tau_0^2 A} \exp\left(-\frac{2\Delta H}{RT}\right)$  with  $N_0$  the number of oxidation nuclei,  $\lambda$  the length of an elemental polymeric chain,  $\tau_0$  the pre-exponential factor of the relaxation time,  $A$  the area of the polymer film,  $\Delta H$  the variation of the conformational energy in absence of electric field,  $Q_r$  the charge consumed to relax and open the polymeric structure;  $Q_d$  is the charge consumed during oxidation-swelling completion;  $i_0$  is the initial current;  $\tau$  is the time constant.

Thus, from equations (29) and (26):

$$E_n(t) = E_0 + E_z + (n-1)\Delta E + \frac{RT}{(1-\alpha)F} \left\{ \ln \left( \frac{2aQ_r t \exp(-at^2) + bQ_d \exp(-bt) + i_0 \left[ 1 - \exp\left(\frac{t}{\tau}\right) \right]}{FV} \right) - d \ln[A^-] - e \ln \left( \left[ Pol^* \right]_{initial} - \frac{Q}{FV} \right) - \ln k_0 \right\} \quad (30)$$

where  $E_z$  is the potential due to the cell impedance and  $Q=Q_r+Q_d+Q_{EDL}$  is the total consumed charge.

Experimental and theoretical chronopotentiometric responses obtained from films reduced at high cathodic potentials as specified in the experimental part (figure 21) present an initial peak attributed to the increment of energy required for the relaxation of packed conformational polymeric structures: this is a structural electrochemical response. After reduction at a lower cathodic potential than the closing potential this initial peak is not present: a continuous increase of the potential is observed during oxidation, getting a very similar response from those chronopotentiograms shown in the previous works. However, starting from rising conformational packed initial states, increasing initial chronopotentiometric peaks are observed. Beyond the peak the potential drops trying to recover the potential evolution from a reduced and non-closed structure.

The experiments were repeated, from the same conformational packed initial state in different concentration of electrolyte or by flow of different anodic currents. Theoretical chronopotentiograms from equation (30) fit the experimental chronopotentiometric responses under influence of each of the studied variables. It is worth to mention that whatever the conformational packing, the sensing properties keep working for the variables studied in the previous papers and it was possible to obtain the sensing calibration curves. A new step in the proprioceptive model was achieved in this work, being able to simulate the effect of conformational effects in complex gels including polymeric chains, ions and solvent mimicking living cell content.

## **‘Physical and chemical awareness from sensing polymeric artificial muscles. Experiments and modeling’**

Toribio F. Otero and Jose G. Martinez.

Published in **Progress in Polymer Science**, year 2014, DOI: 10.1016/j.progpolymsci.2014.09.002. (IF=26.854, Q1 in ‘Polymer science’).

## ***Experimental***

No new experimental work was performed for this work.

## ***Results and achievements***

This paper is a critical review of the state of the art of polymeric and multifunctional sensing-motors driven by electrochemical reactions, in which mechanical consistence is kept during actuation. Simultaneously a general revision is presented of the model developed from electrochemical, mechanical and polymeric principles for the description of polymeric motors sensing while working under mechanical, chemical, thermal and electrical conditions.

The term artificial muscle has been used in the literature to name almost any family of actuators. The term mechanical actuator (or usually just actuator) is applied to any transducer from any kind of energy to mechanical energy. We are concerned with electrical actuators. Here electrical artificial muscles have been differentiated between electromechanical (the transducer is based on a physical property: electrostriction, piezoelectricity, coulombic migration, electro-osmosis, electrophoresis) and electro-chemo-mechanical (the transducer is based on an electrochemical reaction) actuators. This review concerns the sensing properties of the electro-chemo-mechanical actuators, from a molecular motor (a single polymer chain) to nanoscopic, microscopic or macroscopic devices.

The origin of the actuating properties is the Faradaic volumetric variation driven by reactions (1), (2) or others (p-doping, n-doping, anion exchange or cation exchange). The result is that both, bending and linear actuators are Faradaic motors: the movement rate follows a linear dependence of the driving current, equation (5) [99,182–184].

The muscle displacement,  $\alpha$  (degrees) is under linear control of the consumed specific charge, equation (4).

After re-formulation of the Le-Chatelier principle [215] for devices working under current flow, the general actuating-sensing equations (19), (20) and (22) are reconsidered here. By substituting there  $i$  and  $Q$  obtained from equations (5) and (6) the attained equations include, for a physically uniform device, the movement rate, position and sense of the movement at any time of an actuator sensing simultaneously mechanical, thermal, chemical and electrical conditions of work. Summarising: one actuator, a mechanical sensor, a thermal sensor, a chemical sensor and an electrical sensor work simultaneously in a physically uniform device. Actuating

(current and charge) and sensing (potential and electrical work) signals are present, at any time, in the two connecting wires and can be read by the computer. Any parallel device does not exist in present technologies. Only biological evolution presents some similarity: haptic muscles. They send to our brain simultaneous information about the weight of a grasped object, the relative position of our hand at any time, the energy required to move it. This information treated by our brain produces mechanical proprioception. All this information is included by equation (19) for artificial muscles: equation (19) describes a primitive artificial proprioception.

As a first step the very simple linear or semilogarithmic sensing equations for the dual devices: artificial muscle-mechanical sensor, artificial muscle-chemical sensor, artificial muscle-thermal sensor and artificial muscle-electrical sensors were attained and checked with experimental results from previous papers getting the concomitant sensing calibration curves. Once again the good correlation between theoretical and experimental results is underlined.

In addition the model also describes the reaction end and the concomitant muscle potential step, allowing for the specific discrimination between capacitive and faradic assignment of the consumed charges.

Both the reproducibility and the robustness of those artificial muscles described by equation (5) and (6) are highlighted. The Faradaic nature described by equations (5) and (6) is kept for different muscles having different geometries or including different amounts of conducting polymers and for both artificial muscles based on conducting polymers exchanging anions or based on conducting polymers exchanging cations.

Finally, challenges are presented: the study of new materials bearing proprioceptive properties, the development of more intelligent proprioceptive robots and the open window to quantitatively describe new behavioural and psychological concepts as proprioception, thinking, memory or consciousness by physico-chemical equations. The concepts, principles, theoretical descriptions and experimental methodologies presented here could be extended in the next future to similar materials, artificial or biological, and devices or organs based on electrochemical or chemical reactions.

## **'Polyurethane microfibrinous mat template polypyrrole: Preparation and biomimetic reactive sensing capabilities'**

Yahya A. Ismail, Jose G. Martinez and Toribio F. Otero.

Published in **Journal of Electroanalytical Chemistry**, year 2014, volume 719, pages 47-53. (IF=2.871, Q2 in 'Chemistry, analytical' and 'Electrochemistry').

### ***Experimental***

Polyurethane microfibrinous mats were supplied by one of our collaborators, Dr. Yahya A. Ismail. It was put into a solution containing 0.01 M each of Lithium Trifluoromethanesulfonate (LiTFMS) and Pyrrole in 50 mL of 2:1 (v/v) mixture of water and ethanol for 2 hours at 5 °C. Then 25 mL of a 0.015 M FeCl<sub>3</sub> (oxidant) aqueous solution was slowly added to the previous solution at a rate of 2 mL/minute. The polymerization reaction was carried out at a temperature of 5 °C for a period of 4 hours. After this time the reaction mixture was maintained at 0 °C for 20 hours more. The hybrid Polyurethane/polypyrrole (PU/PPy) microfibrinous mat was taken out from the solution and washed thoroughly with distilled water and then with ethanol, after which was dried in air at room temperature.

SEM and FTIR results were attained as specified in the general experimental part.

A sample of a microfibrinous mat of length 14.2 mm and 0.7 mm width having a mass of 171 µg was stabilized by recording the voltammetric results for up to 10 consecutive cycles between -0.5 and 0.5 V versus Ag/AgCl at 20 mV s<sup>-1</sup> in 1M NaCl aqueous solution in order to get stationary voltammetric responses. The last cycle is the one studied. Then, chronopotentiometric results were obtained by submitting the sample to consecutive square waves changing one of the experimental variables: electrolyte concentration, working temperature or applied current every time, maintaining the rest constant (room temperature, 25 °C, 1 M NaCl aqueous solution, ±0.2 mA kept for 120 s each).

### ***Results and achievements***

Free-standing conducting polymer films or artificial muscles constituted by conducting polymers act, as proved in previous papers, as reactive sensors or as dual actuator-sensors. In order to improve different physical, chemical or biocompatible properties new composite and blend materials based in CPs are emerging very fast. The question here is if those materials still keep

the reactive sensing properties of the basic conducting polymers. In this work, polypyrrole coated polyurethane microfibrous mat was obtained by in situ chemical polymerization of pyrrole from aqueous solution using tetrafluoromethane sulfonate as dopant and a polyurethane microfibrous mat produced by electrospinning of a polyurethane solution as a template.

A common characterization of this new material was performed including common techniques as SEM or FTIR. SEM images showed homogeneous growth of nanostructured polypyrrole interpenetrated with the external part of each fibre of the polyurethane microfibrous mat. A uniform material with very high specific area (due to the great porosity of the polyurethane microfibrous mat) was attained.

A full electrochemical characterization was also performed, showing (for voltammetric experiments) an oxidation peak at 0.22 V and a reduction peak at -0.08 V pointing that the electroactivity of the material is given by polypyrrole. Besides, the process is diffusion controlled up to 100 mV s<sup>-1</sup> and the results are very stable during cycling.

The sensing properties of the material were studied under constant currents flow (chronopotentiometry) varying each of the experimental variables every time: temperature, electrolyte concentration or applied current. The calibration sensing curves of the electrical energy sensor of: the electrolyte concentration, the temperature or the applied current were attained. Concentration sensitivities of -1.91 mJ M<sup>-1</sup> for the material oxidation and 1.37 mJ M<sup>-1</sup> for the material reduction (concentration sensor), -7.91 x 10<sup>-2</sup> mJ K<sup>-1</sup> for the oxidation and -3.49 x 10<sup>-2</sup> mJ K<sup>-1</sup> for the reduction (temperature sensor) and 15.57 mJ A<sup>-1</sup> for oxidation and -13.99 mJ A<sup>-1</sup> for the reduction (current sensor) were attained.

The proprioceptive equation developed in previous papers also describes the reactive sensing abilities of very thin conducting polymer films coating polyurethane microfibers getting sensing calibration curves with correlation coefficients (r<sup>2</sup>) higher than 0.95 for all the studied variables.

The voltammetric responses also are influenced by changes of the experimental variables: higher concentrations and higher temperatures give more visible oxidation and reduction peaks and at lower anodic and cathodic potentials respectively.

## **'Fibroin/Polyaniline microfibrinous mat. Preparation and electrochemical characterization as reactive sensor'**

Yahya A. Ismail, Jose G. Martinez and Toribio F. Otero.

Published in **Electrochimica Acta**, year 2014, volume 123, pages 501-510. (IF: 4.086, Q1 in Electrochemistry).

### ***Experimental***

Silk fibroin microfibrinous mesh was supplied by our collaborators from IMIDA (Instituto Murciano de Investigación y Desarrollo Agrario, Murcia). It was prepared as stated in [269].

To get the Silk fibroin/PANI hybrid microfibrinous mat, the silk fibroin microfibrinous mesh was put into 50 mL of 0.005 M aniline, 1 M methanesulfonic acid (MSA) aqueous solution for 2 hours at 5 °C. 50 mL of 0.0065 M Ammonium persulfate (APS), 1 M MSA aqueous solution was slowly added to the previous solution (containing the silk fibroin mesh) at a rate of 2 mL/minute with gentle stirring. The polymerization reaction was carried out at 10 °C for 4 hours after which the temperature was kept at 5 °C for over 18 hours. The microfibrinous mat was then washed with deionized water thoroughly and dried in air at room temperature. By repeating the full procedure the thicker and most uniform polyaniline coats were attained. Two consecutive chemical polymerization processes were enough to ensure a uniform polyaniline coating of the silk fibroin mesh.

Electrical conductivity was measured by two point probe method using an Agilent 34410 multimeter at room temperature. Two metallic clamps were used to ensure the electrical contact and to keep the distance between them constant. Lengths were measured using a digital calliper (COMECTA,  $\pm 10$   $\mu\text{m}$ ) and the thickness was measured using an electronic micrometre ( $\pm 1$   $\mu\text{m}$ ).

SEM and FTIR results were attained as specified in the general experimental part.

In this case, voltammetric, coulombometric and chronopotentiometric results were obtained for the study of the sensing properties and thus, to check the model developed in the previous papers for the new materials. Again, before getting chronopotentiometric results, the microfibrinous mat was stabilized by recording the voltammetric results for up to 10 consecutive cycles between -0.15 and 0.80 V versus Ag/AgCl at a scan rate of 10 mV s<sup>-1</sup> at 27 °C in order to get a stationary voltammetric response. The last cycle is



the one studied. Then, chronopotentiometric results were obtained for different electrolyte concentrations, working temperature or applied current, changing only one variable every time from the standard experimental conditions (room temperature, 25 °C, 1 M MSA aqueous solution,  $\pm 0.3$  mA).

### ***Results and achievements***

In this work, another example of a new material having dual actuating-sensing properties is presented. In this case, microfibrinous silk fibroin mats were coated with polyaniline through in situ chemical polymerization.

The voltammetric characterization shows the two characteristic peaks of the polyaniline corroborating that the electroactivity of the mats is imparted by the polyaniline component. In the studied potential range, the consumed charge during cyclic voltammetry is reversible (the same charge was consumed to oxidize and to reduce the material), indicating that only reversible polyaniline oxidation/reduction reactions occur there. The current of the anodic and cathodic peaks increases linearly as a function of square root of the scan rate up to  $200 \text{ mV s}^{-1}$  indicating that the electrode process is diffusion controlled up to that scan rate.

Sensing properties of the mats were also studied employing the experimental procedure used during the model development: chronopotentiograms were recorded in different experimental conditions, varying only one experimental variable every time, keeping constant the applied charge (same initial/final redox states). Electrolyte concentration, pH, temperature and driving current are sensed by the material during electrochemical reaction following the same relationships stated by the model developed in the previous point: semilogarithmic relationships between the consumed electrical energy and the electrolyte concentration (and pH) was obtained, while linear relationships were attained between the consumed electrical energy and the temperature or the applied current. Thus, the model developed in previous works is also followed by the new material.

The reversible charge consumed during cyclic voltammetry also senses the reaction experimental conditions acting on the conformational movements getting deeper oxidation states for rising energetic working conditions.

This is a first report on sensing reactive properties of polyaniline based materials.

# Conclusions

New soft, wet, ionic and reactive artificial dense gels based on CPs mimic the content of the intracellular matrix (ICM) in living cells. During electrochemical reactions in liquid electrolytes the ionic content in the film changes under Faradaic reversible control. The magnitude of different concentration dependent properties also changes in a reversible way: volume, colour, stored charge, porosity, ionic or solvent content (stored chemicals), material potential, wettability, etc. Those properties are the basis of new exciting devices mimicking the behaviour of biological organs and biological functions, such as artificial muscles, smart membranes, smart drug delivery systems, sensors and biosensors and computer/neuron interfaces. A revision of the state of the art related to the different biomimetic properties and devices was performed at the beginning of this thesis.

One of the key points for the development of the different devices in order to get industrial products is whether full polymeric devices can be developed or metallic supports are required to guarantee its reversible oxidation/reduction during any device actuation. Most of the literature supports that reduced polymer films are insulators requiring metal supports. Here we have proved that, according with the literature the electronic conductivity and the parallel ionic content decrease for both, rising reduced CPs films exchanging anions or for rising oxidized CPs films exchanging cations. Nevertheless after reduction, for polymer films exchanging anions, at high cathodic potentials for 30 min or after deep oxidation, for CP films exchanging cations, over 15% of the balancing counterions remain trapped giving electronic conductivities around  $10^{-3}$  S  $\text{cm}^{-1}$ , in the semiconductors range, and allowing the subsequent cycling when reverse currents are applied. That means that under usual working conditions the lower conductivity of the materials is high enough to allow the development of full polymeric devices not requiring back metal electronic conductors. In addition it has been proved that those back metals support irreversible electrochemical reactions from moisture traces that promote the material and device degradation. Those results are in accordance with the ESCR model: the polymer reduction drives its shrinking, closing (trapping over 30% of the involved counterions) and packing its conformational structure. Getting very deep reduced states showing lower electronic conductivities than  $10^{-3}$  S  $\text{cm}^{-1}$  becomes a very difficult task taking very long (days) reduction times at high potentials.

The film reaction driven ionic exchange for charge balance and solvent exchange for osmotic balance originates reversible film volume variations, which are responsible for the material actuation in artificial muscles. Here bilayer muscles studied up to -2.5 V corroborate that the CP film reduction with expulsion of anions goes on up to a high cathodic potential. The faradaic nature of the movement (the charge controls the muscle displacement and the current controls the movement rate) was corroborated from the coulodynamic responses in the full potential range. Slopes from the coulovoltammetric responses differentiate each of the reaction driven structural processes: reduction-shrinking, reduction-compactation, oxidation-relaxation and oxidation-swelling. Thus, artificial muscles are useful tools to characterize both, ionic exchanges and structural processes driven by the CP film reaction.

During the CP reaction each of the intermolecular forces acting inside the film (polymer-polymer, polymer-anion, polymer-solvent, solvent-anion) change. The result is the exchange of balancing ions and solvent. Voltammetric, coulovoltammetric and coulodynamic responses from bilayer muscles in aqueous solutions of different anions also become suitable tools for a quantitative determination of the number of water molecules exchanged (associated with each anion) per reaction unit: pseudo ion solvation or pseudo polymer hydration number. From linear actuators checked in a large range of ionic concentrations it was corroborated that the actuation amplitude depends on both the ion concentration and the free water concentration giving a maximum. At high concentrations most of the water in solution solvates ions, decreasing the water exchanged per ion and the actuation amplitude.

The next basic question related to the polymer ionic content variation allows the development of reacting sensors. Under chemical equilibrium conditions the Le Chatelier principle and the Nernst equation describe chemical sensors. Under reaction we have reformulated the Le Chatelier principle: any energetic (mechanical, thermal, chemical, electrical) perturbation during the material reaction shifts the reaction energy adapting it to new energetic conditions.

For electroactive materials, as conducting polymers, being oxidized and reduced by square current waves any variation of the electrolyte concentration (chemical energy), temperature (thermal energy), driving current (electrical energy) or mechanical conditions (mechanical energy) must be detected by the evolution of the material potential.

## Conducting polymer actuators: From basic concepts to proprioceptive systems.

Responses from self-supported polypyrrole films (exchanging anions), from PPy-DBS films (exchanging cations), from polypyrrole coating polyurethane microfiber or from polyaniline films coating fibroin microfibers corroborate the sensing ability of the driving reaction.

The CP chemical reaction drives through the flowing current and the consumed charge the artificial muscle actuation and the same reaction drives, through the material potential evolution, mechanical, chemical, thermal and electrical sensors. Based on the simultaneity of both processes in artificial muscles the next goal was checking the dual and simultaneous actuating-sensing capability of the muscle.

Using bending bilayer muscles the dual nature: actuator-mechanical sensor, actuator-thermal sensor, actuator-chemical sensor and actuator-electrical sensor was corroborated. One uniform device works simultaneously as actuator and sensor. Both, actuating ( $I$  and  $Q$ ) and sensing ( $E$  and  $U$ ) signals are present simultaneously in the two connecting wires. It does not exist in any parallel dual device in today's technologies. Only haptic muscles from biological beings should present some similarity. Based on haptic muscles brain from humans and animals have developed proprioception.

From basic electrochemical (Buttler-Volmer kinetic equation), polymeric ( $n$  electrons are extracted or injected in a polymer chain through  $n$  consecutive energetic steps each involving one electron) and mechanical (bending and gravimetric energies) a basic multifunctional equation was developed. It describes one actuator (movement, position and consumed energy), a mechanical sensor, a thermal sensor, a chemical sensor and an electrical sensor working simultaneously (driven by the same reaction) in a physically uniform device. Theoretical results overlap experimental results for the above dual devices.

The attained multifunctional equation includes all the basic components of the human mechanical proprioception (weight of a trailed object, rate and sense of the movement, position related to a relative initial one, energy required to move it, moreover working temperature and chemical conditions or muscle fatigue): it describes the artificial mechanical proprioception.

More advanced, simpler and proprioceptive tools and robots can be developed from dual sensing-actuators.

The door is now open for, selecting from table 1, two or three different properties to develop new two, three or four tool devices. An enlarged proprioceptive equation should require the quantitative description of each of the new composition dependent property and tool.

Proprioception is considered as a psychological mechanism. Its theoretical description by a physicochemical equation opens the possibility, through the development of neuronal interfaces and electro-chemo-conformational memories, to a physicochemical quantification of other brain functions as memory, thinking or consciousness.

## References

- [1] K.J. Astrom, B. Wittenmark, Adaptive Control, 2 edition, Prentice Hall, Reading, Mass, 1994.
- [2] J.-J. Slotine, W. Li, Applied Nonlinear Control, Prentice Hall, Englewood Cliffs, N.J, 1991.
- [3] T. Gilb, Competitive Engineering: A Handbook For Systems Engineering, Requirements Engineering, and Software Engineering Using Planguage, Butterworth-Heinemann, Oxford, 2005.
- [4] H. Janocha, ed., Actuators: Basics and Applications, Springer, Berlin, 2004. [http://download.springer.com/static/pdf/988/bok%253A978-3-662-05587-8.pdf?auth66=1399453222\\_b140904f94ebfcab233df068fdaf967d&ext=.pdf](http://download.springer.com/static/pdf/988/bok%253A978-3-662-05587-8.pdf?auth66=1399453222_b140904f94ebfcab233df068fdaf967d&ext=.pdf).
- [5] N. Boysen, M. Fliedner, A. Scholl, A classification of assembly line balancing problems, *Eur. J. Oper. Res.* 183 (2007) 674–693. doi:10.1016/j.ejor.2006.10.010.
- [6] N.S. Nise, Control Systems Engineering, John Wiley & Sons, Inc., Danvers, 2008.
- [7] K. Ogata, Modern Control Engineering, 5th ed., Prentice Hall, Upper Saddle River, 2009.
- [8] A. O'Dwyer, Handbook of PI and PID Controller Tuning Rules (2nd Edition), Imperial College Press, London, GBR, 2006. <http://site.ebrary.com/lib/alltitles/docDetail.action?docID=10201146> (accessed June 17, 2014).
- [9] R.R. Schaller, Moore's law: past, present and future, *IEEE Spectr.* 34 (1997) 52–59. doi:10.1109/6.591665.
- [10] R. Burns, Advanced Control Engineering, 1 edition, Butterworth-Heinemann, Oxford ; Boston, 2001.
- [11] Aqeel-ur-Rehman, A.Z. Abbasi, N. Islam, Z.A. Shaikh, A review of wireless sensors and networks' applications in agriculture, *Comput. Stand. Interfaces.* 36 (2014) 263–270. doi:10.1016/j.csi.2011.03.004.
- [12] D. Bhattacharyya, T. Kim, S. Pal, A Comparative Study of Wireless Sensor Networks and Their Routing Protocols, *Sensors.* 10 (2010) 10506–10523. doi:10.3390/s101210506.
- [13] J.A. Stankovic, T.F. Abdelzaher, C.Y. Lu, L. Sha, J.C. Hou, Real-time communication and coordination in embedded sensor networks, *Proc. Ieee.* 91 (2003) 1002–1022. doi:10.1109/JPROC.2003.814620.

- [14] D.S. Correa, E.S. Medeiros, J.E. Oliveira, L.G. Paterno, L.H.C. Mattoso, Nanostructured Conjugated Polymers in Chemical Sensors: Synthesis, Properties and Applications, *J. Nanosci. Nanotechnol.* 14 (2014) 6509–6527. doi:10.1166/jnn.2014.9362.
- [15] C.M. Hangarter, N. Chartuprayoon, S.C. Hernandez, Y. Choa, N.V. Myung, Hybridized conducting polymer chemiresistive nano-sensors, *Nano Today*. 8 (2013) 39–55. doi:10.1016/j.nantod.2012.12.005.
- [16] D. Wei, M.J.A. Bailey, P. Andrew, T. Ryhaenen, Electrochemical biosensors at the nanoscale, *Lab. Chip.* 9 (2009) 2123–2131. doi:10.1039/b903118a.
- [17] S. Guo, E. Wang, Functional Micro/Nanostructures: Simple Synthesis and Application in Sensors, Fuel Cells, and Gene Delivery, *Acc. Chem. Res.* 44 (2011) 491–500. doi:10.1021/ar200001m.
- [18] S.A. Wilson, R.P.J. Jourdain, Q. Zhang, R.A. Dorey, C.R. Bowen, M. Willander, et al., New materials for micro-scale sensors and actuators An engineering review, *Mater. Sci. Eng. R-Rep.* 56 (2007) 1–129. doi:10.1016/j.mser.2007.03.001.
- [19] V. Ngo, A. Anpalagan, A detailed review of energy-efficient medium access control protocols for mobile sensor networks, *Comput. Electr. Eng.* 36 (2010) 383–396. doi:10.1016/j.compeleceng.2009.03.005.
- [20] M. Abbasi, M.S. Bin Abd Latiff, H. Chizari, Bioinspired Evolutionary Algorithm Based for Improving Network Coverage in Wireless Sensor Networks, *Sci. World J.* (2014) 839486. doi:10.1155/2014/839486.
- [21] G.P. Joshi, S.Y. Nam, S.W. Kim, Cognitive Radio Wireless Sensor Networks: Applications, Challenges and Research Trends, *Sensors*. 13 (2013) 11196–11228. doi:10.3390/s130911196.
- [22] J. Li, L.L.H. Andrew, C.H. Foh, M. Zukerman, H.-H. Chen, Connectivity, Coverage and Placement in Wireless Sensor Networks, *Sensors*. 9 (2009) 7664–7693. doi:10.3390/s91007664.
- [23] M. Radi, B. Dezfouli, K. Abu Bakar, M. Lee, Multipath Routing in Wireless Sensor Networks: Survey and Research Challenges, *Sensors*. 12 (2012) 650–685. doi:10.3390/s120100650.
- [24] J.A. Ashton-Miller, E.M. Wojtys, L.J. Huston, D. Fry-Welch, Can proprioception really be improved by exercises?, *Knee Surg. Sports Traumatol. Arthrosc.* 9 (2001) 128–136.
- [25] C.S. Sherrington, *The integrative action of the nervous system*, Yale University Press, New Haven, 1920.
- [26] S. Kim, C. Laschi, B. Trimmer, Soft robotics: a bioinspired evolution in robotics, *Trends Biotechnol.* 31 (2013) 23–30. doi:10.1016/j.tibtech.2013.03.002.

- [27] S. Thakoor, N. Cabrol, N. Lay, J. Chahl, D. Soccol, B. Hine, et al., Review: The benefits and applications of bioinspired flight capabilities, *J. Robot. Syst.* 20 (2003) 687–706. doi:10.1002/rob.10116.
- [28] N. Franceschini, F. Ruffier, J. Serres, A Bio-Inspired Flying Robot Sheds Light on Insect Piloting Abilities, *Curr. Biol.* 17 (2007) 329–335. doi:10.1016/j.cub.2006.12.032.
- [29] J. Chahl, S. Thakoor, N. Le Bouffant, G. Stange, M.V. Srinivasan, B. Hine, et al., Bioinspired Engineering of Exploration Systems: A Horizon Sensor/Attitude Reference System Based on the Dragonfly Ocelli for Mars Exploration Applications, *J. Robot. Syst.* 20 (2003) 35–42. doi:10.1002/rob.10068.
- [30] P. Arena, L. Fortuna, M. Frasca, G. Sicurella, An adaptive, self-organizing dynamical system for hierarchical control of bio-inspired locomotion, *IEEE Trans. Syst. Man Cybern. Part B Cybern.* 34 (2004) 1823–1837. doi:10.1109/TSMCB.2004.828593.
- [31] C. Alvarez-Lorenzo, A. Concheiro, Bioinspired drug delivery systems, *Curr. Opin. Biotechnol.* 24 (2013) 1167–1173. doi:10.1016/j.copbio.2013.02.013.
- [32] S. Fukuzumi, Bioinspired energy conversion systems for hydrogen production and storage, *Eur. J. Inorg. Chem.* (2008) 1351–1362. doi:10.1002/ejic.200701369.
- [33] S. Fukuzumi, Development of bioinspired artificial photosynthetic systems, *Phys. Chem. Chem. Phys.* 10 (2008) 2283–2297. doi:10.1039/B801198M.
- [34] L. Kong, W. Chen, Carbon Nanotube and Graphene-based Bioinspired Electrochemical Actuators, *Adv. Mater.* 26 (2014) 1025–1043. doi:10.1002/adma.201303432.
- [35] R. Potyrailo, R.R. Naik, Bionanomaterials and Bioinspired Nanostructures for Selective Vapor Sensing, *Annu. Rev. Mater. Res.* Vol 43. 43 (2013) 307–334. doi:10.1146/annurev-matsci-071312-121710.
- [36] M.E. McConney, K.D. Anderson, L.L. Brott, R.R. Naik, V.V. Tsukruk, Bioinspired Material Approaches to Sensing, *Adv. Funct. Mater.* 19 (2009) 2527–2544. doi:10.1002/adfm.200900606.
- [37] R. Mueller, R. Kuc, Biosonar-inspired technology: goals, challenges and insights, *Bioinspir. Biomim.* 2 (2007) S146–S161. doi:10.1088/1748-3182/2/4/S04.
- [38] R.H. Jacobsen, Q. Zhang, T.S. Toftegaard, Bioinspired Principles for Large-Scale Networked Sensor Systems: An Overview, *Sensors.* 11 (2011) 4137–4151. doi:10.3390/s110404137.



- [39] N. Melab, S. Cahon, E.-G. Talbi, Grid computing for parallel bioinspired algorithms, *J. Parallel Distrib. Comput.* 66 (2006) 1052–1061. doi:10.1016/j.jpdc.2005.11.006.
- [40] L. Quan-Yong, J. Lei, Bionics and Biomimetic Materials Bioinspired by Natural Spider Silks, *Chem. J. Chin. Univ.-Chin.* 31 (2010) 1065–1071.
- [41] A.R. Studart, Towards High-Performance Bioinspired Composites, *Adv. Mater.* 24 (2012) 5024–5044. doi:10.1002/adma.201201471.
- [42] A.E. Barron, R.N. Zuckermann, Bioinspired polymeric materials: in-between proteins and plastics, *Curr. Opin. Chem. Biol.* 3 (1999) 681–687. doi:10.1016/S1367-5931(99)00026-5.
- [43] J.S. Mohammed, W.L. Murphy, Bioinspired Design of Dynamic Materials, *Adv. Mater.* 21 (2009) 2361–2374. doi:10.1002/adma.200803785.
- [44] P.-Y. Chen, J. McKittrick, M.A. Meyers, Biological materials: Functional adaptations and bioinspired designs, *Prog. Mater. Sci.* 57 (2012) 1492–1704. doi:10.1016/j.pmatsci.2012.03.001.
- [45] F. Xia, L. Jiang, Bio-inspired, smart, multiscale interfacial materials, *Adv. Mater.* 20 (2008) 2842–2858. doi:10.1002/adma.200800836.
- [46] W. Barthlott, K. Koch, Biomimetic materials, *Beilstein J. Nanotechnol.* 2 (2011) 135–136. doi:10.3762/bjnano.2.16.
- [47] J. Aizenberg, P. Fratzl, Biological and Biomimetic Materials, *Adv. Mater.* 21 (2009) 387–388. doi:10.1002/adma.200803699.
- [48] F. Brandl, F. Sommer, A. Goepferich, Rational design of hydrogels for tissue engineering: Impact of physical factors on cell behavior, *Biomaterials.* 28 (2007) 134–146. doi:10.1016/j.biomaterials.2006.09.017.
- [49] P.X. Ma, Biomimetic materials for tissue engineering, *Adv. Drug Deliv. Rev.* 60 (2008) 184–198. doi:10.1016/j.addr.2007.08.041.
- [50] H. Shin, S. Jo, A.G. Mikos, Biomimetic materials for tissue engineering, *Biomaterials.* 24 (2003) 4353–4364. doi:10.1016/S0142-9612(03)00339-9.
- [51] M. Uchida, M.T. Klem, M. Allen, P. Suci, M. Flenniken, E. Gillitzer, et al., Biological containers: Protein cages as multifunctional nanoplatforms, *Adv. Mater.* 19 (2007) 1025–1042. doi:10.1002/adma.200601168.
- [52] L. Zhang, T.J. Webster, Nanotechnology and nanomaterials: Promises for improved tissue regeneration, *Nano Today.* 4 (2009) 66–80. doi:10.1016/j.nantod.2008.10.014.
- [53] L.A. Estroff, A.D. Hamilton, At the interface of organic and inorganic chemistry: Bioinspired synthesis of composite materials, *Chem. Mater.* 13 (2001) 3227–3235. doi:10.1021/cm010110k.

- [54] A.-W. Xu, Y. Ma, H. Coelfen, Biomimetic mineralization, *J. Mater. Chem.* 17 (2007) 415–449. doi:10.1039/b611918m.
- [55] X. Hou, W. Guo, L. Jiang, Biomimetic smart nanopores and nanochannels, *Chem. Soc. Rev.* 40 (2011) 2385–2401. doi:10.1039/c0cs00053a.
- [56] F.M.P. Tonelli, A.K. Santos, K.N. Gomes, E. Lorencon, S. Guatimosim, L.O. Ladeira, et al., Carbon nanotube interaction with extracellular matrix proteins producing scaffolds for tissue engineering., *Int. J. Nanomedicine.* 7 (2012) 4511–29. doi:10.2147/IJN.S33612.
- [57] A. Shekaran, A.J. Garcia, Nanoscale engineering of extracellular matrix-mimetic bioadhesive surfaces and implants for tissue engineering, *Biochim. Biophys. Acta-Gen. Subj.* 1810 (2011) 350–360. doi:10.1016/j.bbagen.2010.04.006.
- [58] K.G. Cornwell, A. Landsman, K.S. James, Extracellular matrix biomaterials for soft tissue repair., *Clin. Podiatr. Med. Surg.* 26 (2009) 507–23. doi:10.1016/j.cpm.2009.08.001.
- [59] L. Stryer, *Biochemistry*, W.H. Freeman and Company, New York, 1995.
- [60] T.F. Otero, J.G. Martinez, Biomimetic intracellular matrix (ICM) materials, properties and functions. Full integration of actuators and sensors, *J. Mater. Chem. B.* 1 (2013) 26–38. doi:10.1039/C2TB00176D.
- [61] T.F. Otero, Soft, wet, and reactive polymers. Sensing artificial muscles and conformational energy, *J. Mater. Chem.* 19 (2009) 681–689. doi:10.1039/b809485c.
- [62] T.F. Otero, J.G. Martinez, J. Arias-Pardilla, Biomimetic electrochemistry from conducting polymers. A review: Artificial muscles, smart membranes, smart drug delivery and computer/neuron interfaces, *Electrochimica Acta.* 84 (2012) 112–128. doi:10.1016/j.electacta.2012.03.097.
- [63] T.F. Otero, Biomimetic Conducting Polymers: Synthesis, Materials, Properties, Functions, and Devices, *Polym. Rev.* 53 (2013) 311–351. doi:10.1080/15583724.2013.805772.
- [64] T.F. Otero, Biomimicking materials with smart polymers, in: M. Elices, R.W. Cahn (Eds.), *Struct. Biol. Mater. Des. Struct.-Prop. Relatsh.*, Pergamon, Amsterdam, 2000.
- [65] V.K. Thakur, G. Ding, J. Ma, P.S. Lee, X. Lu, Hybrid Materials and Polymer Electrolytes for Electrochromic Device Applications, *Adv. Mater.* 24 (2012) 4071–4096. doi:10.1002/adma.201200213.
- [66] T.F. Otero, J. Padilla, Anodic shrinking and compaction of polypyrrole blend: electrochemical reduction under conformational relaxation kinetic control, *J. Electroanal. Chem.* 561 (2004) 167–171. doi:10.1016/j.jelechem.2003.08.001.

- [67] D.R. Rosseinsky, R.J. Mortimer, Electrochromic systems and the prospects for devices, *Adv. Mater.* 13 (2001) 783–793. doi:10.1002/1521-4095(200106)13:11<783::AID-ADMA783>3.0.CO;2-D.
- [68] J.D. Stenger-Smith, Intrinsically electrically conducting polymers. Synthesis, characterization, and their applications, *Prog. Polym. Sci.* 23 (1998) 57–79. doi:10.1016/S0079-6700(97)00024-5.
- [69] J.A. Irvin, D.J. Irvin, J.D. Stenger-Smith, Electroactive Polymers for Batteries and Supercapacitors, in: T.A. Skotheim, R.L. Elsenbaumer, J.R. Reynolds (Eds.), *Handb. Conduct. Polym.*, CRC Press, Boca Raton, 2007.
- [70] H.E. Katz, P.C. Searson, T.O. Poehler, Batteries and charge storage devices based on electronically conducting polymers, *J. Mater. Res.* 25 (2010) 1561–1574. doi:10.1557/JMR.2010.0201.
- [71] P. Novak, K. Muller, K. Santhanam, O. Haas, Electrochemically active polymers for rechargeable batteries, *Chem. Rev.* 97 (1997) 207–281. doi:10.1021/cr941181o.
- [72] D. Svirskis, J. Travas-Sejdic, A. Rodgers, S. Garg, Electrochemically controlled drug delivery based on intrinsically conducting polymers, *J. Controlled Release.* 146 (2010) 6–15. doi:10.1016/j.jconrel.2010.03.023.
- [73] A.A. Entezami, B. Massoumi, Artificial muscles, biosensors and drug delivery systems based on conducting polymers: A review, *Iran. Polym. J.* 15 (2006) 13–30.
- [74] T.K. Das, S. Prusty, Review on Conducting Polymers and Their Applications, *Polym.-Plast. Technol. Eng.* 51 (2012) 1487–1500. doi:10.1080/03602559.2012.710697.
- [75] S. Geetha, C.R.K. Rao, M. Vijayan, D.C. Trivedi, Biosensing and drug delivery by polypyrrole, *Anal. Chim. Acta.* 568 (2006) 119–125. doi:10.1016/j.aca.2005.10.011.
- [76] T.F. Otero, Conducting Polymers, Electrochemistry, and Biomimicking Processes, in: R.E. White, J.O. Bockris, B.E. Conway (Eds.), *Mod. Asp. Electrochem.*, Springer US, New York, 1999: pp. 307–434. [http://link.springer.com/chapter/10.1007/0-306-46917-0\\_3](http://link.springer.com/chapter/10.1007/0-306-46917-0_3) (accessed January 9, 2013).
- [77] D.T. Simon, S. Kurup, K.C. Larsson, R. Hori, K. Tybrandt, M. Gojny, et al., Organic electronics for precise delivery of neurotransmitters to modulate mammalian sensory function, *Nat. Mater.* 8 (2009) 742–746. doi:10.1038/NMAT2494.
- [78] R. Ravichandran, S. Sundarrajan, J.R. Venugopal, S. Mukherjee, S. Ramakrishna, Applications of conducting polymers and their issues in biomedical engineering, *J. R. Soc. Interface.* 7 (2010) S559–S579. doi:10.1098/rsif.2010.0120.focus.

- [79] M. Asplund, T. Nyberg, O. Inganäs, Electroactive polymers for neural interfaces, *Polym. Chem.* 1 (2010) 1374–1391. doi:10.1039/c0py00077a.
- [80] R.A. Green, N.H. Lovell, L.A. Poole-Warren, Impact of co-incorporating laminin peptide dopants and neurotrophic growth factors on conducting polymer properties, *Acta Biomater.* 6 (2010) 63–71. doi:10.1016/j.actbio.2009.06.030.
- [81] A.F. Quigley, J.M. Razal, B.C. Thompson, S.E. Moulton, M. Kita, E.L. Kennedy, et al., A Conducting-Polymer Platform with Biodegradable Fibers for Stimulation and Guidance of Axonal Growth, *Adv. Mater.* 21 (2009) 4393–4396. doi:10.1002/adma.200901165.
- [82] M.J. Ariza, T.F. Otero, Ionic diffusion across oxidized polypyrrole membranes and during oxidation of the free-standing film, *Colloids Surf. Physicochem. Eng. Asp.* 270–271 (2005) 226–231. doi:10.1016/j.colsurfa.2005.06.006.
- [83] M.J. Ariza, T.F. Otero, Nitrate and chloride transport through a smart membrane, *J. Membr. Sci.* 290 (2007) 241–249. doi:10.1016/j.memsci.2006.12.040.
- [84] P. Burgmayer, R. Murray, An ion gate membrane - electrochemical control of ion permeability through a membrane with an embedded electrode, *J. Am. Chem. Soc.* 104 (1982) 6139–6140. doi:10.1021/ja00386a061.
- [85] P. Burgmayer, R. Murray, Ion Gate Electrodes - Polypyrrole as a Switchable Ion Conductor Membrane, *J. Phys. Chem.* 88 (1984) 2515–2521. doi:10.1021/j150656a017.
- [86] M.N. Akieh, A. Varga, R.-M. Latonen, S.F. Ralph, J. Bobacka, A. Ivaska, Simultaneous monitoring of the transport of anions and cations across polypyrrole based composite membranes, *Electrochimica Acta.* 56 (2011) 3507–3515. doi:10.1016/j.electacta.2010.08.095.
- [87] T. Ahuja, I.A. Mir, D. Kumar, Rajesh, Biomolecular immobilization on conducting polymers for biosensing applications, *Biomaterials.* 28 (2007) 791–805. doi:10.1016/j.biomaterials.2006.09.046.
- [88] Deepshikha, T. Basu, A Review on Synthesis and Characterization of Nanostructured Conducting Polymers (NSCP) and Application in Biosensors, *Anal. Lett.* 44 (2011) 1126–1171. doi:10.1080/00032719.2010.511734.
- [89] M. Singh, P.K. Kathuroju, N. Jampana, Polypyrrole based amperometric glucose biosensors, *Sens. Actuators B-Chem.* 143 (2009) 430–443. doi:10.1016/j.snb.2009.09.005.
- [90] L. Xia, Z. Wei, M. Wan, Conducting polymer nanostructures and their application in biosensors, *J. Colloid Interface Sci.* 341 (2010) 1–11. doi:10.1016/j.jcis.2009.09.029.

- [91] U. Lange, N.V. Roznyatouskaya, V.M. Mirsky, Conducting polymers in chemical sensors and arrays, *Anal. Chim. Acta.* 614 (2008) 1–26. doi:10.1016/j.aca.2008.02.068.
- [92] B. Adhikari, S. Majumdar, Polymers in sensor applications, *Prog. Polym. Sci.* 29 (2004) 699–766. doi:10.1016/j.progpolymsci.2004.03.002.
- [93] M.A. Rahman, P. Kumar, D.-S. Park, Y.-B. Shim, Electrochemical sensors based on organic conjugated polymers, *Sensors.* 8 (2008) 118–141. doi:10.3390/s8010118.
- [94] T.F. Otero, E. Angulo, J. Rodríguez, C. Santamaría, Electrochemomechanical properties from a bilayer: polypyrrole / non-conducting and flexible material — artificial muscle, *J. Electroanal. Chem.* 341 (1992) 369–375. doi:10.1016/0022-0728(92)80495-P.
- [95] Q. Pei, O. Inganas, Conjugated Polymers and the Bending Cantilever Method - Electrical Muscles and Smart Devices, *Adv. Mater.* 4 (1992) 277–278. doi:10.1002/adma.19920040406.
- [96] T.F. Otero, M.T. Cortes, A sensing muscle, *Sens. Actuators B-Chem.* 96 (2003) 152–156.
- [97] T. Otero, M. Cortes, G. Arenas, Linear movements from two bending triple-layers, *Electrochimica Acta.* 53 (2007) 1252–1258. doi:10.1016/j.electacta.2007.01.081.
- [98] F. García-Córdova, L. Valero, Y.A. Ismail, T.F. Otero, Biomimetic polypyrrole based all three-in-one triple layer sensing actuators exchanging cations, *J. Mater. Chem.* 21 (2011) 17265–17272. doi:10.1039/C1JM13374H.
- [99] L.V. Conzuelo, J. Arias-Pardilla, J.V. Cauich-Rodríguez, M.A. Smit, T.F. Otero, Sensing and Tactile Artificial Muscles from Reactive Materials, *Sensors.* 10 (2010) 2638–2674. doi:10.3390/s100402638.
- [100] Y.A. Ismail, J.G. Martínez, A.S. Al Harrasi, S.J. Kim, T.F. Otero, Sensing characteristics of a conducting polymer/hydrogel hybrid microfiber artificial muscle, *Sens. Actuators B Chem.* 160 (2011) 1180–1190. doi:10.1016/j.snb.2011.09.044.
- [101] L. Valero, J. Arias-Pardilla, M. Smit, J. Cauich-Rodríguez, T.F. Otero, Polypyrrole free-standing electrodes sense temperature or current during reaction, *Polym. Int.* 59 (2010) 337–342. doi:10.1002/pi.2750.
- [102] T. Otero, M. Cortes, Artificial muscles with tactile sensitivity, *Adv. Mater.* 15 (2003) 279–282. doi:10.1002/adma.200390066.
- [103] F. Vidal, C. Plesse, P.-H. Aubert, L. Beouch, F. Tran-Van, G. Palaprat, et al., Poly(3,4-ethylenedioxythiophene)-containing semi-interpenetrating polymer networks: a versatile concept for the design of optical or mechanical electroactive devices, *Polym. Int.* 59 (2010) 313–320. doi:10.1002/pi.2772.

- [104] J.-G. Barbara, F. Clarac, Historical concepts on the relations between nerves and muscles, *Brain Res.* 1409 (2011) 3–22.  
doi:10.1016/j.brainres.2011.06.009.
- [105] G.G. Matthews, *Cellular Physiology of Nerve and Muscle*, Wiley-Blackwell, Hoboken, NJ, USA, 2009.  
<http://site.ebrary.com/lib/alltitles/docDetail.action?docID=10303743>  
(accessed May 26, 2014).
- [106] Q. Pei, O. Inganas, Electrochemical Applications of the Bending Beam Method .1. Mass-Transport and Volume Changes in Polypyrrole During Redox, *J. Phys. Chem.* 96 (1992) 10507–10514.  
doi:10.1021/j100204a071.
- [107] A. Katchalsky, Rapid Swelling and Deswelling of Reversible Gels of Polymeric Acids by Ionization, *Experientia.* 5 (1949) 319–320.  
doi:10.1007/BF02172636.
- [108] A. Katchalsky, H. Eisenberg, Polyvinylphosphate Contractile Systems, *Nature.* 166 (1950) 267–267. doi:10.1038/166267a0.
- [109] W. Kuhn, B. Hargitay, A. Katchalsky, H. Eisenberg, Reversible Dilation and Contraction by Changing the State of Ionization, *Nature.* 165 (1950) 514–516. doi:10.1038/165514a0.
- [110] Y. Osada, Y. Saito, Mechanochemical Energy-Conversion in a Polymer Membrane by Thermo-Reversible Polymer-Polymer Interactions, *Makromol. Chem.-Macromol. Chem. Phys.* 176 (1975) 2761–2764.
- [111] T. Tanaka, D. Fillmore, Kinetics of Swelling of Gels, *J. Chem. Phys.* 70 (1979) 1214–1218. doi:10.1063/1.437602.
- [112] T. Tanaka, I. Nishio, S. Sun, S. Uenonishio, Collapse of Gels in an Electric-Field, *Science.* 218 (1982) 467–469.  
doi:10.1126/science.218.4571.467.
- [113] T.A. Skotheim, J. Reynolds, eds., *Handbook of Conducting Polymers*, 3rd ed., CRC Press, New York, 2006.
- [114] R. Tiwari, E. Garcia, The state of understanding of ionic polymer metal composite architecture: a review, *Smart Mater. Struct.* 20 (2011) 083001. doi:10.1088/0964-1726/20/8/083001.
- [115] D. Pugal, K. Jung, A. Aabloo, K.J. Kim, Ionic polymer-metal composite mechano-electrical transduction: review and perspectives, *Polym. Int.* 59 (2010) 279–289. doi:10.1002/pi.2759.
- [116] T. Mirfakhrai, J.D.W. Madden, R.H. Baughman, Polymer artificial muscles, *Mater. Today.* 10 (2007) 30–38. doi:10.1016/S1369-7021(07)70048-2.
- [117] P. Brochu, Q. Pei, Advances in Dielectric Elastomers for Actuators and Artificial Muscles, *Macromol. Rapid Commun.* 31 (2010) 10–36.  
doi:10.1002/marc.200900425.

- [118] A. DellaSanta, D. DeRossi, A. Mazzoldi, Performance and work capacity of a polypyrrole conducting polymer linear actuator, *Synth. Met.* 90 (1997) 93–100.
- [119] V. Balzani, A. Credi, B. Ferrer, S. Silvi, M. Venturi, Artificial Molecular Motors and Machines: Design Principles and Prototype Systems, in: T.R. Kelly (Ed.), *Mol. Mach.*, Springer Berlin Heidelberg, Berlin, 2005: pp. 1–27.  
[http://link.springer.com/chapter/10.1007/128\\_008](http://link.springer.com/chapter/10.1007/128_008) (accessed August 19, 2013).
- [120] A.P. Davis, Nanotechnology: Synthetic molecular motors, *Nature.* 401 (1999) 120–121. doi:10.1038/43576.
- [121] T.F. Otero, From Electrochemically-Driven Conformational Polymeric States to Macroscopic and Sensing Artificial Muscles., in: J.-P. Sauvage, P. Gaspard (Eds.), *Non-Covalent Assem. Mol. Mach.*, Wiley-VCH, Weinheim, 2011: pp. 443–452.
- [122] R. Kiefer, S.Y. Chu, P.A. Kilmartin, G.A. Bowmaker, R.P. Cooney, J. Travas-Sejdic, Mixed-ion linear actuation behaviour of polypyrrole, *Electrochimica Acta.* 52 (2007) 2386–2391.  
 doi:10.1016/j.electacta.2006.08.058.
- [123] L. Bay, K. West, P. Sommer-Larsen, S. Skaarup, M. Benslimane, A Conducting Polymer Artificial Muscle with 12 % Linear Strain, *Adv. Mater.* 15 (2003) 310–313. doi:10.1002/adma.200390075.
- [124] A. Mazzoldi, C. Degl’Innocenti, M. Michelucci, D. De Rossi, Actuating properties of polyaniline fibers under electrochemical stimulation, *Mater. Sci. Eng. C-Biomim. Mater. Sens. Syst.* 6 (1998) 65–72.  
 doi:10.1016/S0928-4931(98)00036-8.
- [125] G.M. Spinks, L. Liu, G.G. Wallace, D.Z. Zhou, Strain response from polypyrrole actuators under load, *Adv. Funct. Mater.* 12 (2002) 437–440. doi:10.1002/1616-3028(20020618)12:6/7<437::AID-ADFM437>3.0.CO;2-I.
- [126] B.H. Qi, W. Lu, B.R. Mattes, Strain and energy efficiency of polyaniline fiber electrochemical actuators in aqueous electrolytes, *J. Phys. Chem. B.* 108 (2004) 6222–6227. doi:10.1021/jp031092s.
- [127] J.M. Sansinena, J.B. Gao, H.L. Wang, High-performance, monolithic polyaniline electrochemical actuators, *Adv. Funct. Mater.* 13 (2003) 703–709. doi:10.1002/adfm.200304347.
- [128] K. Kaneto, H. Fujisue, M. Kunifusa, W. Takashima, Conducting polymer soft actuators based on polypyrrole films - energy conversion efficiency, *Smart Mater. Struct.* 16 (2007) S250–S255.  
 doi:10.1088/0964-1726/16/2/S08.
- [129] T.F. Otero, J.J. Lopez Cascales, G. Vazquez Arenas, Mechanical characterization of free-standing polypyrrole film, *Mater. Sci. Eng. C-*

- Biomim. Supramol. Syst. 27 (2007) 18–22.  
doi:10.1016/j.msec.2005.11.002.
- [130] T.F. Otero, G. Vazquez Arenas, J.J. Lopez Cascales, Effect of the doping ion on the electrical response of a free-standing polypyrrole strip subjected to different preloads: Perspectives and limitations associated with the use of these devices as actuators, *Macromolecules*. 39 (2006) 9551–9556. doi:10.1021/ma062067y.
- [131] E. Smela, N. Gadegaard, Surprising volume change in PPy(DBS): An atomic force microscopy study, *Adv. Mater.* 11 (1999) 953–956. doi:10.1002/(SICI)1521-4095(199908)11:11<953::AID-ADMA953>3.0.CO;2-H.
- [132] M.S. Cho, J.J. Choi, T.S. Kim, Y. Lee, In situ three-dimensional analysis of the linear actuation of polypyrrole micro-rod actuators using optical microscopy, *Sens. Actuators B-Chem.* 156 (2011) 218–221. doi:10.1016/j.snb.2011.04.021.
- [133] K. Bienkowski, M. Strawski, M. Szklarczyk, The determination of the thickness of electrodeposited polymeric films by AFM and electrochemical techniques, *J. Electroanal. Chem.* 662 (2011) 196–203. doi:10.1016/j.jelechem.2011.06.014.
- [134] E. Smela, N. Gadegaard, Volume change in polypyrrole studied by atomic force microscopy, *J. Phys. Chem. B.* 105 (2001) 9395–9405. doi:10.1021/jp004126u.
- [135] D. Melling, S. Wilson, E.W.H. Jager, The effect of film thickness on polypyrrole actuation assessed using novel non-contact strain measurements, *Smart Mater. Struct.* 22 (2013) 104021. doi:10.1088/0964-1726/22/10/104021.
- [136] K. Yamato, K. Kaneto, Tubular linear actuators using conducting polymer, polypyrrole, *Anal. Chim. Acta.* 568 (2006) 133–137. doi:10.1016/j.aca.2005.12.030.
- [137] S. Hara, T. Zama, S. Sewa, W. Takashima, K. Kaneto, Highly Stretchable and Powerful Polypyrrole Linear Actuators, *Chem. Lett.* 32 (2003) 576–577. doi:10.1246/cl.2003.576.
- [138] S. Hara, T. Zama, W. Takashima, K. Kaneto, Tris(trifluoromethylsulfonyl)methide-doped polypyrrole as a conducting polymer actuator with large electrochemical strain, *Synth. Met.* 156 (2006) 351–355. doi:10.1016/j.synthmet.2006.01.001.
- [139] K. Kaneto, H. Suematsu, K. Yamato, Conducting Polymer Soft Actuators Based on Polypyrrole -Training Effect and Fatigue, *Adv. Sci. Technol.* 61 (2008) 122–130. doi:10.4028/www.scientific.net/AST.61.122.



- [140] K. Kaneto, H. Suematsu, K. Yamato, Training effect and fatigue in polypyrrole-based artificial muscles, *Bioinspir. Biomim.* 3 (2008) 035005. doi:10.1088/1748-3182/3/3/035005.
- [141] T.F. Otero, J.G. Martinez, Artificial Muscles: A Tool To Quantify Exchanged Solvent during Biomimetic Reactions, *Chem. Mater.* 24 (2012) 4093–4099. doi:10.1021/cm302847r.
- [142] A.S. Hutchison, T.W. Lewis, S.E. Moulton, G.M. Spinks, G.G. Wallace, Development of polypyrrole-based electromechanical actuators, *Synth. Met.* 113 (2000) 121–127. doi:10.1016/S0379-6779(00)00190-9.
- [143] W. Lu, A. Fadeev, B. Qi, E. Smela, B. Mattes, J. Ding, et al., Use of ionic liquids for pi-conjugated polymer electrochemical devices, *Science.* 297 (2002) 983–987. doi:10.1126/science.1072651.
- [144] T.F. Otero, E. Angulo, F. Rodríguez, C. Santamaría, Dispositivos laminares que emplean polímeros conductores capaces de provocar movimientos mecánicos., *ES 2 048 086*, 1994.
- [145] T.F. Otero, J. Rodriguez, C. Santamaria, Músculos artificiales formados por multicapas: polímeros conductores-polímeros no conductores, *ES 2062930*, n.d.
- [146] E. Smela, O. Inghanas, Q. Pei, I. Lundstrom, Electrochemical Muscles - Micromachining Fingers and Corkscrews, *Adv. Mater.* 5 (1993) 630–632. doi:10.1002/adma.19930050905.
- [147] E.W.H. Jager, E. Smela, O. Inghanas, Microfabricating conjugated polymer actuators, *Science.* 290 (2000) 1540–1545. doi:10.1126/science.290.5496.1540.
- [148] E.W.H. Jager, O. Inghanas, I. Lundstrom, Microrobots for micrometer-size objects in aqueous media: Potential tools for single-cell manipulation, *Science.* 288 (2000) 2335–2338. doi:10.1126/science.288.5475.2335.
- [149] S.D. Deshpande, J. Kim, S.R. Yun, New electro-active paper actuator using conducting polypyrrole: actuation behaviour in LiClO(4) acetonitrile solution, *Synth. Met.* 149 (2005) 53–58. doi:10.1016/j.synthmet.2004.11.001.
- [150] S.D. Deshpande, J. Kim, S.R. Yun, Studies on conducting polymer electroactive paper actuators: effect of humidity and electrode thickness, *Smart Mater. Struct.* 14 (2005) 876–880. doi:10.1088/0964-1726/14/4/048.
- [151] S.J. Higgins, K.V. Lovell, R.M.G. Rajapakse, N.M. Walsby, Grafting and electrochemical characterisation of poly-(3,4-ethylenedioxythiophene) films, on Nafion and on radiation-grafted polystyrenesulfonate-polyvinylidene fluoride composite surfaces, *J. Mater. Chem.* 13 (2003) 2485–2489. doi:10.1039/b303424k.

- [152] R.H. Baughman, Conducting polymer artificial muscles, *Synth. Met.* 78 (1996) 339–353. doi:10.1016/0379-6779(96)80158-5.
- [153] G. Alici, A. Punning, H.R. Shea, Enhancement of actuation ability of ionic-type conducting polymer actuators using metal ion implantation, *Sens. Actuators B-Chem.* 157 (2011) 72–84. doi:10.1016/j.snb.2011.03.028.
- [154] G. Alici, N.N. Huynh, Predicting force output of trilayer polymer actuators, *Sens. Actuators -Phys.* 132 (2006) 616–625. doi:10.1016/j.sna.2006.02.046.
- [155] U.L. Zainudeen, M.A. Careem, S. Skaarup, PEDOT and PPy conducting polymer bilayer and trilayer actuators, *Sens. Actuators B-Chem.* 134 (2008) 467–470. doi:10.1016/j.snb.2008.05.027.
- [156] S. John, G. Alici, C. Cook, Frequency response of polypyrrole trilayer actuator displacement, in: Y. Bar-Cohen (Ed.), *Electroact. Polym. Actuators Devices Eapad 2008*, Spie-Int Soc Optical Engineering, Bellingham, 2008.
- [157] G.Y. Han, G.Q. Shi, High-response tri-layer electrochemical actuators based on conducting polymer films, *J. Electroanal. Chem.* 569 (2004) 169–174. doi:10.1016/j.jelechem.2004.02.025.
- [158] Q. Yao, G. Alici, G.A. Spinks, Feedback control of tri-layer polymer actuators to improve their positioning ability and speed of response, *Sens. Actuators -Phys.* 144 (2008) 176–184. doi:10.1016/j.sna.2008.01.005.
- [159] J.M. Gere, B.J. Goodno, Gere, *Mechanics of Materials*, Edición: Revised., Cengage Learning, Stamford, CT, 2012.
- [160] S. Timoshenko, Analysis of bi-metal thermostats, *J. Opt. Soc. Am. Rev. Sci. Instrum.* 11 (1925) 233–255. doi:10.1364/JOSA.11.000233.
- [161] Q. Pei, O. Ingnas, Electrochemical Applications of the Bending Beam Method .2. Electroshrinking and Slow Relaxation in Polypyrrole, *J. Phys. Chem.* 97 (1993) 6034–6041. doi:10.1021/j100124a041.
- [162] Q. Pei, O. Ingnas, Electrochemical Applications of the Bending Beam Method, a Novel Way to Study Ion-Transport in Electroactive Polymers, *Solid State Ion.* 60 (1993) 161–166. doi:10.1016/0167-2738(93)90291-A.
- [163] M. Christophersen, B. Shapiro, E. Smela, Characterization and modeling of PPy bilayer microactuators - Part 1. Curvature, *Sens. Actuators B-Chem.* 115 (2006) 596–609. doi:10.1016/j.snb.2005.10.023.
- [164] G. Alici, B. Mui, C. Cook, Bending modeling and its experimental verification for conducting polymer actuators dedicated to manipulation applications, *Sens. Actuators -Phys.* 126 (2006) 396–404. doi:10.1016/j.sna.2005.10.020.

- [165] G. Alici, G. Spinks, N.N. Huynh, L. Sarmadi, R. Minato, Establishment of a biomimetic device based on tri-layer polymer actuators-propulsion fins, *Bioinspir. Biomim.* 2 (2007) S18–S30. doi:10.1088/1748-3182/2/2/S03.
- [166] P. Du, X. Lin, X. Zhang, A multilayer bending model for conducting polymer actuators, *Sens. Actuators -Phys.* 163 (2010) 240–246. doi:10.1016/j.sna.2010.06.002.
- [167] K.-J. Bathe, Finite Element Method, in: *Wiley Encycl. Comput. Sci. Eng.*, John Wiley & Sons, Inc., Hoboken, New Jersey, 2009. <http://onlinelibrary.wiley.com/doi/10.1002/9780470050118.ecse159/abstract> (accessed November 10, 2014).
- [168] G. Alici, P. Metz, G.M. Spinks, A methodology towards geometry optimization of high performance polypyrrole (PPy) actuators, *Smart Mater. Struct.* 15 (2006) 243–252. doi:10.1088/0964-1726/15/2/003.
- [169] P. Metz, G. Alici, G.M. SpinkS, A finite element model for bending behaviour of conducting polymer electromechanical actuators, *Sens. Actuators -Phys.* 130 (2006) 1–11. doi:10.1016/j.sna.2005.12.010.
- [170] B. Shapiro, E. Smela, Bending actuators with maximum curvature and force and zero interfacial stress, *J. Intell. Mater. Syst. Struct.* 18 (2007) 181–186. doi:10.1177/1045389X06063801.
- [171] S. Gutta, J. Realmuto, W. Yim, K.J. Kim, Dynamic model of a cylindrical ionic polymer-metal composite actuator, in: *2011 8th Int. Conf. Ubiquitous Robots Ambient Intell. URAI*, 2011: pp. 326–330. doi:10.1109/URAI.2011.6145985.
- [172] W. Albery, A. Mount, Application of a Transmission-Line Model to Impedance Studies on a Poly(vinylferrocene)-Modified Electrode, *J. Chem. Soc.-Faraday Trans.* 89 (1993) 327–331. doi:10.1039/ft9938900327.
- [173] J. Bisquert, G.G. Belmonte, F.F. Santiago, N.S. Ferriols, M. Yamashita, E.C. Pereira, Application of a distributed impedance model in the analysis of conducting polymer films, *Electrochem. Commun.* 2 (2000) 601–605. doi:10.1016/S1388-2481(00)00089-8.
- [174] G. Paasch, The transmission line equivalent circuit model in solid-state electrochemistry, *Electrochem. Commun.* 2 (2000) 371–375. doi:10.1016/S1388-2481(00)00040-0.
- [175] X. Ren, P. Pickup, Impedance Measurements of Ionic-Conductivity as a Probe of Structure in Electrochemically Deposited Polypyrrole Films, *J. Electroanal. Chem.* 396 (1995) 359–364. doi:10.1016/0022-0728(95)04064-U.
- [176] Y. Fang, X. Tan, Y. Shen, N. Xi, G. Alici, A scalable model for trilayer conjugated polymer actuators and its experimental validation, *Mater.*

- Sci. Eng. C-Biomim. Supramol. Syst. 28 (2008) 421–428.  
doi:10.1016/j.msec.2007.04.024.
- [177] Y. Fang, X. Tan, G. Alici, Robust Adaptive Control of Conjugated Polymer Actuators, *IEEE Trans. Control Syst. Technol.* 16 (2008) 600–612. doi:10.1109/TCST.2007.912112.
- [178] T. Shoa, D.S. Yoo, K. Walus, J.D.W. Madden, A Dynamic Electromechanical Model for Electrochemically Driven Conducting Polymer Actuators, *Ieee-Asme Trans. Mechatron.* 16 (2011) 42–49. doi:10.1109/TMECH.2010.2090166.
- [179] T. Shoa, J.D.W. Madden, N.R. Munce, V. Yang, Analytical modeling of a conducting polymer-driven catheter, *Polym. Int.* 59 (2010) 343–351. doi:10.1002/pi.2783.
- [180] G. Alici, An effective modelling approach to estimate nonlinear bending behaviour of cantilever type conducting polymer actuators, *Sens. Actuators B-Chem.* 141 (2009) 284–292. doi:10.1016/j.snb.2009.06.017.
- [181] W. Yim, J. Lee, K.J. Kim, An artificial muscle actuator for biomimetic underwater propulsors, *Bioinspir. Biomim.* 2 (2007) S31. doi:10.1088/1748-3182/2/2/S04.
- [182] T.F. Otero, J.M. Sansiñena, Bilayer dimensions and movement in artificial muscles, *Bioelectrochem. Bioenerg.* 42 (1997) 117–122. doi:10.1016/S0302-4598(96)05112-4.
- [183] T.F. Otero, M.T. Cortes, Artificial muscle: movement and position control, *Chem. Commun.* (2004) 284–285. doi:10.1039/b313132g.
- [184] L. Valero, J. Arias-Pardilla, J. Cauich-Rodríguez, M.A. Smit, T.F. Otero, Characterization of the movement of polypyrrole–dodecylbenzenesulfonate–perchlorate/tape artificial muscles. Faradaic control of reactive artificial molecular motors and muscles, *Electrochimica Acta.* 56 (2011) 3721–3726. doi:10.1016/j.electacta.2010.11.058.
- [185] T.F. Otero, J. Rodriguez, Electrochemomechanical and Electrochemopositioning Devices - Artificial Muscles, in: M. Aldissi (Ed.), *Intrinsically Conduct. Polym. Emerg. Technol.*, Kluwer Academic Publishers, Dordrecht, 1993: pp. 179–190.
- [186] A. Fersht, *Enzyme Structure and Mechanism*, Edición: 2nd Revised edition, W.H. Freeman & Co Ltd, New York, 1984.
- [187] T. Attwood, P. Campbell, H. Parish, A. Smith, F. Vella, J. Stirling, et al., *Oxford Dictionary of Biochemistry and Molecular Biology*, Edición: 2, OUP Oxford, Oxford ; New York, 2006.
- [188] F. Bezanilla, *The nerve impulse*, (1998).  
<http://nerve.bsd.uchicago.edu/med98a.htm>.

- [189] T.F. Otero, J.G. Martinez, Structural and Biomimetic Chemical Kinetics: Kinetic Magnitudes Include Structural Information, *Adv. Funct. Mater.* 23 (2013) 404–416. doi:10.1002/adfm.201200719.
- [190] T. Otero, E. Angulo, Oxidation-Reduction of Polypyrrole Films - Kinetics, Structural Model and Applications, *Solid State Ion.* 63-5 (1993) 803–809. doi:10.1016/0167-2738(93)90200-M.
- [191] T. Otero, H. Grande, J. Rodriguez, A New Model for Electrochemical Oxidation of Polypyrrole Under Conformational Relaxation Control, *J. Electroanal. Chem.* 394 (1995) 211–216. doi:10.1016/0022-0728(95)04033-K.
- [192] T.F. Otero, H. Grande, J. Rodriguez, An electromechanical model for the electrochemical oxidation of conducting polymers, *Synth. Met.* 76 (1996) 293–295. doi:10.1016/0379-6779(95)03474-X.
- [193] T.F. Otero, H. Grande, J. Rodriguez, Electrochemical oxidation of polypyrrole under conformational relaxation control. Electrochemical relaxation model, *Synth. Met.* 76 (1996) 285–288. doi:10.1016/0379-6779(95)03472-V.
- [194] T.F. Otero, H. Grande, J. Rodriguez, Conformational relaxation during polypyrrole oxidation: From experiment to theory, *Electrochimica Acta.* 41 (1996) 1863–1869. doi:10.1016/0013-4686(96)86826-5.
- [195] T.F. Otero, H. Grande, J. Rodriguez, Influence of the counterion size on the rate of electrochemical relaxation in polypyrrole, *Synth. Met.* 83 (1996) 205–208. doi:10.1016/S0379-6779(97)80081-1.
- [196] T.F. Otero, H. Grande, Thermally enhanced conformational relaxation during electrochemical oxidation of polypyrrole, *J. Electroanal. Chem.* 414 (1996) 171–176. doi:10.1016/0022-0728(96)04686-4.
- [197] T.F. Otero, H. Grande, J. Rodriguez, A conformational relaxation approach to polypyrrole voltammetry, *Synth. Met.* 85 (1997) 1077–1078.
- [198] T.F. Otero, H.J. Grande, J. Rodriguez, Reinterpretation of polypyrrole electrochemistry after consideration of conformational relaxation processes, *J. Phys. Chem. B.* 101 (1997) 3688–3697. doi:10.1021/jp9630277.
- [199] T.F. Otero, H. Grande, J. Rodriguez, Role of conformational relaxation on the voltammetric behavior of polypyrrole. Experiments and mathematical model, *J. Phys. Chem. B.* 101 (1997) 8525–8533. doi:10.1021/jp9714633.
- [200] H. Grande, T.F. Otero, Intrinsic asymmetry, hysteresis, and conformational relaxation during redox switching in polypyrrole: A coulometric study, *J. Phys. Chem. B.* 102 (1998) 7535–7540. doi:10.1021/jp9815356.

- [201] H. Grande, T.F. Otero, Conformational movements explain logarithmic relaxation in conducting polymers, *Electrochimica Acta*. 44 (1999) 1893–1900. doi:10.1016/S0013-4686(98)00298-9.
- [202] H. Grande, T.F. Otero, I. Cantero, Conformational relaxation in conducting polymers: effect of polymer-solvent interactions, *J. Non-Cryst. Solids*. 235 (1998) 619–622. doi:10.1016/S0022-3093(98)00613-9.
- [203] T.F. Otero, J.G. Martinez, M. Fuchiwaki, L. Valero, Structural Electrochemistry from Freestanding Polypyrrole Films: Full Hydrogen Inhibition from Aqueous Solutions, *Adv. Funct. Mater.* 24 (2014) 1265–1274. doi:10.1002/adfm.201302469.
- [204] T. Otero, I. Boyano, M. Cortes, G. Vazquez, Nucleation, non-stoichiometry and sensing muscles from conducting polymers, *Electrochimica Acta*. 49 (2004) 3719–3726. doi:10.1016/j.electacta.2004.01.085.
- [205] T.F. Otero, I. Boyano, Nucleation and nonstoichiometry in electrochromic conducting polymers, *Chemphyschem*. 4 (2003) 868–872. doi:10.1002/cphc.200300640.
- [206] T.F. Otero, J.M. Garcia de Otazo, Polypyrrole oxidation: Kinetic coefficients, activation energy and conformational energy, *Synth. Met.* 159 (2009) 681–688. doi:10.1016/j.synthmet.2008.12.017.
- [207] T.F. Otero, M. Caballero Romero, Conformational energy from the oxidation kinetics of poly(3,4-ethylenedioxythiophene) films, *Polym. Int.* 59 (2010) 329–336. doi:10.1002/pi.2774.
- [208] T.F. Otero, R. Abadias, Potentiostatic oxidation of poly(3-methylthiophene): Influence of the prepolarization time at cathodic potentials on the kinetics, *J. Electroanal. Chem.* 618 (2008) 39–44. doi:10.1016/j.jelechem.2008.02.019.
- [209] L. Rover, G.D. Neto, L.T. Kubota, Potentiometric transducers based in conducting polymers: Analytical applications., *Quimica Nova*. 20 (1997) 519–527.
- [210] N. Gupta, S. Sharma, I.A. Mir, D. Kumar, Advances in sensors based on conducting polymers, *J. Sci. Ind. Res.* 65 (2006) 549–557.
- [211] S. Nambiar, J.T.W. Yeow, Conductive polymer-based sensors for biomedical applications, *Biosens. Bioelectron.* 26 (2011) 1825–1832. doi:10.1016/j.bios.2010.09.046.
- [212] M. Gerard, A. Chaubey, B.D. Malhotra, Application of conducting polymers to biosensors, *Biosens. Bioelectron.* 17 (2002) 345–359. doi:10.1016/S0956-5663(01)00312-8.
- [213] J. Janata, M. Josowicz, Conducting polymers in electronic chemical sensors, *Nat. Mater.* 2 (2003) 19–24. doi:10.1038/nmat768.
- [214] G.W. Wang, Y.N. Lu, L.P. Wang, H.J. Wang, J.Y. Wang, Nanostructured Conducting Polymers and Their Biomedical

- Applications, *J. Nanosci. Nanotechnol.* 14 (2014) 596–612.  
doi:10.1166/jnn.2014.9084.
- [215] P. Atkins, J. De Paula, *Physical Chemistry*, 7th ed., OUP Oxford, Oxford, 2002.
- [216] L.T.T. Kim, C. Gabrielli, A. Pailleret, H. Perrot, Ions/Solvent Exchanges and Electromechanical Processes in Hexasulfonated Calix[6]Arene Doped Polypyrrole Films: Towards a Relaxation Mechanism, *Electrochem. Solid State Lett.* 14 (2011) F9–F11.  
doi:10.1149/2.022111esl.
- [217] C. Odin, M. Nechtschein, Slow Relaxation in Conducting Polymers, *Phys. Rev. Lett.* 67 (1991) 1114–1117.  
doi:10.1103/PhysRevLett.67.1114.
- [218] C. Jo, H.E. Naguib, R.H. Kwon, Fabrication, modeling and optimization of an ionic polymer gel actuator, *Smart Mater. Struct.* 20 (2011) 045006. doi:10.1088/0964-1726/20/4/045006.
- [219] W. Plieth, A. Bund, U. Rammelt, S. Neudeck, L. Duc, The role of ion and solvent transport during the redox process of conducting polymers, *Electrochimica Acta.* 51 (2006) 2366–2372.
- [220] M.J.M. Jafeen, M.A. Careem, S. Skaarup, A novel method for the determination of membrane hydration numbers of cations in conducting polymers, *J. Solid State Electrochem.* 16 (2012) 1753–1759.  
doi:10.1007/s10008-011-1594-2.
- [221] J.G. Martínez, T.F. Otero, C. Bosch-Navarro, E. Coronado, C. Martí-Gastaldo, H. Prima-Garcia, Graphene electrochemical responses sense surroundings, *Electrochimica Acta.* 81 (2012) 49–57.  
doi:10.1016/j.electacta.2012.07.037.
- [222] J.G. Martinez, T. Sugino, K. Asaka, T.F. Otero, Electrochemistry of Carbon Nanotubes: Reactive Processes, Dual Sensing-Actuating Properties and Devices, *Chemphyschem.* 13 (2012) 2108–2114.  
doi:10.1002/cphc.201100931.
- [223] P. Gimenez, K. Mukai, K. Asaka, K. Hata, H. Oike, T.F. Otero, Capacitive and faradic charge components in high-speed carbon nanotube actuator, *Electrochimica Acta.* 60 (2012) 177–183.  
doi:10.1016/j.electacta.2011.11.032.
- [224] K. Mukai, K. Asaka, K. Hata, T. Fernandez Otero, H. Oike, High-Speed Carbon Nanotube Actuators Based on an Oxidation/Reduction Reaction, *Chem.- Eur. J.* 17 (2011) 10965–10971.  
doi:10.1002/chem.201003641.
- [225] J. Arias-Pardilla, C. Plesse, A. Khaldi, F. Vidal, C. Chevrot, T.F. Otero, Self-supported semi-interpenetrating polymer networks as reactive ambient sensors, *J. Electroanal. Chem.* 652 (2011) 37–43.  
doi:10.1016/j.jelechem.2010.12.002.

- [226] S. Cosnier, A. Karyakin, eds., *Electropolymerization: Concepts, Materials and Applications*, Edición: 1, Wiley Vch Verlag GmbH, Weinheim, 2010.
- [227] N. Ferrer i Felis, *Applications of Fourier transform infrared spectroscopy*, in: *Handb. Instrum. Tech. Mater. Chem. Biosci. Res.*, Centres Científics i Tecnològics. Universitat de Barcelona, Barcelona, 2012: p. 10. <http://diposit.ub.edu/dspace/handle/2445/32136> (accessed September 11, 2014).
- [228] J.C.H. Spence, *High-Resolution Electron Microscopy*, OUP Oxford, Oxford, GBR, 2008.  
<http://site.ebrary.com/lib/alltitles/docDetail.action?docID=10278576> (accessed September 11, 2014).
- [229] R. Verdu, R. Berenguer, J. Morales, G. Vazquez, T.F. Otero, L. Weruaga, *Mechanical characterization of the life cycle of artificial muscles through stereoscopic computer vision and active contours*, in: *2005 Int. Conf. Image Process. ICIP Vols 1-5*, Ieee, New York, 2005: pp. 3705–3708.
- [230] S. Koehler, M. Ueda, I. Efimov, A. Bund, *An EQCM study of the deposition and doping/dedoping behavior of polypyrrole from phosphoric acid solutions*, *Electrochimica Acta*. 52 (2007) 3040–3046. doi:10.1016/j.electacta.2006.09.044.
- [231] M.A. Vorotyntsev, E. Vieil, J. Heinze, *Charging process in polypyrrole films: effect of ion association*, *J. Electroanal. Chem.* 450 (1998) 121–141. doi:10.1016/S0022-0728(97)00623-2.
- [232] S. Bruckenstein, J. Chen, I. Jureviciute, A.R. Hillman, *Ion and solvent transfers accompanying redox switching of polypyrrole films immersed in divalent anion solutions*, *Electrochimica Acta*. 54 (2009) 3516–3525. doi:10.1016/j.electacta.2008.11.061.
- [233] K.P. Vidanapathirana, M.A. Careem, S. Skaarup, K. West, *Ion movement in polypyrrole/dodecylbenzenesulphonate films in aqueous and non-aqueous electrolytes*, *Solid State Ion.* 154 (2002) 331–335. doi:10.1016/S0167-2738(02)00530-1.
- [234] A. Ispas, R. Peipmann, A. Bund, I. Efimov, *On the p-doping of PEDOT layers in various ionic liquids studied by EQCM and acoustic impedance*, *Electrochimica Acta*. 54 (2009) 4668–4675. doi:10.1016/j.electacta.2009.03.056.
- [235] T.F. Otero, M. Alfaro, V. Martinez, M.A. Perez, J.G. Martinez, *Biomimetic Structural Electrochemistry from Conducting Polymers: Processes, Charges, and Energies. Coulovoltammetric Results from Films on Metals Revisited*, *Adv. Funct. Mater.* 23 (2013) 3929–3940. doi:10.1002/adfm.201203502.



- [236] A. Zykwińska, W. Domagała, A. Czardybon, B. Pilawa, M. Lapkowski, In situ EPR spectroelectrochemical studies of paramagnetic centres in poly(3,4-ethylenedioxythiophene) (PEDOT) and poly(3,4-butylendioxythiophene) (PBuDOT) films, *Chem. Phys.* 292 (2003) 31–45. doi:10.1016/S0301-0104(03)00253-2.
- [237] J. Heinze, B.A. Frontana-Urbe, S. Ludwigs, *Electrochemistry of Conducting Polymers—Persistent Models and New Concepts*, *Chem. Rev.* 110 (2010) 4724–4771. doi:10.1021/cr900226k.
- [238] K. Aoki, M. Kawase, Introduction of a Percolation-Threshold Potential at Polyaniline-Coated Electrodes, *J. Electroanal. Chem.* 377 (1994) 125–129. doi:10.1016/0022-0728(94)03446-X.
- [239] J.Q. Li, K. Aoki, Electrochemical gelation of poly(3-hexylthiophene) film, *J. Electroanal. Chem.* 453 (1998) 107–112. doi:10.1016/S0022-0728(98)00238-1.
- [240] J. Fournier, G. Boiteux, G. Seytre, G. Marichy, Percolation network of polypyrrole in conducting polymer composites, *Synth. Met.* 84 (1997) 839–840. doi:10.1016/S0379-6779(96)04173-2.
- [241] L. Vandyke, S. Kuwabata, C. Martin, A Simple Chemical Procedure for Extending the Conductive State of Polypyrrole to More Negative Potentials, *J. Electrochem. Soc.* 140 (1993) 2754–2759. doi:10.1149/1.2220906.
- [242] A.J. Heeger, Semiconducting and metallic polymers: the fourth generation of polymeric materials, *Synth. Met.* 125 (2001) 23–42. doi:10.1016/S0379-6779(01)00509-4.
- [243] J. Heinze, P. Tschuncky, A. Smie, The oligomeric approach - the electrochemistry of conducting polymers in the light of recent research, *J. Solid State Electrochem.* 2 (1998) 102–109. doi:10.1007/s100080050073.
- [244] D.P. Almond, C.R. Bowen, D. a. S. Rees, Composite dielectrics and conductors: simulation, characterization and design, *J. Phys. -Appl. Phys.* 39 (2006) 1295–1304. doi:10.1088/0022-3727/39/7/S03.
- [245] G. Ambrosetti, N. Johnner, C. Grimaldi, T. Maeder, P. Ryser, A. Danani, Electron tunneling in conductor-insulator composites with spherical fillers, *J. Appl. Phys.* 106 (2009) 016103. doi:10.1063/1.3159040.
- [246] M. Heaney, Measurement and Interpretation of Nonuniversal Critical Exponents in Disordered Conductor-Insulator Composites, *Phys. Rev. B.* 52 (1995) 12477–12480. doi:10.1103/PhysRevB.52.12477.
- [247] M.E. Mezeme, S. El Bouazzaoui, M.E. Achour, C. Brosseau, Uncovering the intrinsic permittivity of the carbonaceous phase in carbon black filled polymers from broadband dielectric relaxation, *J. Appl. Phys.* 109 (2011) 074107. doi:10.1063/1.3556431.

- [248] B. Mu, P. Liu, X. Yu, F. Pan, Z. Gao, X. Liu, Preparation and characterization of conductor-insulator-semiconductor sandwich-structured MWCNT/double-layer polymer hybrid nanocomposites, *Synth. Met.* 160 (2010) 2329–2335. doi:10.1016/j.synthmet.2010.09.007.
- [249] H. Naarmann, N. Theophilou, New Process for the Production of Metal-Like, Stable Polyacetylene, *Synth. Met.* 22 (1987) 1–8. doi:10.1016/0379-6779(87)90564-9.
- [250] J. Obrzut, J.F. Douglas, S.B. Kharchenko, K.B. Migler, Shear-induced conductor-insulator transition in melt-mixed polypropylene-carbon nanotube dispersions, *Phys. Rev. B.* 76 (2007) 195420. doi:10.1103/PhysRevB.76.195420.
- [251] D. Ofer, R. Crooks, M. Wrighton, Potential Dependence of the Conductivity of Highly Oxidized Polythiophenes, Polypyrroles, and Polyaniline - Finite Windows of High Conductivity, *J. Am. Chem. Soc.* 112 (1990) 7869–7879. doi:10.1021/ja00178a004.
- [252] V. Panwar, R.M. Mehra, Analysis of Electrical, Dielectric, and Electromagnetic Interference Shielding Behavior of Graphite Filled High Density Polyethylene Composites, *Polym. Eng. Sci.* 48 (2008) 2178–2187. doi:10.1002/pen.21163.
- [253] J.Y. Yi, G.M. Choi, Percolation behavior of conductor-insulator composites with varying aspect ratio of conductive fiber, *J. Electroceramics.* 3 (1999) 361–369. doi:10.1023/A:1009913913732.
- [254] G. Zotti, R. Salmaso, M.C. Gallazzi, R.A. Marin, In situ conductivity of a polythiophene from a branched alkoxy-substituted tetrathiophene. Enhancement of conductivity by conjugated cross-linking of polymer chains, *Chem. Mater.* 9 (1997) 791–795. doi:10.1021/cm960476a.
- [255] C.C.B. Bufon, J. Vollmer, T. Heinzl, P. Espindola, H. John, J. Heinze, Relationship between chain length, disorder, and resistivity in polypyrrole films, *J. Phys. Chem. B.* 109 (2005) 19191–19199. doi:10.1021/jp053516j.
- [256] B.J.S. Jones, M. Kalaji, Influence of electrode geometry on the redox switching characteristics of conducting polymers, *Electrochimica Acta.* 50 (2005) 4505–4512. doi:10.1016/j.electacta.2005.02.019.
- [257] J.C. Lacroix, K. Fraoua, P.C. Lacaze, Moving front phenomena in the switching of conductive polymers, *J. Electroanal. Chem.* 444 (1998) 83–93. doi:10.1016/S0022-0728(97)00561-5.
- [258] T.F. Otero, H. Grande, J. Rodriguez, Reversible electrochemical reactions in conducting polymers: A molecular approach to artificial muscles, *J. Phys. Org. Chem.* 9 (1996) 381–386. doi:10.1002/(SICI)1099-1395(199606)9:6<381::AID-POC796>3.0.CO;2-N.

- [259] T.F. Otero, H.J. Grande, Reversible 2D to 3D electrode transitions in polypyrrole films, *Colloids Surf. -Physicochem. Eng. Asp.* 134 (1998) 85–94. doi:10.1016/S0927-7757(97)00331-2.
- [260] T.F. Otero, I. Boyano, Characterization of polypyrrole degradation by the conformational relaxation model, *Electrochimica Acta.* 51 (2006) 6238–6242. doi:10.1016/j.electacta.2006.04.005.
- [261] T.F. Otero, M. Marquez, I.J. Suarez, Polypyrrole: Diffusion coefficients and degradation by overoxidation, *J. Phys. Chem. B.* 108 (2004) 15429–15433. doi:10.1021/jp0490608.
- [262] K. Vetter, *Electrochemical kinetics : theoretical and experimental aspects*, Academic Press, New York, N.Y, 1967.
- [263] M. (editor) Abramowitz, I.A. (editor) Stegun, *Handbook of mathematical functions with formulas, graphs, and mathematical tables*, Dover, New York, 1964.  
<http://archive.org/details/handbookofmathem1964abra> (accessed January 10, 2013).
- [264] A.J. Bard, L.R. Faulkner, *Electrochemical methods: fundamentals and applications*, Wiley, New York, 1980.
- [265] H. Okuzaki, K. Funasaka, Electromechanical Properties of a Humido-Sensitive Conducting Polymer Film, *Macromolecules.* 33 (2000) 8307–8311. doi:10.1021/ma0000531.
- [266] T. Sendai, H. Suematsu, K. Kaneto, Anisotropic Strain and Memory Effect in Electrochemomechanical Strain of Polypyrrole Films under High Tensile Stresses, *Jpn. J. Appl. Phys.* 48 (2009) 051506. doi:10.1143/JJAP.48.051506.
- [267] T.F. Otero, J.G. Martinez, Activation energy for polypyrrole oxidation: film thickness influence, *J. Solid State Electrochem.* 15 (2011) 1169–1178. doi:10.1007/s10008-010-1170-1.
- [268] T.F. Otero, F. Santos, Polythiophene oxidation: Rate coefficients, activation energy and conformational energies, *Electrochimica Acta.* 53 (2008) 3166–3174. doi:10.1016/j.electacta.2007.10.072.
- [269] S. Aznar-Cervantes, M.I. Roca, J.G. Martinez, L. Meseguer-Olmo, J.L. Cenis, J.M. Moraleda, et al., Fabrication of conductive electrospun silk fibroin scaffolds by coating with polypyrrole for biomedical applications, *Bioelectrochemistry.* 85 (2012) 36–43. doi:10.1016/j.bioelechem.2011.11.008.

# **Annex I: Papers**

## Papers

1. Toribio F. Otero, Jose G. Martinez and Joaquin Arias-Pardilla. Biomimetic electrochemistry from conducting polymers. A review. Artificial muscles, smart membranes, smart drug delivery and computer/neuron interfaces *Electrochimica Acta*, year 2012, volume 84, pages 112-128. (ISI-JCR IF: 4.086, Q1 in Electrochemistry).
2. Toribio F. Otero and Jose G. Martinez. Artificial Muscles: A Tool To Quantify Exchanged Solvent During Biomimetic Reactions *Chemistry of Materials*, year 2012, volume 24, pages 4093-4099. (IF=8.535, Q1 in 'Materials science, Multidisciplinary' and 'Chemistry, Physical').
3. Toribio F. Otero and Jose G. Martinez. Ionic exchanges, structural movements and driven reactions in conducting polymers from bending artificial muscles *Sensors and Actuators B: Chemical*, year 2014, volume 199, pages 27-30. (IF=3.840, Q1 in 'Instruments & instrumentation', 'Chemistry, analytical' and 'Electrochemistry').
4. Toribio F. Otero and Jose G. Martinez. Structural Electrochemistry: Conductivities and Ionic Content from Rising Reduced Polypyrrole Films *Advanced Functional Materials*, year 2014, volume 24, pages 1259-1264. (IF=10.439, Q1 in 'Materials science, multidisciplinary', 'Nanoscience & nanotechnology', 'Physics, applied', 'Chemistry, multidisciplinary', 'Chemistry, physical' and 'Physics, condensed matter').
5. Jose G. Martinez, Toribio F. Otero and Edwin W. H. Jager. Effect of the Electrolyte Concentration and Substrate on Conducting Polymer Actuators *Langmuir*, year 2014, volume 30, pages 3894-3904. (IF=4.384, Q1 in 'Materials science, multidisciplinary', 'Chemistry, multidisciplinary' and 'Chemistry, physical').
6. Toribio F. Otero, Juan J. Sanchez and Jose G. Martinez. Biomimetic Dual Sensing-Actuators Based on Conducting Polymers. Galvanostatic Theoretical Model for Actuators Sensing Temperature *The Journal of Physical Chemistry B*, year 2012, volume 116, pages 5279-5290. (IF=3.377, Q2 in 'Chemistry, physical').
7. Jose G. Martinez and Toribio F. Otero. Biomimetic Dual Sensing-Actuators: Theoretical Description. Sensing Electrolyte Concentration and Driving Current *The Journal of Physical Chemistry B*, year 2012, volume 116, pages 9223-9230. (IF=3.377, Q2 in 'Chemistry, physical').
8. Jose G. Martinez and Toribio F. Otero. Mechanical awareness from sensing artificial muscles: Experiments and modeling *Sensors and Actuators B: Chemical*, year 2014, volume 195, pages 365-372. (IF=3.840, Q1 in 'Instruments & instrumentation', 'Chemistry, analytical', and 'Electrochemistry').
9. Jose G. Martinez and Toribio F. Otero. Structural Electrochemistry. Chronopotentiometric Responses From Rising Compacted Polypyrrole Electrodes: Experiments and Model *RSC Advances*, year 2014, volume 4, pages 29139-29145. (IF=3.708, Q1 in 'Chemistry, multidisciplinary').
10. Toribio F. Otero and Jose G. Martinez. Physical and chemical awareness from sensing polymeric artificial muscles. Experiments and modeling *Progress in Polymer Science*, year 2014, DOI: 10.1016/j.progpolymsci.2014.09.002. (IF=26.854, Q1 in 'Polymer science').
11. Yahya A. Ismail, Jose G. Martinez and Toribio F. Otero. Polyurethane microfibrinous mat template polypyrrole: Preparation and biomimetic reactive sensing capabilities *Journal of Electroanalytical Chemistry*, year 2014, volume 719, pages 47-53. (IF=2.871, Q2 in 'Chemistry, analytical' and 'Electrochemistry').
12. Yahya A. Ismail, Jose G. Martinez and Toribio F. Otero. Fibroin/Polyaniline microfibrinous mat. Preparation and electrochemical characterization as reactive sensor *Electrochimica Acta*, year 2014, volume 123, pages 501-510. (IF: 4.086, Q1 in 'Electrochemistry').